

Squark Production in the R-Symmetric Supersymmetric Standardmodel

Master-Arbeit
zur Erlangung des Hochschulgrades
Master of Science
im Master-Studiengang Physik

vorgelegt von

Sebastian Liebschner
geboren am 08.05.1990 in Meerane

Institut für Kern- und Teilchenphysik Physik
Fachrichtung Physik
Fakultät Mathematik und Naturwissenschaften
Technische Universität Dresden
2016

Eingereicht am xx. Monat 20xx

1. Gutachter: Prof. Dr. XX
2. Gutachter: Prof. Dr. YY

Summary

Abstract

English: motivation: aesthetic: Coleman-Mandula \rightarrow Haag-Lopuszanski-Sohnius-Theorem

Abstract

Deutsch

Contents

1	Introduction	1
2	The Standard Model	2
2.1	Symmetries and Transformations	2
2.2	The Particles of the Standard Model	4
2.3	Electroweak Symmetry Breaking	7
2.4	Quantization	9
2.5	Lagrangian of the SM	9
3	The Minimal Supersymmetric Standard Model	10
3.1	Supersymmetry as Extension of Poincaré Symmetry	10
3.2	A Generic Supersymmetric Model in Superspace Formulation	10
3.3	The Minimal Supersymmetric Standard Model in superspace formulation . . .	12
4	R-Symmetry	14
4.1	R-Symmetry Transformation	14
4.2	The Minimal R-Symmetric Supersymmetric Standard Model	15
4.3	The R-Symmetric Supersymmetric Quantum Chromodynamics	16
5	Squark and Gluino Production at Tree Level	19
5.1	Partonic Processes and their Cross Section	19
5.2	Hadronic Cross Section	25
6	Virtual and Real Corrections	35
6.1	Virtual Correction	35
6.2	Real Corrections	36
6.2.1	Real Gluon Radiation	37
6.2.2	Real Quark Radiation	37
7	Renormalization of the MRSSM	39
7.1	Regularization Schemes	39
7.2	Regularization Scheme Dependences	40
7.3	On-Shell Renormalization	41
7.4	Renormalization of the Gauge Coupling	46
7.5	The Beta Function	51
7.6	Supersymmetry Restoring Counterterm	51
7.7	$\overline{\text{MS}}$ - Renormalization	53

8	Squark Production at One-Loop	54
8.1	The LSZ Theorem	54
8.2	The Cross Section in the Limit of Large Sgluon Masses	56
9	Summary and Outlook	57
10	Appendix	58
10.1	System of Units and Metric	58
10.2	Constants of the Colour Algebra $SU(N)$	58
10.3	Weyl basis and 2-spinor notation	59
10.4	Anticommuting numbers	61
10.5	Feynman rules for the RSQCD	61
10.6	Passarino-Veltman Integrals	64
10.7	Cross section and Phase Space Integration	66
11	References	68

1 Introduction

motivation: aesthetic: Coleman-Mandula \rightarrow Haag-Lopuszanski-Sohnius-Theorem

plots for exclusion of squarks in specific SUSY scenarios (from Michael) \rightarrow R-Symmetry could be possible explanation for that because:

MSSM-Lagrangian \rightarrow trafo rules for superfields under R-symm \rightarrow forbidden terms in MRSSM (write down Lagrangian for R-symmetric SUSYQCD)

suppression of squark production in MRSSM by less diagrams (m_{gluino}^{-4} suppression at low energies in MRSSM and only m_{gluino}^{-2} suppression in MSSM)

R-charges of all fields (show in diagram!) \rightarrow only if R-charges of final / initial particles are zero, a diagram is allowed in R-symm. model

references to build in

- "Matching Squark Pair Production at NLO with Parton Showers" from Gavin, Hangst, Krämer, Mühlleitner,.. for complete treatment of NLO calculation
- "DIRAC gAUGINOS IN susy - sUPPRESSED jETS + <met sIGNALS: a sNOWMASS WHITEPAPER" FROM kRIBS, mARTIN for Squark production at LO, allude to same result
- "Dirac Gaugino Masses and supersoft SUSY breaking" from Fox, Weiner, Nelson for the introduction of the MRSSM

2 The Standard Model

The Standard Model of particle physics is the commonly accepted theory describing the world's fundamental particles and their interactions. It is a gauge quantum field theory which is characterized by its invariance under symmetry groups. The Standard Model contains different fields, whose quantized excitations are interpreted as particles.

This chapter summarizes the most important aspects of the Standard Model.

2.1 Symmetries and Transformations

Spacetime Symmetries

The Standard Model is defined on Minkowski space, whose coordinates are label with x^μ $\mu \in \{0, 1, 2, 4\}$. As a relativistic theory it is invariant under Poincaré transformations, i.e. it is invariant under Lorentz-transformations (with generators $J^{\mu\nu}$) and translations (with generators P^μ) in spacetime. The set of all Poincaré transformations form the Poincaré group, which is a Lie group. Its generators obey the Poincaré-algebra

$$\begin{aligned} [P^\mu, P^\nu] &= 0 \\ [P^\mu, J^{\nu\rho}] &= i(g^{\mu\nu} P^\rho - g^{\mu\rho} P^\nu) \\ [J^{\mu\nu}, J^{\rho\sigma}] &= i(g^{\nu\rho} J^{\mu\sigma} + g^{\mu\sigma} J^{\nu\rho} - g^{\mu\rho} J^{\nu\sigma} - g^{\nu\sigma} J^{\mu\rho}). \end{aligned} \quad (2.1)$$

The fields of the Standard Model transform in different representations of the Poincaré-group [1].

Gauge Symmetries

In order to describe interactions of matter particles gauge theories are used. In the Standard Model matter fields are described by Dirac spinors. The Lagrangian of a free Dirac field reads

$$\mathcal{L}_{Dirac} = \bar{\Psi}(i\not{\partial} - m)\Psi. \quad (2.2)$$

To include interactions one imposes a local group symmetry (gauge symmetry) upon this Lagrangian. A spinor transforms under a generic gauge transformation like

$$\Psi(x) \rightarrow U(x)\Psi(x), \quad (2.3)$$

where $U(x)$ is an element of the gauge group in question. Because the gauge group is a unitary matrix Lie group it can be written in the form $U(x) = \exp(-igT^a\theta^a(x))$. Here T^a are the

self-adjoint generators of the associated Lie algebra which obey

$$[T^a, T^b] = if_{abc}T^c \quad (2.4)$$

where f_{abc} are the structure constants of a Lie algebra, g is the coupling constant of the gauge group and $\theta^a(x)$ are local parameters.

Because the parameters of the gauge group are local the derivative in 2.2 spoils the gauge invariance. In order to rectify gauge invariance of the Lagrangian one introduces a further field for each index a of the generators - the gauge vector $G^{a\mu}$. Defining the transformation of the matrix valued gauge vector $G^\mu := G^{a\mu}T^a$ as

$$G^\mu(x) \rightarrow U^{-1}(x) \left(G^\mu(x) + \frac{i}{g} \partial^\mu \right) U(x) \quad (2.5)$$

and introducing the gauge covariant derivative

$$D^\mu = \partial^\mu + igT^a G^{a\mu} \quad (2.6)$$

one finds that the expression $D_\mu \Psi(x)$ transforms as

$$D_\mu \Psi(x) \rightarrow U(x) D_\mu \Psi(x) \quad (2.7)$$

Therefore gauge invariance is restored in eq. 2.2 by replacing ∂_μ with D_μ . But if the gauge vector is interpreted as a physical field there must apart from the so far introduced interaction term also be a kinetic term associated with it. Using eq. 2.7 one defines the field strength tensor¹ $F^{a\mu\nu}$ whose matrix valued form

$$F^{\mu\nu} = F^{a\mu\nu}T^a := \frac{1}{ig}[D^\mu, D^\nu] = \partial^\mu G^\nu - \partial^\nu G^\mu - gf_{abc}T^c G^{a\mu}G^{b\nu} \quad (2.8)$$

transforms as $F^{\mu\nu} \rightarrow U(x)F^{\mu\nu}U^{-1}(x)$. Using the cyclic property of the trace and the Dynkin index $T(F)$ defined in eq. 10.6 in the appendix one can write down a gauge invariant kinetic term for the gauge vector:

$$\mathcal{L}_{\text{gauge}} = -\frac{1}{2}\text{Tr}(F^{\mu\nu}F_{\mu\nu}) = -\frac{T(F)}{2}F^{a\mu\nu}F_{\mu\nu}^a \quad (2.9)$$

This completes the construction of a Lagrangian which is invariant under non-abelian gauge group transformations. The result is the famous Yang and Mills Lagrangian [3]

$$\mathcal{L}_{\text{Yang-Mills}} = \bar{\Psi}i\not{D}\Psi - \frac{1}{4}F^{a\mu\nu}F_{\mu\nu}^a \quad (2.10)$$

¹An alternative construction of the field strength tensor makes use of the gauge invariant Wilson loop. This gives some insights into the geometry of gauge transformations [2].

This Lagrangian gives rise to spin- $\frac{1}{2}$ (matter) particles which interact with spin-1 (force mediator) particles. Furthermore if the gauge group is non-abelian, i.e. $f_{abc} \neq 0$, there are self interactions among the spin-1 particles.

The gauge group of the Standard Model is a direct product of the three gauge groups²: $U_Y(1)$, $SU_L(2)$ and $SU_C(3)$. The elements $U(x)$ of those are given in table 2.1.

These gauge groups give rise to 3 forces: the strong force, the weak force and the electromagnetic force.

Gauge Group	Group Element
$U_Y(1)$	$U(x) = \exp\left(-ig_Y \frac{\hat{Y}}{2} \theta_Y(x)\right)$
$SU_L(2)$	$U(x) = \exp\left(-ig_w \vec{\tau} \cdot \vec{\theta}_w(x)\right)$
$SU_C(3)$	$U(x) = \exp(-ig_s T^a \cdot \theta_s^a(x))$

Table 2.1: The table lists the explicit element $U(x)$ of the gauge groups $U_Y(1)$, $SU_L(2)$ and $SU_C(3)$. The hypercharge operator \hat{Y} gives the eigenvalue of the hypercharge of the field it is applied to (see table 2.3). $\vec{\tau}$ and T^a are the generators of $SU_L(2)$ and $SU_C(3)$ respectively. In the fundamental representation $\vec{\tau} = \frac{\vec{\sigma}}{2}$ where $\vec{\sigma}$ has the 3 Pauli matrices as components and $T^a = \frac{\lambda^a}{2}$ where λ^a are the 8 Gell-Mann matrices. ε_{abc} and f_{abc} are the structure constants of $SU_L(2)$ and $SU_C(3)$ respectively.

2.2 The Particles of the Standard Model

In the Standard Model different matter particles take part in different interactions, i.e. their corresponding spinor couples to different gauge vectors.

If a spinor couples to a certain gauge vector it transforms non trivially (like indicated in table 2.1) under the gauge group which is associated with this gauge vector³. This means if a particle couples to a certain force its charge which is associated with this force is nonzero.

The charges of particles for a force are defined as the eigenvalues of the generators which correspond to the force.

The Quarks:

Quarks are strongly interacting fermions, which means their spinors transform non trivially under $SU_C(3)$. Because they transform in the fundamental representation of $SU_C(3)$ this means a quark spinor is built up by 3 spinors each carrying another color. This splitting of the quark spinor in colors is often suppressed for the sake of simplicity. This convention is adopted throughout this thesis.

²The subscript stands for the associated charge of the groups respectively: Y for hypercharge, L for left handedness (weak Isospin I_3) and C for color

³In the Standard Model all matter particles transform in the fundamental (or trivial) representation of gauge groups.

Furthermore the left handed component of quarks interact weakly, which means that their spinors⁴ transform (in the fundamental representation) under $SU_L(2)$ transformations meaning that 2 left handed quark spinors are assembled within a doublet.

Finally all quarks carry a hypercharge. In section 2.3 the mechanism of electroweak symmetry breaking is described. This mechanism explains how electromagnetism arises from the groups $SU_L(2)$ and $U_Y(1)$. All quarks interact electromagnetically.

After all there are 6 quarks which are listed in table 2.2. They are categorized in 3 generations because their quantum numbers except for their masses reoccur in each generation. The two types of quarks within a generation which have distinct quantum numbers are referred to as up-type and down-type quarks. An up-type-quark and the down-type quark of the same generation built up a doublet.

The Leptons:

Leptons do not interact strongly. They take part in the weak and the electromagnetic interaction, i.e. their spinors transform under the fundamental representation of $SU_L(2)$ and $U_Y(1)$. As for the quarks only the left handed components interact weakly.

As for the quarks there are 6 leptons which are classified into 3 generations (see table 2.2). In each generation is a lepton with a negative electrical charged and an electrically neutral lepton. The latter ones are referred to as neutrinos. Right handed neutrinos have not been observed (yet) and are therefore absent in the SM. The former are called electron, muon and tau. Each left handed leptons with an electric charge is assembled with its neutrino in a doublet.

Particle	1 st generation	2 nd generation	3 rd generation
u_i up-type-Quark	u up-Quark	c charm-Quark	t top-Quark
d_i down-type-Quark	d down-Quark	s strange-Quark	b bottom-Quark
e_i Charged Lepton	e Electron	μ Muon	τ Tau
ν_i Neutrino	ν_e Electron Neutrino	ν_μ Muon Neutrino	ν_τ Tau Neutrino

Table 2.2: The matter particles of the SM. Listed are the symbol and the name of the particles.

Quarks and Leptons are the matter particles of the Standard Model. They are listed together with their charges for the different forces in table 2.3. There is the color for strong interactions, the third component of the weak isospin I_3 for weak interactions (the eigenvalue of the third generator of the $SU_L(2)$) and the half of the hypercharge $\frac{Y}{2}$ to obtain the electric charge Q via the Gell-Mann–Nishijima formula: $Q = I_3 + \frac{Y}{2}$.

Because the left and right-handed parts of spinors transform differently under the $SU_L(2)$ they

⁴The left handed part of a 4-spinor Ψ is projected out by the appropriate projector P_L . This is explained in Appendix 10.3.

are listed separately. All quarks occur with three different colors.

In the last row the Higgs-boson is listed. Its associated field is responsible for the mass of elementary particles. That is explained in section 2.3.

Particle	Symbol	color	I_3	$\frac{Y}{2}$	Q
Left handed Quarks	$Q_{iL} = \begin{pmatrix} u_{iL} \\ d_{iL} \end{pmatrix}$	red, green, blue	$\begin{pmatrix} +\frac{1}{2} \\ -\frac{1}{2} \end{pmatrix}$	$+\frac{1}{6}$	$\begin{pmatrix} +\frac{2}{3} \\ -\frac{1}{3} \end{pmatrix}$
Right-handed Quarks	u_{iR}	red, green, blue	0	$+\frac{2}{3}$	$+\frac{2}{3}$
	d_{iR}	red, green, blue	0	$-\frac{1}{3}$	$-\frac{1}{3}$
Left-handed Leptons	$\ell_{iL} = \begin{pmatrix} \nu_{iL} \\ e_{iL} \end{pmatrix}$	-	$\begin{pmatrix} +\frac{1}{2} \\ -\frac{1}{2} \end{pmatrix}$	$-\frac{1}{2}$	$\begin{pmatrix} 0 \\ -1 \end{pmatrix}$
Right-handed Leptons	e_{iR}	-	0	+1	+1
Higgs	H	-	$-\frac{1}{2}$	$+\frac{1}{2}$	0

Table 2.3: This table lists all matter particles in the Standard Model and the Higgs particle with their charges for all forces. This is the color, the weak isospin I_3 , the half of their hypercharge and their electrical charge. The index $i = 1, 2, 3$ labels the generation of the matter particles and is written out in table 2.2. If there are no colors specified or charges are zero this means that the fields in question transform trivially under the pertaining gauge transformation.

The Force Particles

before EWSB			after EWSB		
group	coupling constant	gauge field	coupling constant	gauge field	Particle
$SU_C(3)$	g_s	G_μ^a	g_s	G_μ^a	Gluon
$SU_L(2)$	g_w	W_μ^b	$g_W = \sqrt{2}g_w,$ $g_Z = \sqrt{g_w^2 + g_Y^2}$	$W_\mu^\pm,$ Z_μ^0	$W^\pm,$ Z^0 Boson
$U_Y(1)$	g_Y	B_μ	$e = g_Y \cdot c_w$	A_μ	Photon

Table 2.4: The gauge fields and their coupling constants before and after electro weak symmetry breaking (EWSB). The Gluon field is not affected by EWSB. $a = 1, \dots, 8$ and $b = 1, 2, 3$ label the number of gauge fields. c_w is the cosine of the electroweak mixing angle defined in 2.3

The force particles are described by gauge fields. The gauge field of $SU_C(3)$ is the gluon field. Because the $SU_C(3)$ has 8 generators there are 8 gluons. Their coupling constant is denoted with g_s .

For the other force particles in the Standard Model - the W^\pm bosons, the Z_0 boson and the

photon the situation is slightly more involved. They are obtained as a mixture of the W_μ^b ($b = 1, 2, 3$) and the B_μ field which are the gauge fields of $SU_L(2)$ and $U_Y(1)$ respectively. This mixing procedure is explained in section 2.3.

For the moment being the coupling constants and gauge fields before and after this mixing are quoted in table 2.4.

The Lagrangian of the SM is built up by qualitatively different terms. Firstly there are the kinetic and minimal coupling terms of the matter fields

$$\mathcal{L}_{\text{matter}} = \sum_{i=1}^3 (\bar{\ell}_{iL} i \not{D} \ell_{iL} + \bar{e}_{iR} i \not{D} e_{iR} + \bar{q}_{iL} i \not{D} q_{iL} + \bar{u}_{iR} i \not{D} u_{iR} + \bar{d}_{iR} i \not{D} d_{iR}) \quad (2.11)$$

where $i \in \{1, 2, 3\}$ labels the generations of matter. The gauge covariant derivative is given by

$$D_\mu = \partial_\mu + ig_Y \frac{\hat{Y}}{2} + ig_w \vec{\tau} \cdot \vec{W}^\mu + ig_s T^a G_a^\mu \quad (2.12)$$

where for each field the corresponding representation (fundamental or trivial) of the gauge group is to be inserted (see table 2.3). The hyper charge operator \hat{Y} gives the eigenvalue of the hypercharge of the field it is applied to. These can also be found in table 2.3. The kinetic terms of the gauge fields are given by

$$\mathcal{L}_{\text{gauge}} = -\frac{1}{4} F^{\mu\nu} F_{\mu\nu} - \frac{1}{4} W^{a\mu\nu} W_{\mu\nu}^a - \frac{1}{4} G^{a\mu\nu} G_{\mu\nu}^a. \quad (2.13)$$

2.3 Electroweak Symmetry Breaking

So far no mass terms like in the Dirac Lagrangian 2.2 have been introduced. The reason for this is that they are not gauge invariant for left- and right-handed spinors transform differently. The same argument forbids terms like $-\frac{m^2}{2} A^\mu A_\mu$ for a generic gauge boson. Electroweak symmetry breaking (EWSB) ascribes masses to those particles [4], [5], [6], [7], [8], [9], [?]. To this end one considers a complex scalar doublet

$$\Phi = \begin{pmatrix} \phi^+ \\ \phi^0 \end{pmatrix} \quad (2.14)$$

which receives a vacuum expectation value (VEV) $\langle \Phi \rangle = \frac{1}{\sqrt{2}} \begin{pmatrix} 0 \\ v \end{pmatrix}$ by the Higgs potential

$$V(\Phi^\dagger \Phi) = -\mu^2 \Phi^\dagger \Phi + \lambda (\Phi^\dagger \Phi)^2 \quad (2.15)$$

where $\mu^2, \lambda > 0$. The Higgs sector of the Standard Model reads

$$\mathcal{L}_{Higgs} = (D_\mu \Phi)^\dagger (D^\mu \Phi) - V(\Phi^\dagger \Phi). \quad (2.16)$$

The Higgs doublet couples to the gauge fields of $SU_L(2)$ and $U_Y(1)$ in the fundamental representation. Inserting an expansion⁵ around the VEV $\Phi = \begin{pmatrix} \phi^+(x) \\ \frac{1}{\sqrt{2}}(v + H(x) + i\sigma(x)) \end{pmatrix}$ one obtains quadratic terms, i.e. mass terms, for the gauge fields in question. In order to obtain mass eigenstates out of B_μ and W_μ^3 and charge eigenstates for Q and I_3 out of W_μ^1 and W_μ^2 one performs the transformation

$$\begin{pmatrix} A_\mu \\ Z_\mu^0 \end{pmatrix} = \begin{pmatrix} \cos \theta_w & \sin \theta_w \\ -\sin \theta_w & \cos \theta_w \end{pmatrix} \begin{pmatrix} B_\mu \\ W_\mu^3 \end{pmatrix} \quad W_\mu^\pm = \frac{1}{\sqrt{2}}(W_\mu^1 \mp iW_\mu^2), \quad (2.17)$$

where the electroweak mixing angle is given by $\cos \theta_w = \frac{g_w}{\sqrt{g_w^2 + g_Y^2}}$. These gauge fields acquire masses:

$$m_W = \frac{g_w}{2}v \quad m_Z = \frac{\sqrt{g_w^2 + g_Y^2}}{2}v \quad m_A = 0. \quad (2.18)$$

Apart from the massive bosons W_μ^\pm and Z_μ^0 one obtains the massless photon A_μ . As the photon is massless it is still associated with a gauge symmetry called $U_{em}(1)$. One therefore often writes EWSB as the breaking of the gauge group $SU_L(2) \times U_Y(1)$ to $U_{em}(1)$.

Matter particles acquire mass via Yukawa couplings to the Higgs doublet. For up-type-quarks one uses that the charge conjugate of Φ : $\Phi^C = i\sigma^2 \Phi^*$ also transform as Φ .

$$\mathcal{L}_{Yukawa} = \sum_{i,j=1}^3 (y_{ij}^e \bar{\ell}_L \Phi e_R + y_{ij}^d \bar{q}_L \Phi d_R + y_{ij}^u \bar{q}_L \Phi^C u_R) + h.c. \quad (2.19)$$

where y^e, y^d, y^u are 3×3 matrices in generation space. The fermion mass matrices are therefore:

$$m_{ij}^e = \frac{y_{ij}^e}{\sqrt{2}}v \quad m_{ij}^d = \frac{y_{ij}^d}{\sqrt{2}}v \quad m_{ij}^u = \frac{y_{ij}^u}{\sqrt{2}}v. \quad (2.20)$$

The quark mass matrices are not diagonal, which is the precondition of the violation of CP-invariance.⁶ One therefore has to distinguish between interaction and mass eigenstates of the quarks. The corresponding transformation matrix is the well known CKM-matrix [11], [12]. Throughout this thesis, the CKM-matrix is approximated with the unit matrix as it will have

⁵The complex $\phi^+(x)$ and the real $\sigma(x)$ are the fields of the so called massless Goldstone bosons. These degrees of freedom can be absorbed in the longitudinally polarized degrees of freedom of the arising gauge bosons W^\pm and Z^0 . This is referred to as unitary gauge [10]. The real $H(x)$ is the Higgs field, whose excitation is the Higgs boson.

⁶The actual CP-violating term is the coupling term from quarks to the W -bosons.

a minor influence upon the results

The upshot of EWSB are masses for all matter particles except for the neutrinos and masses for the gauge bosons W^\pm and Z^0 .

2.4 Quantization

The Quantization of Spin 0 and Spin $\frac{1}{2}$ fields yield no complication in the Lagrangian formalism. To quantize Spin 1 fields it turns out that the usual gauge invariance needs to be replaced by the so called BRST invariance [13], [14], [15]. This results in two extra contributions in the Lagrangian. Firstly there are the gauge fixing terms:

$$\mathcal{L}_{R_\xi} = -\frac{1}{2\xi_A}(\partial^\mu A_\mu)^2 - \frac{1}{\xi_W}|\partial^\mu W_\mu^+ - im_W\xi_W\phi^+|^2 - \frac{1}{2\xi_Z}(\partial^\mu Z_\mu - m_Z\xi_Z\sigma)^2 - \frac{1}{2\xi_G}(\partial^\mu G_\mu^a)^2. \quad (2.21)$$

Here R_ξ -gauge is chosen, where the parameters ξ_i specify the gauge further. The two terms in the middle are modified with the Goldstone bosons from section 2.3. This is to cancel terms of the form $V_\mu\partial^\mu\phi$ up to a total derivative arising from EWSB which would lead to non-diagonal propagators, where V stands for a gauge boson W^\pm or Z^0 and ϕ for a Goldstone boson.

Secondly there is a ghost Lagrangian

$$\mathcal{L}_{\text{ghost}} = -\bar{c}_a\partial^\mu(\partial_\mu c_a + g_s f_{abc}c_b G_{c\mu}) + \mathcal{L}_{\text{weak ghosts}}. \quad (2.22)$$

The ghost Lagrangian corresponding to the electroweak sector is not needed within this thesis and due to its lengthy form not quoted here. It can be found in [10]. In eq. 2.22 c_a and \bar{c}_a are the Faddeev-Popov ghost and antighosts. These fields do not correspond to physical particles because they violate the spin-statistics theorem, i.e. they anticommute while being spin 0 fields. Ghost fields are an elegant way of accounting for an additional term in the Lagrangian of non-abelian gauge fields which is best seen in the path integral quantization [2].

2.5 Lagrangian of the SM

The complete Lagrangian of the SM reads

$$\mathcal{L}_{\text{SM}} = \mathcal{L}_{\text{matter}} + \mathcal{L}_{\text{gauge}} + \mathcal{L}_{\text{Higgs}} + \mathcal{L}_{\text{Yukawa}} + \mathcal{L}_{R_\xi} + \mathcal{L}_{\text{ghost}} \quad (2.23)$$

with the corresponding parts of the previous chapters. For further reading, see [10].

3 The Minimal Supersymmetric Standard Model

3.1 Supersymmetry as Extention of Poincaré Symmetry

....The superalgebra is defined by

$$\begin{aligned}
\{Q_\alpha, Q_\beta\} &= \{\bar{Q}_{\dot{\alpha}}, \bar{Q}_{\dot{\beta}}\} = 0, \\
\{Q_\alpha, \bar{Q}_{\dot{\alpha}}\} &= 2\sigma_{\alpha\dot{\alpha}}^\mu P_\mu, \\
[P^\mu, Q_\alpha] &= [P^\mu, \bar{Q}_{\dot{\alpha}}] = 0, \\
[Q_\alpha, J^{\mu\nu}] &= \frac{1}{2}(\sigma^{\mu\nu})_\alpha{}^\beta Q_\beta
\end{aligned} \tag{3.1}$$

A representation in the form of differential operators is given by

$$\begin{aligned}
P^\mu &= i\partial^\mu \\
J^{\mu\nu} &= i(x^\mu\partial^\nu - x^\nu\partial^\mu) \\
Q_\alpha &= i(\partial_\alpha + i\sigma_{\alpha\dot{\alpha}}^\mu \bar{\theta}^{\dot{\alpha}} \partial_\mu) \\
\bar{Q}_{\dot{\alpha}} &= i(-\bar{\partial}_{\dot{\alpha}} - i\theta^\alpha \sigma_{\alpha\dot{\alpha}}^\mu \partial_\mu).
\end{aligned} \tag{3.2}$$

INTRODUCE AND MOTIVATE SUSY COVARIANT DERIVATIVES $\mathcal{D}_\alpha = \frac{\partial}{\partial\theta^\alpha} - i(\sigma^\mu\bar{\theta})_\alpha\partial_\mu$ is the chiral covariant derivative and $\bar{\mathcal{D}}\mathcal{D} = \bar{\mathcal{D}}_{\dot{\alpha}}\bar{\mathcal{D}}^{\dot{\alpha}}$

3.2 A Generic Supersymmetric Model in Superspace Formulation

This chapter outlines the generic ingredients and terms of a supersymmetric model. To this end it is practical to work in the language of superspace and superfields.

Superspace is a manifold obtained by enlarging Minkowski space, whose coordinates are label with x^μ , with four anticommuting numbers: θ^α and $\bar{\theta}^{\dot{\alpha}}$, where $\alpha, \dot{\alpha} = 1, 2$. Superfields are functions on superspace.

The for the MSSM relevant superfields⁷ are the chiral superfield $\hat{\Phi}$, the antichiral superfield $\hat{\bar{\Phi}}$ and the vector superfield V . Chiral superfields are defined by the restriction $\bar{\mathcal{D}}_{\dot{\alpha}}\hat{\Phi} = 0$, antichiral superfields by $\mathcal{D}_\alpha\hat{\bar{\Phi}} = 0$ and vector superfields by the condition of being real $V^\dagger = V$. Their component decomposition reads⁸

$$\begin{aligned}
\hat{\Phi}(x, \theta, \bar{\theta}) &= A(x) + \sqrt{2}\theta\psi(x) + \theta\theta F(x) - i\theta\sigma^\mu\bar{\theta}\partial_\mu A(x) - \frac{1}{4}\theta\theta\bar{\theta}\bar{\theta}\partial_\mu\partial^\mu A(x) - \frac{i}{\sqrt{2}}\theta\theta\bar{\theta}\bar{\sigma}^\mu\partial_\mu\psi(x) \\
\hat{\bar{\Phi}}(x, \theta, \bar{\theta}) &= A^\dagger(x) + \sqrt{2}\bar{\theta}\bar{\psi}(x) + \bar{\theta}\bar{\theta}F^\dagger(x) + i\theta\sigma^\mu\bar{\theta}\partial_\mu A^\dagger(x) - \frac{1}{4}\theta\theta\bar{\theta}\bar{\theta}\partial_\mu\partial^\mu A^\dagger(x) - \frac{i}{\sqrt{2}}\bar{\theta}\bar{\theta}\theta\sigma^\mu\partial_\mu\bar{\psi}(x) \\
\hat{V}(x, \theta, \bar{\theta}) &= \theta\sigma^\mu\bar{\theta}v_\mu + i\theta\theta\bar{\theta}\bar{\lambda}(x) - i\bar{\theta}\bar{\theta}\theta\lambda(x) + \frac{1}{2}\theta\theta\bar{\theta}\bar{\theta}D(x),
\end{aligned} \tag{3.3}$$

⁷Superfield are throughout this thesis labeled with a hat.

⁸For the vector superfield Wess-Zumino-gauge is applied.

where $A(x)$ and $F(x)$ are complex scalar fields, $\psi(x)$ and $\lambda(x)$ are left handed Weyl spinors and $D(x)$ being a real scalar field.

The superfields transform under a generic gauge transformation as

$$\begin{aligned}\hat{\Phi} &\rightarrow e^{-2ig\hat{\Lambda}}\hat{\Phi} \\ \hat{\bar{\Phi}} &\rightarrow \hat{\bar{\Phi}}e^{2ig\bar{\Lambda}} \\ e^{2g\hat{V}} &\rightarrow e^{-2ig\hat{\Lambda}}e^{2g\hat{V}}e^{2ig\hat{\Lambda}},\end{aligned}\tag{3.4}$$

where $\hat{\Lambda} = \hat{\Lambda}^a T^a$ and $\hat{V} = \hat{V}^a T^a$. $\hat{\Lambda}^a$ is an arbitrary chiral superfield and the T^a are the generators of the Lie algebra, which is associated to the gauge group in question. g is the gauge coupling constant of the gauge group.

One can therefore construct the important gauge invariant term $\int d^4\theta \hat{\bar{\Phi}}e^{2g\hat{V}}\hat{\Phi}$. If one introduces the gauge covariant derivative $D_\mu = \partial + igT^a v_\mu^a$ the component decomposition reads

$$\begin{aligned}\int d^4\theta \hat{\bar{\Phi}}e^{2g\hat{V}}\hat{\Phi} &= F^\dagger F + (D_\mu A)^\dagger (D^\mu A) + \bar{\psi}\bar{\sigma}^\mu i D_\mu \psi \\ &\quad - \sqrt{2}g \left(-i(A^\dagger T^a A)\lambda^a + i\bar{\lambda}^a (AT^a A^\dagger) \right) + g(A^\dagger T^a A)D^a.\end{aligned}\tag{3.5}$$

Therefore this term gives rise to the kinetic terms of the components of the chiral and antichiral superfields A , A^\dagger , ψ and $\bar{\psi}$, their minimal coupling to the gauge fields v_μ^a and their superpartners λ^a and $\bar{\lambda}^a$ and terms involving the auxiliary fields F , F^\dagger and D .

With the field-strength chiral superfields $\hat{W}_\alpha = -\frac{1}{4}\overline{\mathcal{D}}\mathcal{D}(e^{-2gV}\mathcal{D}_\alpha e^{2gV})$ one can write down a gauge invariant term yielding the kinetic terms of the gauge fields and their superpartners:

$$\int d^2\theta \frac{1}{16g^2} \hat{W}^{\alpha\alpha} \hat{W}_\alpha^a + h.c. = \frac{1}{2} D^a D^a - \frac{1}{4} F_{\mu\nu}^a F^{a\mu\nu} + \frac{i}{2} \bar{\lambda}^a \bar{\sigma}^\mu (D_\mu \lambda^a) + \frac{i}{2} \lambda^a \sigma^\mu (D_\mu \bar{\lambda}^a).\tag{3.6}$$

A third generic term in a supersymmetric theory arises from the superpotential $W(\hat{\Phi})$ which is a holomorphic function in the chiral superfields:

$$\int d^2\theta W(\hat{\Phi}).\tag{3.7}$$

A renormalizable superpotential is given by $W(\hat{\Phi}) = c_i \hat{\Phi} + \frac{m_{ij}}{2} \hat{\Phi}_i \hat{\Phi}_j + \frac{g_{ijk}}{3!} \hat{\Phi}_i \hat{\Phi}_j \hat{\Phi}_k$. The component decomposition of the corresponding terms is

$$\begin{aligned}\int d^2\theta \hat{\Phi}_1 &= F_1 \\ \int d^2\theta \hat{\Phi}_1 \hat{\Phi}_2 &= A_1 F_2 + F_1 A_2 - \psi_1 \psi_2 \\ \int d^2\theta \hat{\Phi}_1 \hat{\Phi}_2 \hat{\Phi}_3 &= F_1 A_2 A_3 + A_1 F_2 A_3 + A_1 A_2 F_3 - A_1 \psi_2 \psi_3 - \psi_1 A_2 \psi_3 - \psi_1 \psi_2 A_3.\end{aligned}\tag{3.8}$$

The Lagrangian for a supersymmetric theory is therefore given by

$$\begin{aligned}\mathcal{L}_{SUSY} &= \mathcal{L}_{matter} + \mathcal{L}_{gauge} + \mathcal{L}_{superpot} \\ &= \int d^4\theta \hat{\Phi} e^{2g\hat{V}} \hat{\Phi} + \left(\int d^2\theta \frac{1}{16g^2} \hat{W}^{\alpha\alpha} \hat{W}_\alpha^a + h.c. \right) + \int d^2\theta W(\hat{\Phi})\end{aligned}\quad (3.9)$$

Observing the component decomposition 3.5, 3.6, 3.8 of the 3 parts of this Lagrangian, one observes that the F and D fields have no kinetic term and are therefore auxiliary fields which can be eliminated by their equation of motion $\frac{\partial \mathcal{L}}{\partial \phi} = \partial_\mu \frac{\partial \mathcal{L}}{\partial (\partial_\mu \phi)}$ with $\phi = F, D$. Doing this one obtains

$$\begin{aligned}\mathcal{L}_D &= \frac{1}{2} D^a D^a + g A^\dagger T^a D^a A \quad \Rightarrow \quad D^a = -A^\dagger T^a A \\ \mathcal{L}_D &= -\frac{1}{2} (A^\dagger T^a A)^2\end{aligned}\quad (3.10)$$

and

$$\begin{aligned}\mathcal{L}_F &= F_i^\dagger F_i + \left(c_i F_i + m_{ij} F_i A_j + \frac{g_{ijk}}{2} F_i A_j A_k + h.c. \right) \quad \Rightarrow \quad F_i^\dagger = -\frac{\partial W(A)}{\partial A_i} \\ \mathcal{L}_F &= -\left| \frac{\partial W(A)}{\partial A_i} \right|^2\end{aligned}\quad (3.11)$$

3.3 The Minimal Supersymmetric Standard Model in superspace formulation

The Lagrangian for the MSSM⁹ reads

$$\begin{aligned}\mathcal{L}_{MSSM} &= \int d^4\theta \left[\hat{\bar{Q}} e^{2g'\hat{V}'+2g\hat{V}+2g_s\hat{V}_s} \hat{Q} + \hat{\bar{U}} e^{2g'\hat{V}'+2g\hat{V}-2g_s\hat{V}_s^T} \hat{U} + \hat{\bar{D}} e^{2g'\hat{V}'+2g\hat{V}-2g_s\hat{V}_s^T} \hat{D} \right. \\ &\quad + \hat{\bar{L}} e^{2g'\hat{V}'+2g\hat{V}} \hat{L} + \hat{\bar{E}} e^{2g'\hat{V}'+2g\hat{V}} \hat{E} \\ &\quad \left. + \hat{\bar{H}}_d e^{2g'\hat{V}'+2g\hat{V}} \hat{H}_d + \hat{\bar{H}}_u e^{2g'\hat{V}'+2g\hat{V}} \hat{H}_u \right] \\ &\quad + \int d^2\theta \left[\frac{1}{16g'^2} \hat{W}'^\alpha \hat{W}'_\alpha + \frac{1}{16g^2} \hat{W}^{a\alpha} \hat{W}_\alpha^a + \frac{1}{16g_s^2} \hat{W}_s^{a\alpha} \hat{W}_{s\alpha}^a \right] + h.c. \\ &\quad + \int d^2\theta W_{MSSM} + h.c. \\ &\quad + \mathcal{L}_{soft}.\end{aligned}\quad (3.12)$$

Apart from the already discussed terms in the first 4 lines of 3.12 there is a superpotential W_{MSSM} :

$$W_{MSSM} = y_d \hat{H}_d \hat{Q} \hat{D} + y_u \hat{H}_u \hat{Q} \hat{U} + y_e \hat{H}_d \hat{L} \hat{E} - \mu \hat{H}_d \hat{H}_u \quad (3.13)$$

⁹This is the Lagrangian on the classical level, i.e. there are neither gauge fixing nor ghost terms.

and terms which break supersymmetry softly, i.e. terms with coupling constants with positive mass dimension.

$$\begin{aligned}
\mathcal{L}_{soft} = & -M_Q^2 |\tilde{q}_L|^2 - M_U^2 |\tilde{u}_R|^2 - M_D^2 |\tilde{d}_R|^2 \\
& - M_L^2 |\tilde{l}_L|^2 - M_E^2 |\tilde{e}_R|^2 - M_{H_d}^2 |H_d|^2 - M_{H_u}^2 |H_u|^2 \\
& + \frac{1}{2} (M_1 \lambda \lambda + M_2 \lambda^a \lambda^a + M_3 \lambda_s^a \lambda_s^a) + h.c. \\
& - \left(A_d y_d H_d \tilde{q}_L \tilde{d}_R^\dagger + A_u y_u H_u \tilde{q}_L \tilde{u}_R^\dagger + A_e y_e H_d \tilde{l}_L \tilde{e}_R^\dagger - B \mu H_d H_u \right) + h.c.
\end{aligned} \tag{3.14}$$

The field content of the MSSM is summarized in 3.1

Superfield	Components	$SU_C(3) \times SU_L(2) \times U_Y(1)$
$\hat{\Phi}$	A, ψ	
\hat{V}	λ, v_μ	
\hat{Q}	$\tilde{q}_L = \begin{pmatrix} \tilde{u}_L \\ \tilde{d}_L \end{pmatrix}, q_L = \begin{pmatrix} u_L \\ d_L \end{pmatrix}$	$(3, 2, \frac{1}{6})$
\hat{U}	\tilde{u}_R^\dagger, u_R	$(3^*, 1, -\frac{2}{3})$
\hat{D}	\tilde{d}_R^\dagger, d_R	$(3^*, 1, +\frac{1}{3})$
\hat{L}	$\tilde{l}_L = \begin{pmatrix} \tilde{\nu}_L \\ \tilde{e}_L \end{pmatrix}, l_L = \begin{pmatrix} \nu_L \\ e_L \end{pmatrix}$	$(1, 2, -\frac{1}{2})$
\hat{E}	\tilde{e}_R^\dagger, e_R	$(1, 1, 1)$
\hat{H}_d	H_d, \tilde{H}_d	$(1, 2, -\frac{1}{2})$
\hat{H}_u	H_u, \tilde{H}_u	$(1, 2, +\frac{1}{2})$
\hat{V}'	λ', B_μ	$(1, 1, 0)$
\hat{V}^a	λ^a, W_μ^a	$(1, 3, 0)$
\hat{V}_s^a	λ_s^a, G_μ^a	$(8, 1, 0)$

Table 3.1: The table shows the field content of the MSSM in terms of the superfields and their component decomposition. The first two lines show the decomposition of the generic superfields (cf. 3.3).

The third column shows the representation (for $SU_C(3)$ and $SU_L(2)$) in which the fields transform and the charges of the fields for $U_Y(1)$.

4 R-Symmetry

4.1 R-Symmetry Transformation

R-symmetry is a global $U(1)$ symmetry. R-symmetry should not be confused with R-parity which is a discrete Z_2 symmetry. A continuous global symmetry implies according to Noether's theorem a conserved charge. In the case of R-symmetry this charge is called R-charge and one therefore refers to R-symmetry as $U_R(1)$.

The defining property of $U_R(1)$ is that the anticommuting coordinates θ^α and $\bar{\theta}^{\dot{\alpha}}$ transform like

$$\theta \rightarrow e^{i\alpha}\theta \qquad \bar{\theta} \rightarrow e^{-i\alpha}\bar{\theta}, \quad (4.1)$$

where α parametrizes the transformation. This in turn implies that R-symmetry does not commute with supersymmetry, meaning that superpartners do not have the same R-charge.

The transformation of chiral and vector superfields reads

$$\begin{aligned} \hat{\Phi}(x, \theta, \bar{\theta}) &\rightarrow e^{ir_{\hat{\Phi}}\alpha} \hat{\Phi}(x, e^{i\alpha}\theta, e^{-i\alpha}\bar{\theta}) \\ \hat{V}(x, \theta, \bar{\theta}) &\rightarrow \hat{V}(x, e^{i\alpha}\theta, e^{-i\alpha}\bar{\theta}). \end{aligned} \quad (4.2)$$

If one inserts the component decomposition 3.3 of the superfields one can read off the R-charges of the component fields.

4.2 The Minimal R-Symmetric Supersymmetric Standard Model

The MSSM with additional R-symmetry is called minimal R-symmetric supersymmetric standard model (MRSSM). If one imposes R-symmetry upon the MSSM one is faced with a certain arbitrariness, i.e. the choice of the R-charges of the chiral superfields. In this thesis the R-charges are chosen in that way, that every Standard model particle has R-charge zero. Following this one obtains the R-charges of all particles which are summed up in table 4.2. The gauge, matter and H -Higgs fields are the fields of the MSSM. Below the horizontal line one finds the fields which are not present in the MSSM, i.e. the R -Higgs and adjoint chiral fields. These occur for the following reason.

Since in the MSSM the gauginos are Majorana particles their mass terms reads

$$\mathcal{L}_{Majorana\ mass} = -m\lambda\lambda + h.c. \quad (4.3)$$

which is not R-invariant because the Weyl fermion λ has R-charge $+1$. The only other way to account for a fermion mass is to write down a Dirac mass term.

$$L_{Dirac\ mass} = -m\chi\lambda + h.c. \quad (4.4)$$

Maybe refer to mixed Majorana/Dirac gauginos, Mass matrix for spinors

In order to get a R-symmetric mass term one has to choose the R-charge of the new Weyl-spinor χ to be the opposite of λ .

This explains the necessity of enlarging the field content if one imposes R-symmetry.

Of course the new Weyl-spinor χ must have also a superpartner. One chooses this superpartner to be a scalar, i.e. the additional Weyl fermion comes from a chiral superfield. In order to maintain gauge invariance this chiral superfield has to transform in the adjoint representation, hence the name adjoint chiral in table 4.2. To fix notation the component decomposition of the 8 chiral supermultiplets associated to the gluons is given by

$$\hat{O}^a(x, \theta, \bar{\theta}) = \sigma^a + \sqrt{2}\theta\chi^a + \dots \quad a = 1, \dots, 8. \quad (4.5)$$

superfield		boson		fermion	
$\hat{\Phi}$	$r_{\hat{\Phi}}$	A	$r_{\hat{\Phi}}$	ψ	$r_{\hat{\Phi}} - 1$
\hat{V}	0	v^μ	0	λ	+1

Table 4.1: This table shows the R-charges of a generic chiral and vector superfield.

Field	Superfield		Boson		Fermion	
Gauge Vector	$\hat{g}, \hat{W}, \hat{B}$	0	g, W, B	0	$\tilde{g}, \tilde{W}, \tilde{B}$	+1
Matter	\hat{L}, \hat{E}	0	\tilde{l}, \tilde{e}_R	+1	l, e_R	0
	$\hat{Q}, \hat{D}, \hat{U}$	+1	$\tilde{q}, \tilde{d}_R^\dagger, \tilde{u}_R^\dagger$	+1	q, d_R, u_R	0
<i>H</i> -Higgs	$\hat{H}_{d,u}$	0	$H_{d,u}$	0	$\tilde{H}_{d,u}$	-1
<i>R</i> -Higgs	$\hat{R}_{d,u}$	+2	$R_{d,u}$	+2	$\tilde{R}_{d,u}$	+1
Adjoint Chiral	$\hat{O}, \hat{T}, \hat{S}$	0	O, T, S	0	$\tilde{O}, \tilde{T}, \tilde{S}$	-1

Table 4.2: This table shows the R-charges of all particles in the MRSSM.

The scalar components σ^a are called scalar gluons and the Weyl spinors χ^a are called octinos. The same argument as for the adjoint chiral explains the existence of additional Higgs-superfields which are referred to as *R*-Higgs fields.

But instead of including more fields in the model *R*-symmetry also forbids terms which are allowed by supersymmetry. For the above choice of R-charges the μ -term in 3.13 and the *A*-terms in the last line of 3.14 are excluded. As a consequence terms which allow flavor violating processes like $\mu \rightarrow e\gamma$ are allowed in the MSSM but forbidden in the MRSSM [Kribs, Popitz, Weiner].

4.3 The R-Symmetric Supersymmetric Quantum Chromodynamics

The subject of this thesis is the phenomenology of the strongly coupling sector of the MRSSM. The R-symmetric supersymmetric quantumchromodynamics (RSQCD) is therefore considered closer. Its Lagrangian reads

$$\begin{aligned}
\mathcal{L}_{RSQCD} = & \int d^4\theta \left(\hat{\bar{Q}}_L e^{2g_s \hat{V}_s} \hat{Q}_L + \hat{\bar{Q}}_R e^{-2g_s \hat{V}_s^T} \hat{Q}_R + \hat{\bar{O}} e^{2g_s \hat{V}_s^{fund}} \hat{O} \right) \\
& + \left(\int d^2\theta \frac{1}{16g_s^2} \hat{W}_s^{a\alpha} \hat{W}_{s\alpha}^a + h.c. \right) + \mathcal{L}_{soft}
\end{aligned} \tag{4.6}$$

where in terms of component fields the terms are given by

$$\begin{aligned} \int d^4\theta \hat{\bar{Q}}_L e^{2g_s \hat{V}_s} \hat{Q}_L &= F_L^\dagger F_L + (D_\mu \tilde{q}_L)^\dagger (D^\mu \tilde{q}_L) + \bar{q}_L \bar{\sigma}^\mu i D_\mu q_L \\ &\quad - \sqrt{2} g_s \left(-i(\tilde{q}_L^\dagger T^a q_L) \lambda^a + i\bar{\lambda}^a (\bar{q}_L T^a \tilde{q}_L) \right) + g_s \tilde{q}_L^\dagger T^a D^a \tilde{q}_L \end{aligned} \quad (4.7)$$

$$\begin{aligned} \int d^4\theta \hat{\bar{Q}}_R e^{-2g_s \hat{V}_s^T} \hat{Q}_R &= F_R^\dagger F_R + (D_\mu \tilde{q}_R)^\dagger (D^\mu \tilde{q}_R) + \bar{q}_R \bar{\sigma}^\mu i D_\mu q_R \\ &\quad + \sqrt{2} g_s \left(-i(\tilde{q}_R T^{*a} q_R) \lambda^a + i\bar{\lambda}^a (\bar{q}_R T^{*a} \tilde{q}_R^\dagger) \right) - g_s \tilde{q}_R T^{*a} D^a \tilde{q}_R^\dagger \end{aligned} \quad (4.8)$$

$$\begin{aligned} \int d^4\theta \hat{\bar{O}} e^{2g_s \hat{V}_s^{fund}} \hat{O} &= F_O^\dagger F_O + (D_\mu \sigma^a)^\dagger (D^\mu \sigma^a) + \bar{\chi} \bar{\sigma}^\mu i D_\mu \chi \\ &\quad - \sqrt{2} g_s \left(-i(\sigma_{b\dagger}(-if_{abc})(-i\chi^c)) \lambda^a + i\bar{\lambda}^a (i\bar{\chi}_b(+if_{abc})\sigma^{c\dagger}) \right) \\ &\quad - ig_s \sigma^{b\dagger} f^{abc} D^a \sigma^c \end{aligned} \quad (4.9)$$

where in the gauge covariant derivative $D_\mu = \partial_\mu + ig_s T^a G_\mu^a$ the generator T^a needs to be replaced by $-T^{*a}$ or $-if^{abc}$ if applied to a field transforming in the antifundamental or adjoint representation respectively.

The soft breaking Lagrangian accounts for the squark, gaugino and scalar gluon masses. These mass terms arise from a hidden sector spurion. For the gauginos the D-type spurion is given by $\hat{W}'_\alpha = \theta_\alpha D$ and mediates super symmetry breaking at the mediation scale M : $\int d\theta^2 \frac{\hat{W}'_\alpha}{M} W_s^\alpha \hat{O}$. After integrating out the spurion one obtains

$$\begin{aligned} \mathcal{L}_{soft} &= -\frac{m_{\tilde{q}}^2}{2} (|\tilde{q}_L|^2 + |\tilde{q}_R|^2) \\ &\quad -\frac{m_{\sigma_1}^2}{2} \sigma_1^2 - \frac{m_{\sigma_2}^2}{2} \sigma_2^2 - m_g (\lambda \chi - \sqrt{2} D^a \sigma^a + h.c.) \end{aligned} \quad (4.10)$$

where the complex scalar gluons $\sigma = \frac{\sigma_1 + i\sigma_2}{\sqrt{2}}$ constitutes of two real scalar gluons with different masses. The equations of motion for the auxiliary fields are

$$D^a = -g_s \tilde{q}_L^\dagger T^a \tilde{q}_L + g_s \tilde{q}_R T^a \tilde{q}_R^\dagger + ig_s \sigma^{\dagger b} f^{abc} \sigma^c - \sqrt{2} m_g (\sigma^a + \sigma^{\dagger a}) \quad (4.11)$$

$$F_i = 0 \quad \text{for} \quad i = L, R, O \quad (4.12)$$

where D^a is still real as the purely imaginary parts do not contribute by virtue of the antisymmetry of the structure constants. After eliminating the auxiliary fields the complete

Lagrangian in 4 spinor notation¹⁰ reads

$$\begin{aligned}
\mathcal{L}_{RSQCD} = & |D_\mu \sigma|^2 + |D_\mu \tilde{q}_R|^2 + |D_\mu \tilde{q}_L|^2 + \bar{q} i \not{D} q + \bar{\tilde{g}}^a i \not{D} P_L \tilde{g}^a + \bar{\tilde{g}}^a i \not{D} P_R \tilde{g}^a - \frac{1}{4} (F_a^{\mu\nu})^2 \\
& - \sqrt{2} g_s \left(\bar{\tilde{g}}^a P_R (q^C T^a \tilde{q}_L) + (\tilde{q}_L^\dagger T^a \bar{q}^C) P_L \tilde{g}^a \right) \\
& + \sqrt{2} g_s \left(\bar{\tilde{g}}^a P_R (q T^{*a} \tilde{q}_R^\dagger) + (\tilde{q}_R T^{*a} \bar{q}) P_L \tilde{g}^a \right) \\
& - \sqrt{2} g_s \left(\bar{\tilde{g}}^a P_R (\tilde{g}^b (i f^{abc}) \sigma^c) + (\sigma^{\dagger b} (-i f^{abc}) \bar{\tilde{g}}^c) P_L \tilde{g}^a \right) \\
& - \frac{m_{\tilde{q}}^2}{2} (|\tilde{q}_L|^2 + |\tilde{q}_R|^2) - \frac{m_{\sigma_1}^2}{2} \sigma_1^2 - \frac{m_{\sigma_2}^2}{2} \sigma_2^2 - m_g \bar{\tilde{g}}^a \tilde{g}^a \\
& - \frac{1}{2} \left(g_s \tilde{q}_L^\dagger T^a \tilde{q}_L - g_s \tilde{q}_R T^{*a} \tilde{q}_R^\dagger - i g_s \sigma^{\dagger b} f^{abc} \sigma^c + \sqrt{2} m_g (\sigma^a + \sigma^{\dagger a}) \right)^2 \quad (4.13)
\end{aligned}$$

Observe that there is no 3 sgluon vertex, because of the antisymmetry of the structure constants f^{abc} . Add relation of sgluon masses: $m_{\sigma_0}^2 = m_{\phi_0}^2 + 4m_{\tilde{g}}$ and table of particle content of RSQCD

¹⁰How a 4 spinor is composed of Weyl-spinors is given in the Appendix 10.3

5 Squark and Gluino Production at Tree Level

Comment on sgluon production: which channels, calculate cross section for at least one configuration of masses.

In this chapter the production of strongly interacting supersymmetric particles¹¹ in the MRSSM is considered. The various processes and their associated cross section is compared to their analogues in the MSSM.

5.1 Partonic Processes and their Cross Section

For the following calculation the top quark is excluded from the initial state as it is too heavy to be significantly present in hadrons. For consistency reasons also the stop is excluded from the final states. One therefore deals with $n_f - 1 = 5$ quark flavors. In view of the renormalization to be performed at the 1-loop level the results are given in $D = 4 - 2\epsilon$ dimensions and it has been distinguished between the gauge coupling g_s from the gluon-quark-quark vertex and its supersymmetric analogue \hat{g}_s from the gluino-squark-quark vertex. The usual Mandelstam variables s, t, u and the following modifications of them are used¹²

$$\begin{aligned}
 s &= (k_a + k_b)^2 = (p_1 + p_2)^2 \\
 t &= (k_a - p_1)^2 = (k_b - p_2)^2 \\
 u &= (k_a - p_2)^2 = (k_b - p_1)^2 \\
 t_{\tilde{g}} &= t - m_{\tilde{g}}^2 & t_{\tilde{q}} &= t - m_{\tilde{q}}^2 \\
 u_{\tilde{g}} &= u - m_{\tilde{g}}^2 & u_{\tilde{q}} &= u - m_{\tilde{q}}^2
 \end{aligned} \tag{5.1}$$

¹¹The production of sgluons is excluded from the analysis for their mass is chosen to be too large to significantly produce them.

¹²The kinematics of the process is like denoted in fig. 5.1.

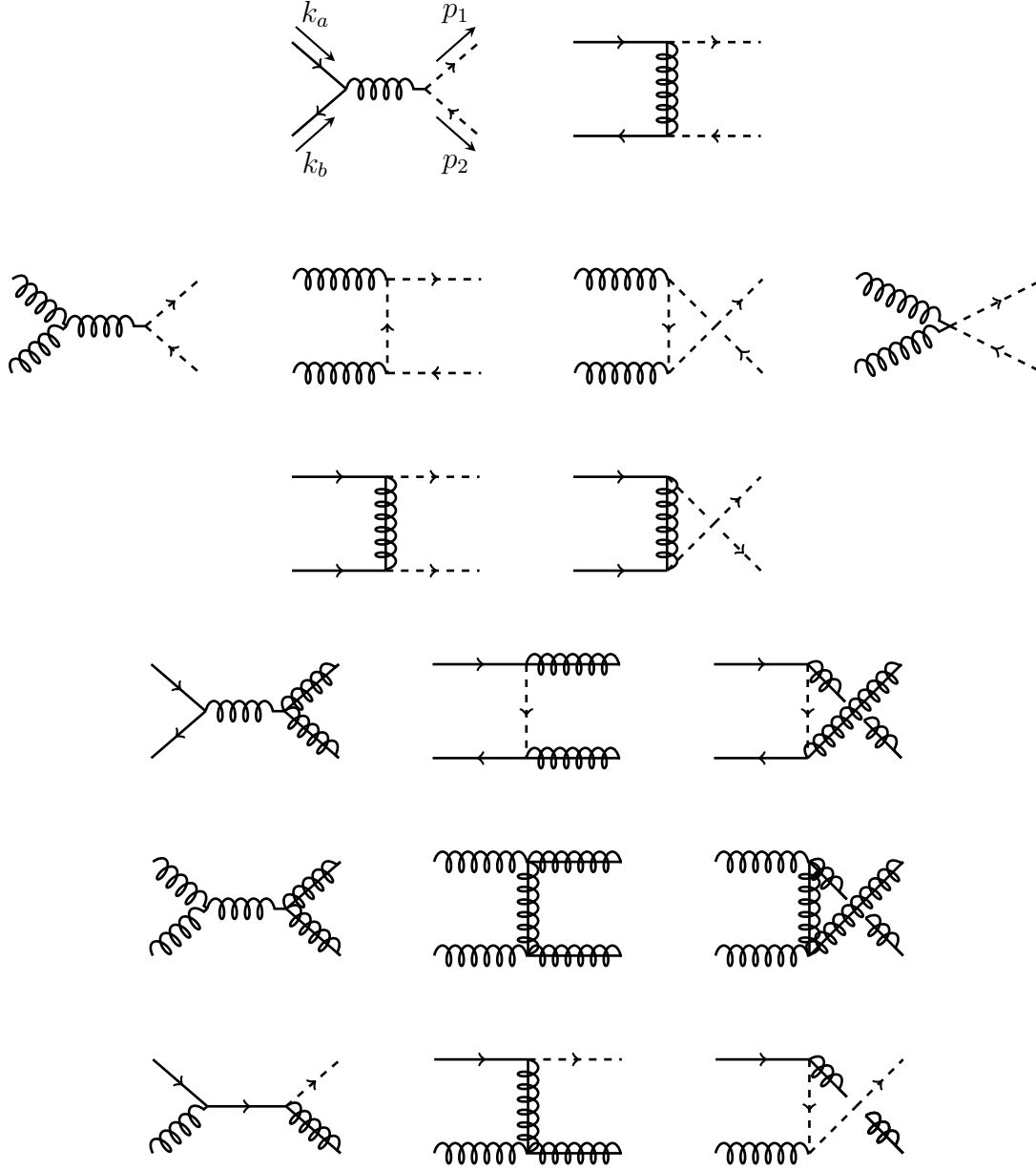


Figure 5.1: Tree level diagrams for squark and gluino production at tree level in the MRSSM. The processes $GG \rightarrow \tilde{q}\tilde{q}$ and $qG \rightarrow \tilde{q}\tilde{g}$ are identical to those in the MSSM. The processes $q\bar{q} \rightarrow \tilde{q}\tilde{q}$ and $qq \rightarrow \tilde{q}\tilde{q}$ involve the production of less chiralities than in the MSSM. Also in the $q\tilde{q} \rightarrow \tilde{g}\tilde{g}$ channel only half of the t-channel squark chiralities occur in the MRSSM. (Anti-)Gluino production via initial gluons $GG \rightarrow \tilde{g}\tilde{g}$ proceeds via the same diagrams like in the MSSM but its cross section is twice as much in the MRSSM for gluino and antigluino are distinguishable particles.

Using the Feynman rules in the Appendix 10.5 one obtains the following sums over absolute squared Feynman amplitudes.

$$\begin{aligned} \sum |\mathcal{M}^B|^2(q_i \bar{q}_j \rightarrow \tilde{q} \tilde{q}^\dagger) &= \delta_{ij} \left[8N_c C(F) g_s^4 \frac{(n_f - 1)}{s^2} + 4N_c C(F) \hat{g}_s^4 \frac{1}{t_{\tilde{g}}^2} - 8C(F) g_s^2 \hat{g}_s^2 \frac{1}{t_{\tilde{g}} s} \right] (tu - m_{\tilde{q}}^4) \\ &\quad + (1 - \delta_{ij}) 4N_c C(F) \hat{g}_s^4 \frac{tu - m_{\tilde{q}}^4}{t_{\tilde{g}}^2} \end{aligned} \quad (5.2)$$

$$\begin{aligned} \sum |\mathcal{M}^B|^2(GG \rightarrow \tilde{q} \tilde{q}^\dagger) &= 4(n_f - 1) g_s^4 \left[2N_c^2 C(F) \left(1 - 2 \frac{t_{\tilde{q}} u_{\tilde{q}}}{s^2} \right) - 2C(F) \right] \\ &\quad \left[1 - \epsilon - 2 \frac{s m_{\tilde{q}}^2}{t_{\tilde{q}} u_{\tilde{q}}} \left(1 - \frac{s m_{\tilde{q}}^2}{t_{\tilde{q}} u_{\tilde{q}}} \right) \right] \end{aligned} \quad (5.3)$$

$$\begin{aligned} \sum |\mathcal{M}^B|^2(q_i q_j \rightarrow \tilde{q} \tilde{q}) &= \delta_{ij} 2 \hat{g}_s^4 N_c C(F) \left[\frac{1}{t_{\tilde{g}}^2} + \frac{1}{u_{\tilde{g}}^2} \right] (tu - m_{\tilde{q}}^4) \\ &\quad + (1 - \delta_{ij}) 4 \hat{g}_s^4 N_c C(F) \frac{tu - m_{\tilde{q}}^4}{t_{\tilde{g}}^2} \end{aligned} \quad (5.4)$$

$$\begin{aligned} \sum |\mathcal{M}^B|^2(q \bar{q} \rightarrow \tilde{g} \tilde{g}) &= 8N_c^2 C(F) g_s^4 \left[\frac{2m_{\tilde{g}}^2 s + t_{\tilde{g}}^2 + u_{\tilde{g}}^2}{s^2} - \epsilon \right] \\ &\quad + 4N_c^2 C(F) g_s^2 \hat{g}_s^2 \left[\frac{m_{\tilde{g}}^2 s + t_{\tilde{g}}^2}{s t_{\tilde{q}}} + \frac{m_{\tilde{g}}^2 s + u_{\tilde{g}}^2}{s u_{\tilde{q}}} + \epsilon \left(\frac{t_{\tilde{g}}}{t_{\tilde{q}}} + \frac{u_{\tilde{g}}}{u_{\tilde{q}}} \right) \right] \\ &\quad + 2C(F) (N_c^2 - 1) \hat{g}_s^4 \left(\frac{t_{\tilde{g}}^2}{t_{\tilde{q}}^2} + \frac{u_{\tilde{g}}^2}{u_{\tilde{q}}^2} \right) \end{aligned} \quad (5.5)$$

$$\begin{aligned} \sum |\mathcal{M}^B|^2(GG \rightarrow \tilde{g} \tilde{g}) &= 16N_c^3 C(F) g_s^4 \left(1 - \frac{t_{\tilde{g}} u_{\tilde{g}}}{s^2} \right) \\ &\quad \left[\frac{s^2}{t_{\tilde{g}} u_{\tilde{g}}} (1 - \epsilon)^2 - 2(1 - \epsilon) + 4 \frac{m_{\tilde{g}}^2 s}{t_{\tilde{g}} u_{\tilde{g}}} \left(1 - \frac{m_{\tilde{g}}^2 s}{t_{\tilde{g}} u_{\tilde{g}}} \right) \right] \end{aligned} \quad (5.6)$$

$$\begin{aligned} \sum |\mathcal{M}^B|^2(qg \rightarrow \tilde{q} \tilde{g}) &= 2g_s^2 \hat{g}_s^2 \left[2N_c^2 C(F) \left(1 - 2 \frac{s u_{\tilde{q}}}{t_{\tilde{g}}^2} \right) - 2C(F) \right] \\ &\quad \left[(-1 + \epsilon) \frac{t_{\tilde{g}}}{s} + \frac{2(m_{\tilde{g}}^2 - m_{\tilde{q}}^2) t_{\tilde{g}}}{s u_{\tilde{q}}} \left(1 + \frac{m_{\tilde{q}}^2}{u_{\tilde{q}}} + \frac{m_{\tilde{g}}^2}{t_{\tilde{g}}} \right) \right] \end{aligned} \quad (5.7)$$

Having calculated the absolute squared Feynman amplitudes one obtains the partonic cross sections (see Appendix 10.7) via

$$\begin{aligned} \frac{d^2 \sigma^B}{dt du} &= \frac{K_{ab}}{s^2} \frac{\pi S_\epsilon}{\Gamma(1 - \epsilon)} \left[\frac{tu - m_1^2 m_2^2}{\mu^2 s} \right]^{-\epsilon} \Theta(tu - m_1^2 m_2^2) \\ &\quad \Theta(s - 4m^2) \delta(s + t + u - m_1^2 - m_2^2) \sum |\mathcal{M}^B|^2 \end{aligned} \quad (5.8)$$

where m_1 (m_2) is the mass of the first (second) final state particle and m is their arithmetic

mean. The leading order cross sections are

$$\begin{aligned}\sigma^B(q_i \bar{q}_j \rightarrow \tilde{q} \tilde{q}^\dagger) &= \delta_{ij} \frac{g_s^4}{16\pi s} (n_f - 1) \left[\frac{4}{27} - \frac{16m_{\tilde{q}}^2}{27s} \right] \\ &\quad + \delta_{ij} \frac{g_s^2 \hat{g}_s^2}{16\pi s} \left[\left(\frac{4}{27} + \frac{8m_-^2}{27s} \right) \beta_{\tilde{q}} + \left(\frac{8m_{\tilde{g}}^2}{27s} + \frac{8m_-^4}{27s^2} \right) L_1 \right] \\ &\quad + \frac{\hat{g}_s^4}{16\pi s} \left[-\frac{8}{9} \beta_{\tilde{q}} + \left(-\frac{4}{9} - \frac{8m_-^2}{9s} \right) L_1 \right]\end{aligned}\quad (5.9)$$

$$\sigma^B(GG \rightarrow \tilde{q} \tilde{q}^\dagger) = \frac{(n_f - 1)g_s^4}{16\pi s} \left[\left(\frac{5}{24} + \frac{31m_{\tilde{q}}^2}{12s} \right) \beta_{\tilde{q}} + \left(\frac{4m_{\tilde{q}}^2}{3s} + \frac{m_{\tilde{q}}^4}{3s^2} \right) \ln \frac{1 - \beta_{\tilde{q}}}{1 + \beta_{\tilde{q}}} \right] \quad (5.10)$$

$$\sigma^B(q_i q_j \rightarrow \tilde{q} \tilde{q}) = \frac{\hat{g}_s^4}{16\pi s} \left[-\frac{8}{9} \beta_{\tilde{q}} + \left(-\frac{4}{9} - \frac{8m_-^2}{9s} \right) L_1 \right] \quad (5.11)$$

$$\begin{aligned}\sigma^B(q\bar{q} \rightarrow \tilde{g} \tilde{g}) &= \frac{g_s^4}{16\pi s} \left[\frac{16}{9} + \frac{32m_{\tilde{g}}^2}{9s} \right] \beta_{\tilde{g}} \\ &\quad + \frac{\hat{g}_s^2 g_s^2}{16\pi s} \left[\left(-\frac{4}{3} - \frac{8m_-^2}{3s} \right) \beta_{\tilde{g}} + \left(\frac{8m_{\tilde{g}}^2}{3s} + \frac{8m_-^4}{3s^2} \right) L_2 \right] \\ &\quad + \frac{\hat{g}_s^4}{16\pi s} \left[\left(\frac{32}{27} + \frac{32m_-^4}{27(m_-^4 + m_{\tilde{q}}^2 s)} \right) \beta_{\tilde{g}} - \frac{64m_-^2}{27s} L_2 \right]\end{aligned}\quad (5.12)$$

$$\sigma^B(GG \rightarrow \tilde{g} \tilde{g}) = \frac{g_s^4}{16\pi s} \left[\left(-6 - \frac{51m_{\tilde{g}}^2}{2s} \right) \beta_{\tilde{g}} + \left(-\frac{9}{2} - \frac{18m_{\tilde{g}}^2}{s} + \frac{18m_{\tilde{g}}^4}{s^2} \right) \ln \frac{1 - \beta_{\tilde{g}}}{1 + \beta_{\tilde{g}}} \right] \quad (5.13)$$

$$\begin{aligned}\sigma^B(qG \rightarrow \tilde{q} \tilde{g}) &= \frac{g_s^2 \hat{g}_s^2}{16\pi s} \left[\frac{\kappa}{s} \left(-\frac{7}{9} - \frac{32m_-^2}{9s} \right) + \left(-\frac{8m_-^2}{9s} + \frac{2m_{\tilde{q}}^2 m_-^2}{s^2} + \frac{8m_-^4}{9s^2} \right) L_3 \right. \\ &\quad \left. + \left(-1 - \frac{2m_-^2}{s} + \frac{2m_{\tilde{q}} m_-^2}{s^2} \right) L_4 \right]\end{aligned}\quad (5.14)$$

where the abbreviations [16]

$$\begin{aligned}\beta_{\tilde{q}} &= \sqrt{1 - \frac{4m_{\tilde{q}}^2}{s}} & \beta_{\tilde{g}} &= \sqrt{1 - \frac{4m_{\tilde{g}}^2}{s}} \\ m_-^2 &= m_{\tilde{g}}^2 - m_{\tilde{q}}^2 & \kappa &= \sqrt{(s - m_{\tilde{g}}^2 - m_{\tilde{q}}^2)^2 - 4m_{\tilde{g}}^2 m_{\tilde{q}}^2} \\ L_1 &= \ln \frac{s + 2m_-^2 - s\beta_{\tilde{q}}}{s + 2m_-^2 + s\beta_{\tilde{q}}} & L_2 &= \ln \frac{s - 2m_-^2 - s\beta_{\tilde{g}}}{s - 2m_-^2 + s\beta_{\tilde{g}}} \\ L_3 &= \ln \frac{s - m_-^2 - \kappa}{s - m_-^2 + \kappa} & L_4 &= \ln \frac{s + m_-^2 - \kappa}{s + m_-^2 + \kappa}\end{aligned}\quad (5.15)$$

are used. In the following the considered processes of the MRSSM are compared to those of the MSSM.

The process $q_i \bar{q}_j \rightarrow \tilde{q} \tilde{q}^\dagger$

The production of a squark and an antisquark through a quark and an antiquark in the initial state originates from two types of Feynman diagrams. The first one has an s -channel gluon and is the same in the MSSM and in the MRSSM. The second one exhibits a difference due to the t -channel gluino which is no Majorana particle in the MRSSM. To see this one can either



Figure 5.2: Tree level diagrams for $q\bar{q} \rightarrow \tilde{q}\tilde{q}^\dagger$

just apply the Feynman rules in Appendix 10.5 or think of the conservation of R-charge: Left handed squarks have R-charge +1 and right handed squarks have R-charge -1. Antiparticles have the opposite R-charge of their corresponding particles. The final state particles have to meet the total R-charge zero from the initial state. Because of this one only has $\tilde{q}_L \bar{\tilde{q}}_L$ and $\tilde{q}_R \bar{\tilde{q}}_R$ as the final states in the MRSSM whereas in the MSSM one actually has four instead of two t-channel diagrams: The corresponding final states are $\tilde{q}_L \bar{\tilde{q}}_L$, $\tilde{q}_R \bar{\tilde{q}}_R$, $\tilde{q}_L \bar{\tilde{q}}_R$ and $\tilde{q}_R \bar{\tilde{q}}_L$. Consequently contributions from the t -channel diagrams are suppressed in the MRSSM in comparison to the MSSM. As visible in fig. 5.5 this suppression grows with the masses. The reason for this lies in the gluino mass dependence of the t -channel diagrams which is explained in the discussion of squark production.

If the initial state quarks are of different flavor the s -channel diagram is absent.

The process $GG \rightarrow \tilde{q}\tilde{q}^\dagger$

This process has the same cross section as in the MSSM for also in the MSSM only like chirality squark and antisquark $\tilde{q}_A \bar{\tilde{q}}_A^\dagger$ with $A \in L, R$ can be produced.

The process $q_i q_j \rightarrow \tilde{q}\tilde{q}$

In the MRSSM only the production of unlike chirality squarks $\tilde{q}_L \tilde{q}_R$ is allowed whilst in the MSSM also like chirality squarks can be produced. This is again a consequence of the conservation of R-charge. The upshot of this is a suppression of squark production in the MRSSM in comparison to the MSSM. To be more explicit the suppression of squark production in the MRSSM grows with the gluino mass. This can be understood as follows: As in the MRSSM a left handed squark needs to be produced with a right handed squark one can read off from the Feynman rules given in Appendix 10.5 that the gluino propagator $i \frac{\not{p} + m_{\tilde{g}}}{p^2 - m_{\tilde{g}}^2}$ is sandwiched between the projectors P_L and P_R which leads to the cancellation of the gluino mass in the numerator. Therefore for small momenta of the gluino compared to the gluino mass one gets $\mathcal{M} \sim \frac{1}{m_{\tilde{g}}^2}$ in the MRSSM while in the MSSM one finds a suppression proportional to $\frac{1}{m_{\tilde{g}}}$.

When considering squark production one has to sum over all $|\mathcal{M}|^2$ with different helicity. The diagrams for those different final state helicities are shown for flavor like squark production in tab. 5.1 and for flavor unlike squark production in tab. 5.2 for the MSSM and the MRSSM. To avoid double counting one needs to weight $|\mathcal{M}|^2(qq \rightarrow \tilde{q}_L \tilde{q}_L)$ and $|\mathcal{M}|^2(qq \rightarrow \tilde{q}_R \tilde{q}_R)$ with a statistical factor of $\frac{1}{2}$ as one integrates over all momenta of both particles to arrive at the cross section.

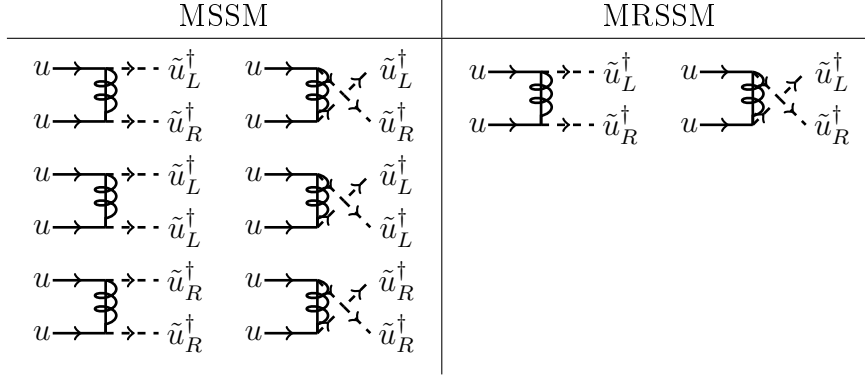


Table 5.1: All Feynman diagrams contributing to flavor like squark production in the MSSM and the MRSSM for the example of u -quarks. For the MSSM the absolute squared Feynman amplitudes from the diagrams with chirality like squarks need to be weighted with a factor of $\frac{1}{2}$.

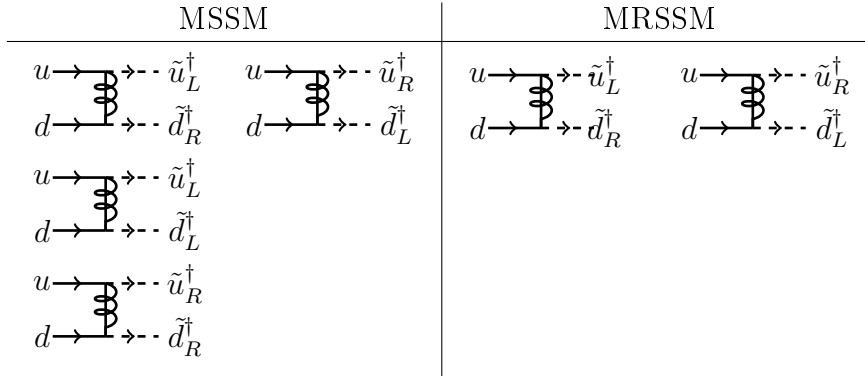


Table 5.2: All Feynman diagrams contributing to flavor unlike squark production in the MSSM and the MRSSM for the example of u - and d -quarks.

Because of the absence of chirality like squarks in the final state in the MRSSM (and a missing interference of the two diagrams in tab. 5.1 in the column of the MRSSM) the partonic cross section of flavor like and unlike squarks is the same in the MRSSM, i.e. on the partonic level:

$$\sigma_{\text{Part, MRSSM}}^{\text{B}}(uu \rightarrow \tilde{u}_L \tilde{u}_R) = \sigma_{\text{Part, MRSSM}}^{\text{B}}(ud \rightarrow \tilde{u}_L \tilde{d}_R) + \sigma_{\text{Part, MRSSM}}^{\text{B}}(ud \rightarrow \tilde{u}_R \tilde{d}_L). \quad (5.16)$$

That is however not true in the MSSM because for flavor like squarks there is a non vanishing interference of the t - and u -channel diagram of the processes $qq \rightarrow \tilde{q}_L \tilde{q}_L$ and $qq \rightarrow \tilde{q}_R \tilde{q}_R$. This

term is given in [16, p.7]

The process $q\bar{q} \rightarrow \tilde{g}\tilde{g}$

In contrast to the MSSM no statistical factor of $\frac{1}{2}$ is taken into account when turning from $|\mathcal{M}|^2$ to σ . This is because gluino and antigluino are distinguishable particles. Still in comparison to the MSSM cross section [16, p.9] only the first line in 5.12 is doubled up as the other two lines originate from an t or u channel squark which occurs in only one instead of two chiralities. Furthermore an interference term from the t and u channel diagram which occurs in the MSSM is absent in the MRSSM.

The process $GG \rightarrow \tilde{g}\tilde{g}$

As in the previous process the MRSSM cross section for $GG \rightarrow \tilde{g}\tilde{g}$ receives no statistical factor of $\frac{1}{2}$ like in the MSSM. As there are no further differences between MSSM and MRSSM in this channel, the MRSSM cross section is simply twice as large as in the MSSM.

The process $qG \rightarrow \tilde{q}\tilde{g}$

This process is exactly the same in the MSSM and MRSSM.

In order to account for the confinement of quarks and gluons within hadrons the hadronic cross sections for the considered processes are calculated in the next subsection.

5.2 Hadronic Cross Section

Quarks, antiquarks and gluons are no free particles but are confined within hadrons. As hadrons consist of a variety of the just mentioned partons which share the hadron's momentum one does not have a definite initial state in hadron collisions which is assumed in the previous subsection. Fortunately the hadronic cross section for the production of a final state X , e.g. $X = \tilde{q}\tilde{q}$, can be obtained by convolving the partonic cross section with parton density functions of the initial hadrons.

$$\sigma_{\text{Had}}^{\text{B}}(P_1 P_2 \rightarrow X) = \int dx_1 dx_2 f_{P_1/H_1}(x_1) f_{P_2/H_2}(x_2) \sigma_{\text{Part}}^{\text{B}}(P_1 P_2 \rightarrow X, s = x_1 x_2 S). \quad (5.17)$$

The parton density functions $f_{P_i/H_j}(x)$ and the momentum fractions x_i are explained below. The hadrons center-of-mass energy is denoted with \sqrt{S} where \sqrt{s} denotes the partons center-of-mass energy.

As the production of the final state X may proceed via various initial partons one has to sum

over all possible possibilities arising from the initial hadrons H_1 and H_2 :

$$\sigma_{\text{Had}}^B(H_1 H_2 \rightarrow X) = \sum_{i,j} \sigma_{\text{Had}}^B(P_i P_j \rightarrow X) \quad (5.18)$$

where the sum runs over all partons P_i (P_j) which are in the hadron H_1 (H_2).

To get an intuitive idea of this factorization regard the hadrons as extended objects consisting of partons¹³ which are permanently interacting with each other. Now consider two colliding hadrons in their center-of-mass frame. Due to Lorentz contraction the hadrons appear as thin discs and the parton's mutual interactions are time-delayed within this frame. This effectively means that a hadron at the time of collision is virtually frozen.

maybe picture of colliding disks

This in turn implies that the hadron consists at the time of collision of a definite number of partons which can be thought of as carrying a definite fraction of the hadron's momentum $p_{\text{Part}} = x p_{\text{Had}}$ with $x \in (0, 1)$. The parton density function $f_{P/H}(x)$ can therefore be understood as the probability of finding a parton P within the hadron H carrying x of its momentum.

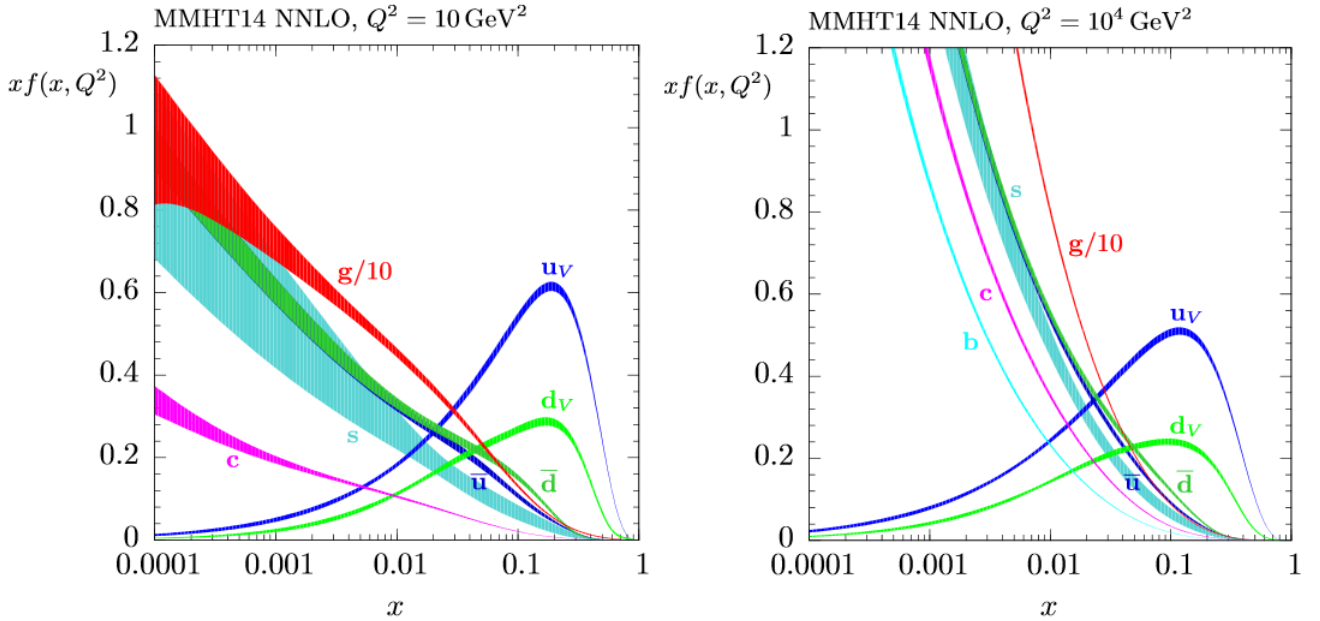


Figure 5.3: Parton density function of the proton, taken from MMHT2014 [17] with 68% confidence level. The parton density function is multiplied by x in order to counteract its peak at $x \rightarrow 0$. The parton density function is given at two different factorisation scales $\mu_F = Q$

They actually depend on an arbitrary energy scale referred to as the factorization scale μ_F . The μ_F evolution is given within the scope of perturbation theory by coupled integro-

¹³The proton is considered as composed of three valence quarks: Two up-quarks and one down-quark. In addition there are gluons and seaquarks, i.e. virtual quark-antiquark pairs.

differential equations named after Gribov, Lipatov, Dokshitzer, Altarelli and Parisi: the DGLAP-equations. For further reading on parton density functions and factorization see [18] and [19]. See [20] for how to determine parton density functions.

Fig. 5.3 shows a parton density function set for the proton. One can see that the partons most probable to carry a high fraction of momentum are the valence quarks. For lower values of x gluons constitute the major component of the proton.

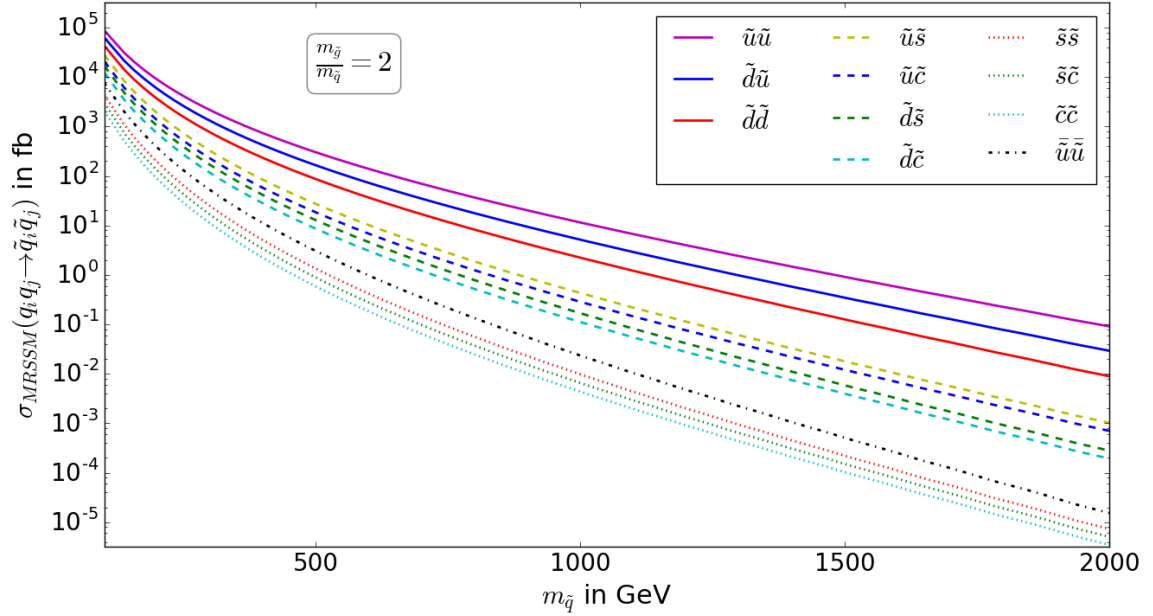


Figure 5.4: Hadronic cross section for squark production in the MRSSM at the LHC at $\sqrt{S} = 13 \text{ GeV}$. The ratio of the gluino and squark mass is fixed to 2. The parton densities used are MMHT2014 LO with $\alpha_s(M_Z) = 0.135$ in the 5-flavor scheme [17]. As renormalization and factorization scale $\mu_R = \mu_F = \frac{m_1 + m_2}{2}$ has been chosen, where m_i are the final state particle masses.

Fig.5.5 shows the hadronic cross section for the production of various squarks in the MRSSM. These can only be produced by their non supersymmetric partner, e.g. two up-squarks can only be produced by two up-quarks. Because the partonic cross section for these processes are the same, cf. eq. 5.16, one can see the influence of the parton density functions quite nicely: The up-squark production is the dominant contribution to squark production. Apart from the solid lines in fig.5.5 which correspond to the production of first generation squarks, also the cross section of mixed first and second generation (dashed lines) and second generation (dotted lines) squarks is shown. The dashed dotted line shows the cross section of the charged conjugated particles of the dominant channel.

REFER TO Kribs, Martin: SNOWMASS WHITEPAPER

REFER TO Vernoica Sanz: How many SUPersymmetries?

The following paragraph discusses fig. 5.5, 5.6 and 5.7, i.e. the hadronic cross section of all considered processes for three successive mass ratios of the gluino and squark: $\frac{m_{\tilde{g}}}{m_{\tilde{q}}} = 0.9$, 2 and 5. Also the corresponding fraction of final states is shown.

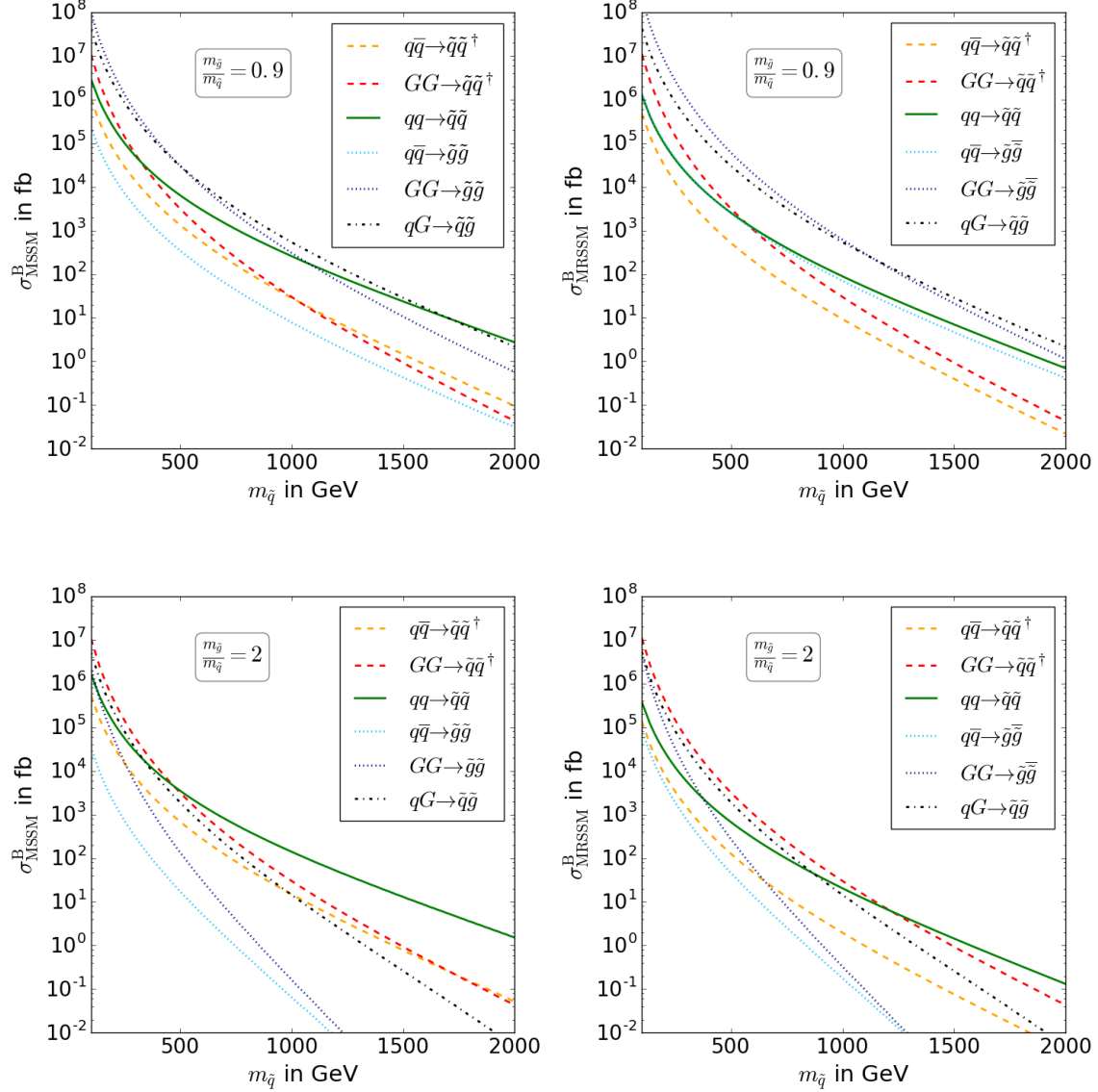


Figure 5.5: Hadronic cross section for squark and gluino production in the MSSM (left-hand side) and MRSSM (right-hand side) at the LHC with $\sqrt{S} = 13$ GeV. The ratio of gluino and squark mass is fixed to 0.9 (first row) and 2 (second row). In the final state it has been summed over all squark flavors except for t -squarks. For the channels $qq \rightarrow \tilde{q}\tilde{q}$ and $qG \rightarrow \tilde{q}\tilde{G}$ also the charge conjugated process is included. The parton densities used are MMHT2014 LO with $\alpha_s(M_Z) = 0.135$ in the 5-flavor scheme [17]. As renormalization and factorization scale $\mu_R = \mu_F = \frac{m_1 + m_2}{2}$ has been chosen, where m_i are the final state particle masses.

For the small mass ratio $\frac{m_{\tilde{g}}}{m_{\tilde{q}}} = 0.9$ and small squark masses the dominant contribution comes

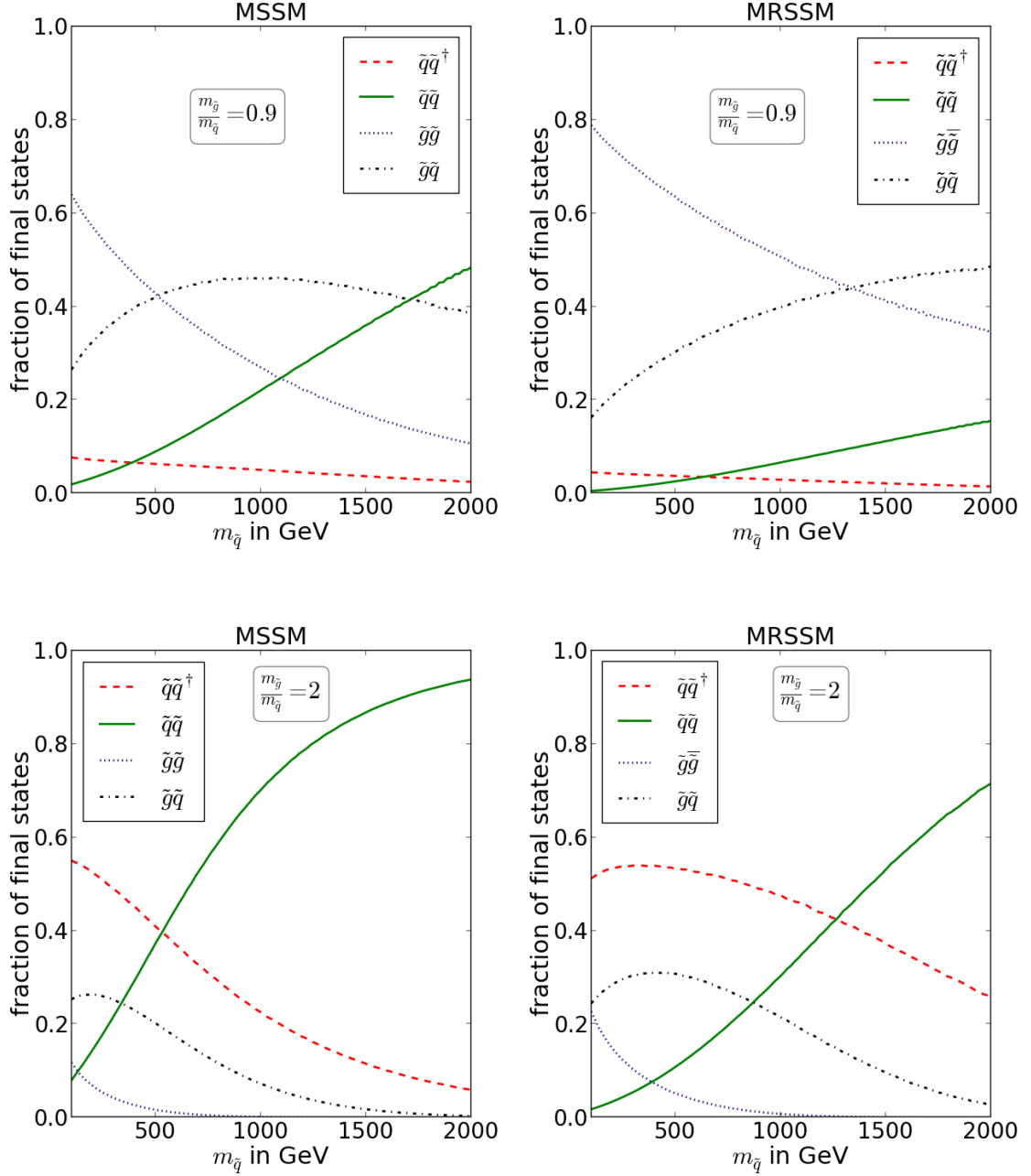


Figure 5.6: Relative contributions of the indicated final states on the total hadronic cross section in the MSSM (left-hand side) and MRSSM (right-hand side) at the LHC with $\sqrt{S} = 13$ GeV. The ratio of gluino and squark mass is fixed to 0.9 (first row) and 2 (second row). In the final state it has been summed over all squark flavors except for t -quarks. For the channels $qq \rightarrow \tilde{q}\tilde{q}$ and $qG \rightarrow \tilde{q}\tilde{G}$ also the charge conjugated process is included. The parton densities and the renormalization and factorization scale are chosen as in fig. 5.5.

from gluino (antigluino) production. This is even more dominant in the MRSSM which can be explained by the above mentioned factor of 2 difference in the $GG \rightarrow \tilde{g}\tilde{g}(\tilde{g})$ channel which comes from the distinguishable gluino and antigluino in the MRSSM. Furthermore there is the above mentioned destructive interference term in the $q\bar{q} \rightarrow \tilde{g}\tilde{g}(\tilde{g})$ channel which makes the cross section in the MRSSM dominant over the one in the MSSM.

For a growing squark mass the previously subdominant gluino-squark production takes over and becomes dominant. A salient difference between the MSSM and the MRSSM is that squark production is strongly suppressed in the MRSSM. While in the MSSM it becomes dominant above about 1700 GeV it is subsubdominant for the whole displayed squark mass in the MRSSM. This suppression has also already been explained above.

Turning from $\frac{m_{\tilde{g}}}{m_{\tilde{q}}} = 0.9$ to $\frac{m_{\tilde{g}}}{m_{\tilde{q}}} = 2$ suppresses quite strongly the production of gluinos in all pertaining channels. For the MSSM one finds above 500 GeV a growing dominance of squark production. The same happens in the MRSSM but for a significantly higher squark mass of about 1300 GeV. This suppression of squark production in the MRSSM increases with a growing gluino masses which can be seen when going from $\frac{m_{\tilde{g}}}{m_{\tilde{q}}} = 0.9$ to $\frac{m_{\tilde{g}}}{m_{\tilde{q}}} = 2$ or even $\frac{m_{\tilde{g}}}{m_{\tilde{q}}} = 5$ in fig. 5.7. This reflects the gluino mass dependence explained in detail in section 5.1. See also ?? for a visualization of this behavior.

Note also that for sufficiently large squark masses squark production becomes the dominant process, see fig. 5.5 and 5.6. This is because the production of heavy particles requires large longitudinal momenta of the colliding partons, i.e. large x . Looking at the parton density functions in fig. 5.3 one sees that within the proton the partons most likely to carry large momentum are quarks. So looking at large x the proton basically consists of quarks and because the only process involving only quarks in the initial state is squark production, this channel dominates for high masses.

The total cross section in the MRSSM is increasingly smaller than in the MSSM in particular from about 500 GeV onwards. The is because for masses below that the $GG \rightarrow \tilde{q}\tilde{q}^\dagger$ channel which is the same for both models is the dominant one.

When raising the gluino squark mass ratio further to $\frac{m_{\tilde{g}}}{m_{\tilde{q}}} = 5$ the above described tendency continues. This is all processes including a gluino get even more negligible and squark production gets further suppressed. While in the MSSM it becomes dominant over $GG \rightarrow \tilde{q}\tilde{q}^\dagger$ at $m_{\tilde{q}} \approx 1000$ GeV it is subdominant in the MRSSM in the whole displayed mass range. even though it does not fall that steeply as the dominant channel.

The following contour plots underline the already announced difference between squark production in the MRSSM and the MSSM. The main difference is a suppression of the cross section for higher gluino masses in the MRSSM.

As a summary of the comparison between MSSM and MRSSM gluino production one can say, that the gluino production is enhanced in the MRSSM due to distinguishable gluino and

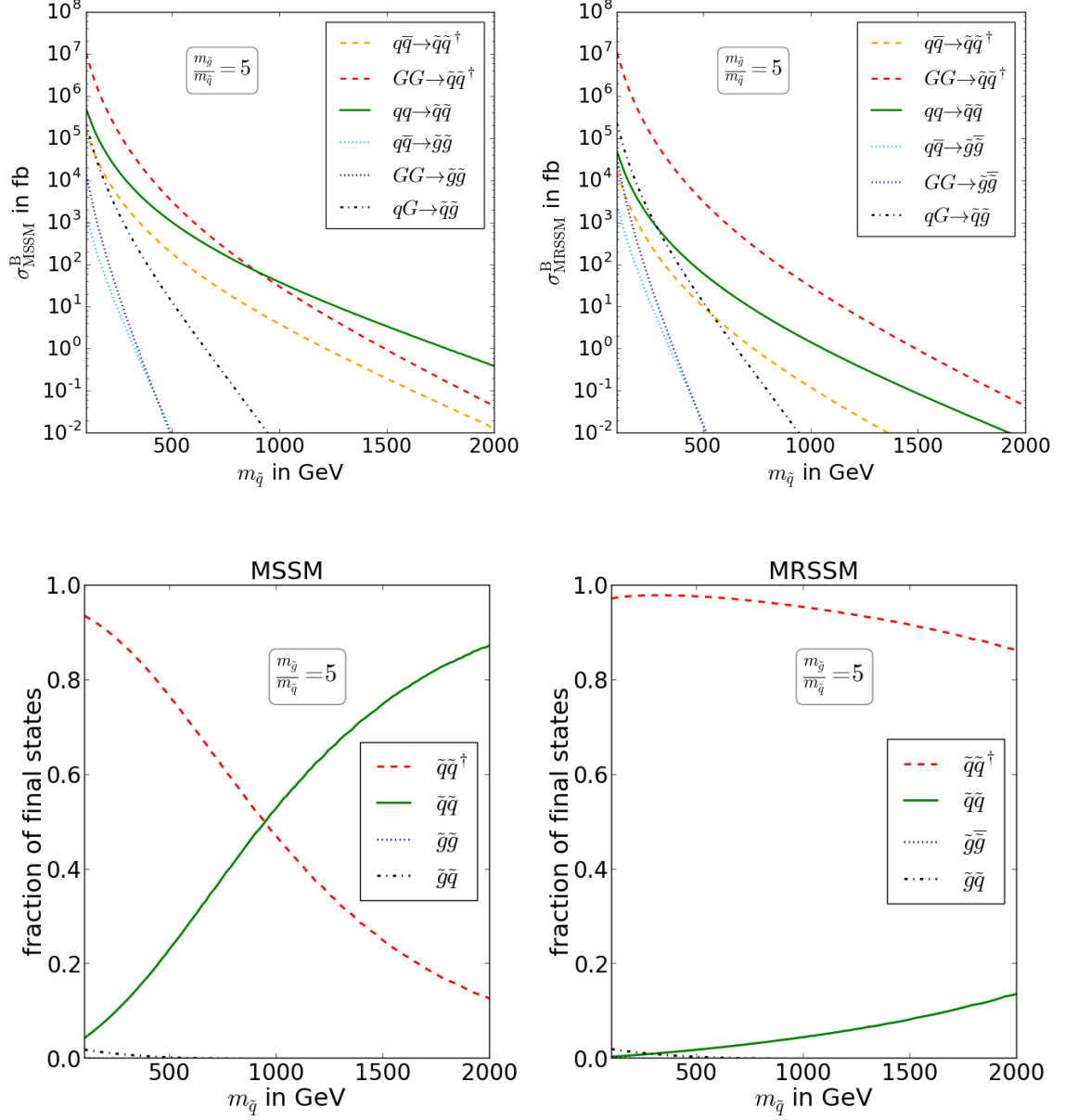


Figure 5.7: Hadronic cross section for squark and gluino production (in the first row) and relative contributions of the indicated final states on the total hadronic cross section (in the second row) in the MSSM (left-hand side) and MRSSM (right-hand side) at the LHC which $\sqrt{S} = 13$ GeV. The ratio of gluino and squark mass is fixed to 5. In the final state it has been summed over all squark flavors expect for staus. For the channels $q\bar{q} \rightarrow \tilde{q}\tilde{q}$ and $q\bar{G} \rightarrow \tilde{q}\tilde{G}$ also the charge conjugated process is included. The parton densities and the renormalization and factorization scale are chosen as in fig. 5.5.

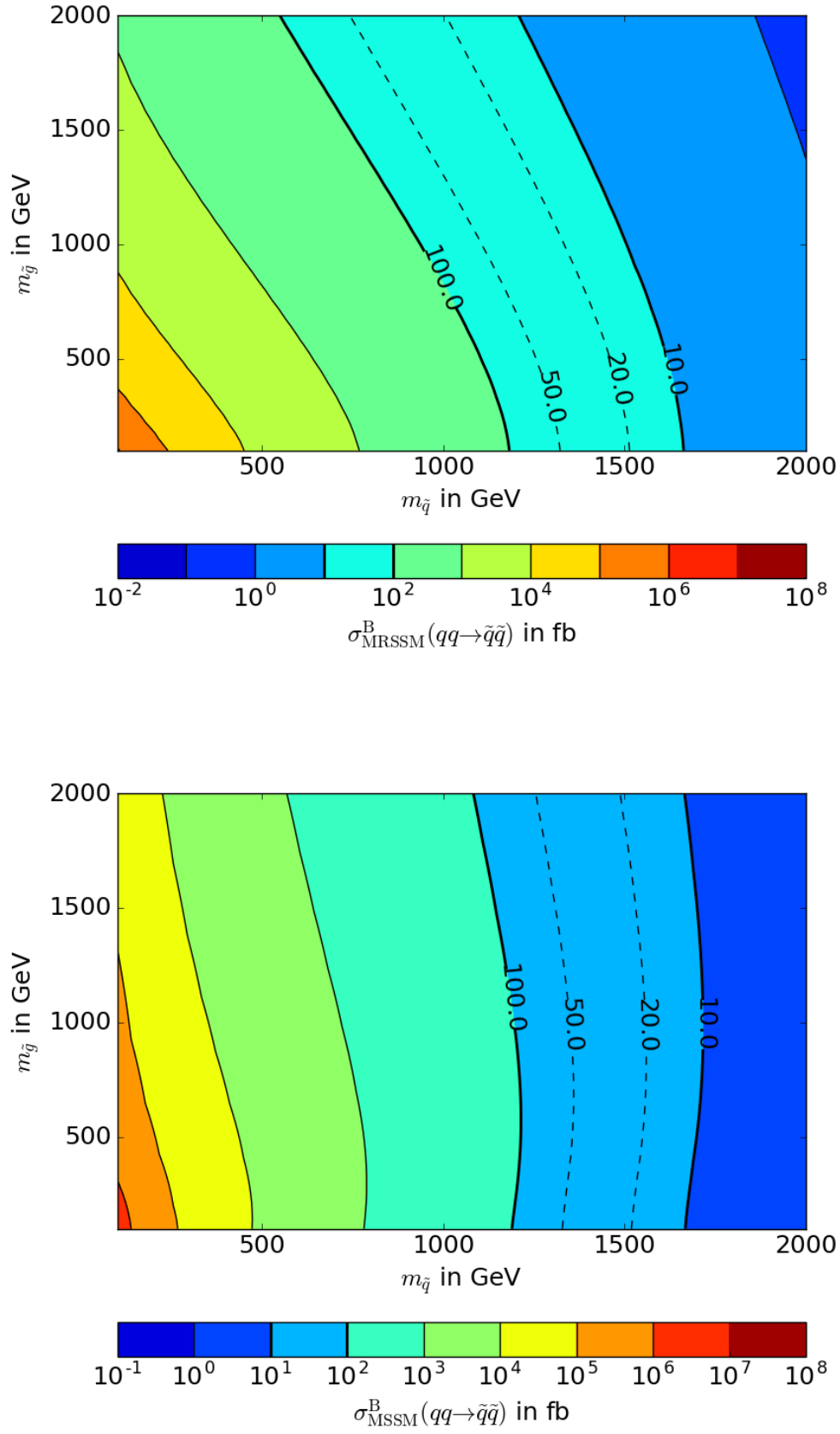


Figure 5.8

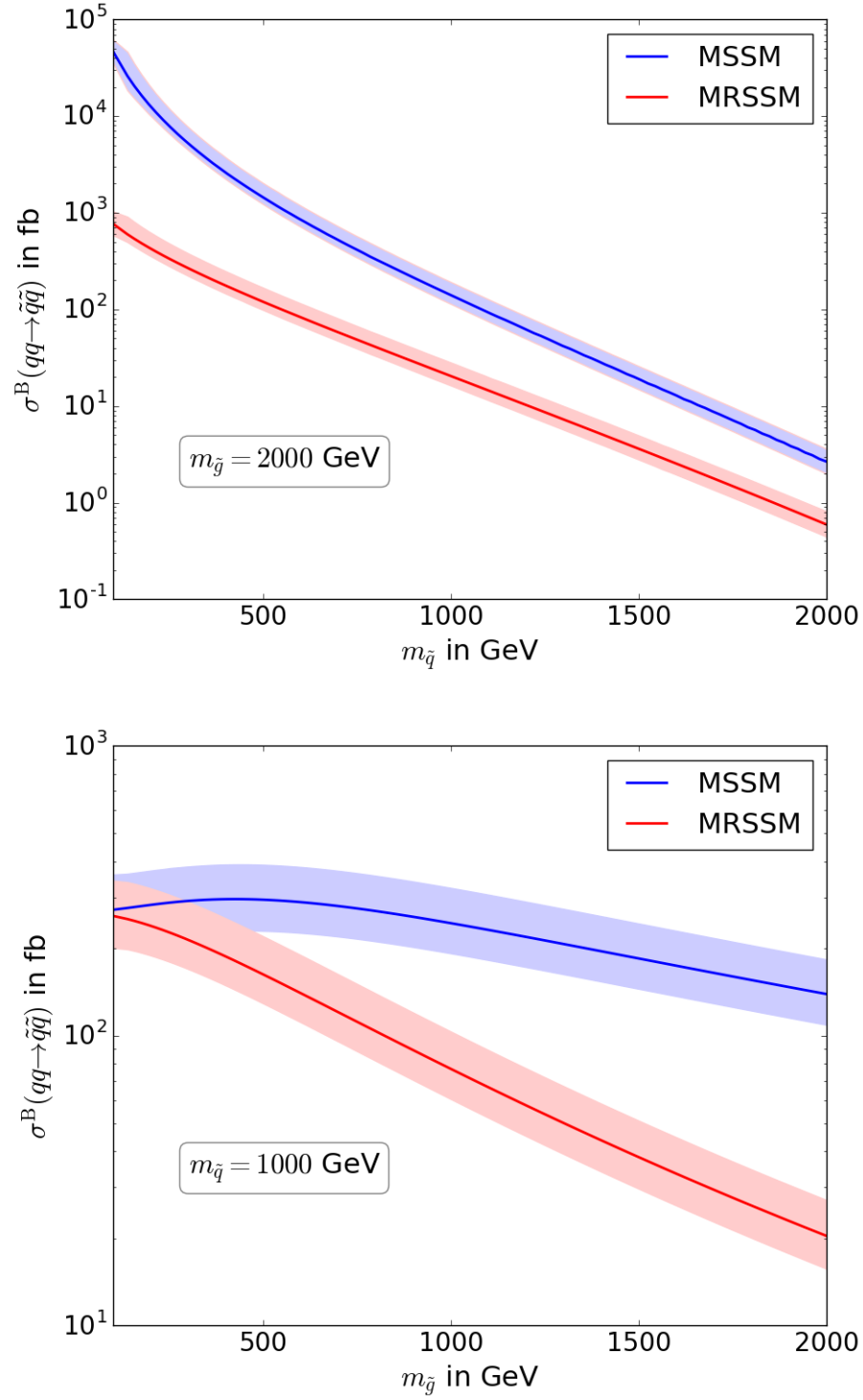


Figure 5.9: add error bars
??

antigluino. In order to meet missing experimental evidence for supersymmetry this suggests that gluinos might be heavier than squarks in the MRSSM. Focusing on $\frac{m_{\tilde{g}}}{m_{\tilde{q}}} \geq 2$ the most significant change between the considered models is the growing suppression of squark production for an increasing gluino mass. This is why this channel is going to be investigated at next-to-leading order in the ensuing sections.

6 Virtual and Real Corrections

The results calculated in the previous chapter are not the full theoretical predictions for the different processes but only the first term in a perturbation theory of α_s .

This section describes the necessary steps in the calculation of the squark production cross section at next-to-leading-order, i.e. its $\mathcal{O}(\alpha_s)$ -correction.

Reason validity of perturbation theory in this context.

6.1 Virtual Correction

According to quantum field theory the $\mathcal{O}(\alpha_s)$ correction to a tree level process includes the computation of one-loop diagrams such as shown in fig. 6.1. To yield $\mathcal{O}(\alpha_s)$ corrections in the cross section the interference term between the one-loop amplitude \mathcal{M}^{1L} and the Born amplitude \mathcal{M}^B needs to be considered. However the virtual amplitude

$$\mathcal{M}^V = \mathcal{M}^B \mathcal{M}^{1L*} + \mathcal{M}^{1L} \mathcal{M}^{B*} = 2\Re(\mathcal{M}^B \mathcal{M}^{1L*}) \quad (6.1)$$

contains divergences. These come from integrals over undetermined momentum and energy of particles running in loops. Due to their origin these divergences are referred to as ultra-

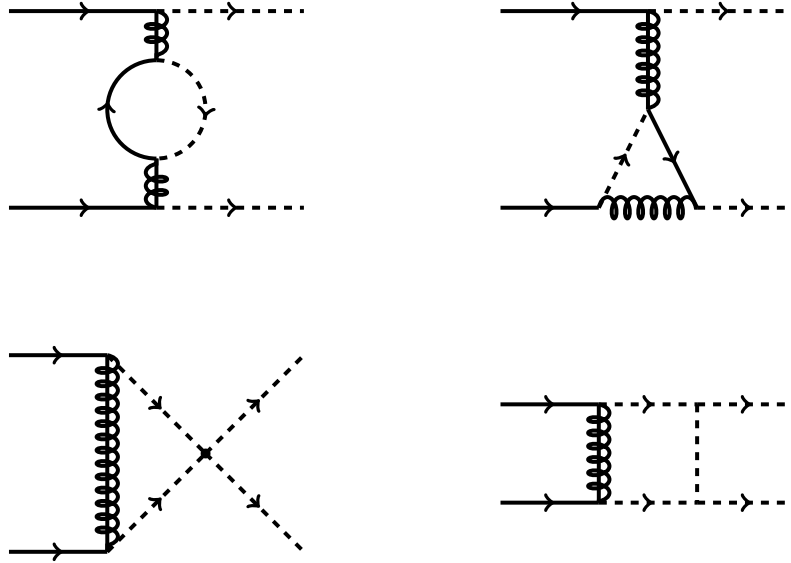


Figure 6.1: A selection of diagrams contributing to the 1-loop matrix element for squark production. Each diagram is a representative of a certain diagram type. In the first line an example for a self-energy and a vertex-correction diagram is shown. The second line lists typical box-diagrams: a three-point box and a four-point box.

violet and infrared divergences. Ultraviolet divergences occur when the loop momenta and energy tend to infinity which corresponds to arbitrary short distance interactions. However, these divergences are cured by first regularizing them and then introducing appropriate coun-

terterms¹⁴ in the Lagrangian to cancel the extracted singularities. The second step is called renormalization and can be understood as a redefinition or rescaling of parameters and fields in the Lagrangian in the first place:

$$\begin{aligned} \phi^0/\sigma^0 &\rightarrow \sqrt{Z_{\phi^0/\sigma^0}} \phi^0/\sigma^0 & \tilde{q}_{L/R} &\rightarrow \sqrt{Z_{\tilde{q}_{L/R}}} \tilde{q}_{L/R} \\ P_L \tilde{g} &\rightarrow \sqrt{Z_{\tilde{g}}^L} P_L \tilde{g} & P_R \tilde{g} &\rightarrow \sqrt{Z_{\tilde{g}}^R} P_R \tilde{g} \\ q &\rightarrow \sqrt{Z_q} q & G_\mu &\rightarrow \sqrt{Z_G} G_\mu \end{aligned} \quad (6.2)$$

$$\begin{aligned} g_s &\rightarrow g_s \text{ bare} & m_{\tilde{q}}^2 &\rightarrow m_{\tilde{q}}^2 \text{ bare} \\ m_\sigma^2 &\rightarrow m_\sigma^2 \text{ bare} & m_{\tilde{g}} &\rightarrow m_{\tilde{g}} \text{ bare} \end{aligned} \quad (6.3)$$

In this thesis the computation is performed in $D = 4 - 2\epsilon$ dimensions in order to regularize it. Ultraviolet divergences show then up as single poles in ϵ . This procedure will be discussed in detail in section 7 and 8.1.

Having removed the ultraviolet divergences the matrix element is not free of divergences as it comprises infrared divergences. These split into soft and collinear (or mass) singularities¹⁵ which cannot be removed by means of renormalization. These additional singularities show up as single and double poles of ϵ in the matrix element \mathcal{M}^{1L} and the virtual cross section which is obtained after performing the 2-body phase space integration as in eq. 5.8 but over $|\mathcal{M}^{\text{V}}|^2$:

$$\begin{aligned} \frac{d^2\sigma^{\text{V}}}{dt du} &= \frac{K_{ab}}{s^2} \frac{\pi S_\epsilon}{\Gamma(1-\epsilon)} \left[\frac{tu - m_1^2 m_2^2}{\mu^2 s} \right]^{-\epsilon} \Theta(tu - m_1^2 m_2^2) \\ &\quad \Theta(s - 4m^2) \delta(s + t + u - m_1^2 - m_2^2) \sum |\mathcal{M}^{\text{V}}|^2. \end{aligned} \quad (6.4)$$

The single poles correspond to soft or collinear divergences whereas the double poles correspond to the coincidence of soft and collinear divergences.

6.2 Real Corrections

A crucial thing to recognize in the calculation of the $\mathcal{O}(\alpha_s)$ correction to the squark production cross section is that not only virtual corrections but also real corrections give rise to this physical observable. This is because one does not measure the final state partons but the jets in which they hadronize in due to confinement. This means that a radiation of a massless particle whose energy tends to zero or the radiation of a particle which is collinear to one of the final state particles is in experiment measured as a two jet event even though there are three particles in the final state of the calculation. However real corrections also contain divergences. Including these contributions to the cross section causes the cancellation of singles

¹⁴These counterterms have to be of the same $\mathcal{O}(\hbar)$ as the loop diagrams they are constructed to cancel.
NOCHMAL IN LAHIRI / PAL NACHSCHAUEN.

¹⁵The names differ in the literature. Often infrared divergences are used as a synonym for soft divergences.

poles coming from soft divergences and the cancellation of double poles. At this point the only singularities which are left in the cross section are the collinear ones.

To see how these are removed consider diagram the second digram in fig. 6.3. The propagator of the quark which radiates off a gluon is giving a contribution of the form

$$\frac{1}{(p_q + p_g)^2 - m_q^2} = \frac{1}{p_q \cdot p_g} = \frac{1}{2E_q E_g (1 - \beta_q \cos \theta_{qg})} \quad \text{with } \beta_q = \frac{\vec{p}_q}{E_q} \quad (6.5)$$

to the the diagram in question. Where p_q, p_g (E_q, E_g) are the quark's and gluon's four-momentum (energy) and θ_{qg} is the angle between the quark's and gluon's three-momentum. One observes two potentially singular limits

$$\text{soft gluon :} \quad E_g \rightarrow 0 \quad (6.6)$$

$$\text{collinear particles :} \quad \theta_{qg} \rightarrow 0 \quad \text{if } m_q \rightarrow 0. \quad (6.7)$$

Within these limits the inner quark can almost be considered as on-shell which means that it may travel a long distance between the emission of a gluon and taking part in the actual interaction. This suggest that some divergences may come from the incoming hadron and are actually not associated with the interaction. In fact this turns out to be the case: The remaining collinear divergences can be absorbed in to a redefinition of the parton density functions. This procedure is referred to as mass factorization. Figure 6.2 summarizes the required steps to render the next-to-leading-order cross section finite.

In fact the Kinoshita-Lee-Naunberg-Theorem [21], [22] guarantees the finiteness of sufficiently inclusive observables.

6.2.1 Real Gluon Radiation

Representative Feynman-diagrams for real gluon emission are shown in fig. 6.3. In order to extract the singularities the so called two-cut method has been adopted. This is the phase space has been divided into different regimes: a soft part, a hard collinear part and a hard non-collinear part.

In the soft part the energy of the outgoing gluon is only integrated up to $\delta_s \frac{\sqrt{s}}{2}$ where δ_s is a cut on which the final result must not depend on.

6.2.2 Real Quark Radiation

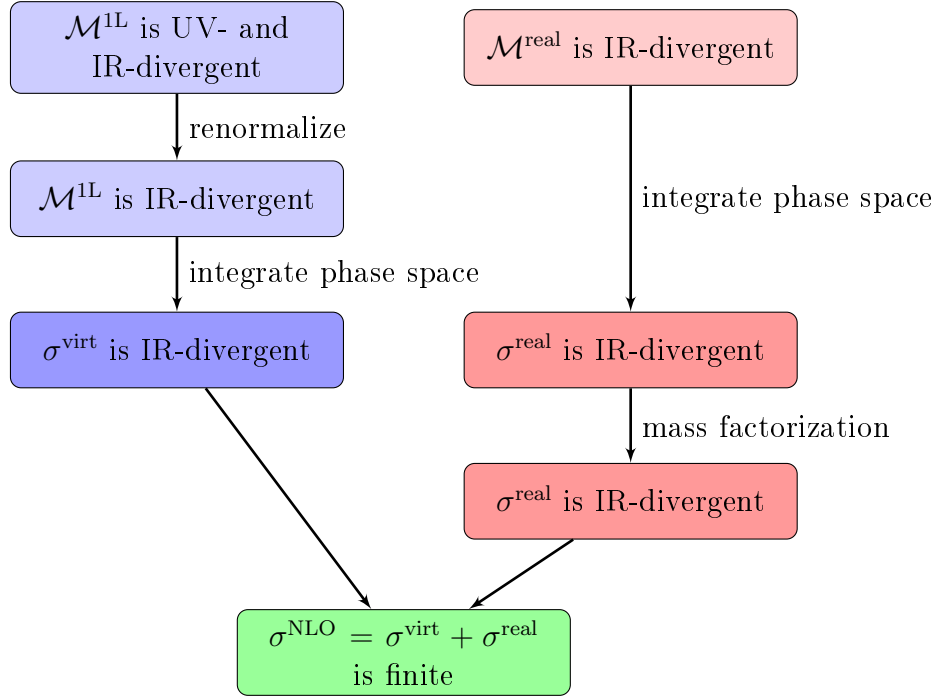


Figure 6.2: This scheme illustrates the necessary steps in the computation of the next-to-leading order cross section which are required to render it finite.

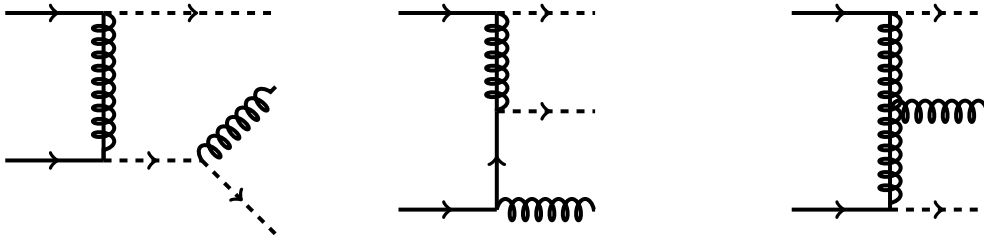


Figure 6.3: A selection of real gluon emission diagrams contributing to squark production. Again each diagram is a representative of a certain diagram type. The first one is final state gluon emission, the second one initial state gluon radiation and the third one is the radiation of a gluon from a virtual particle within the diagram.

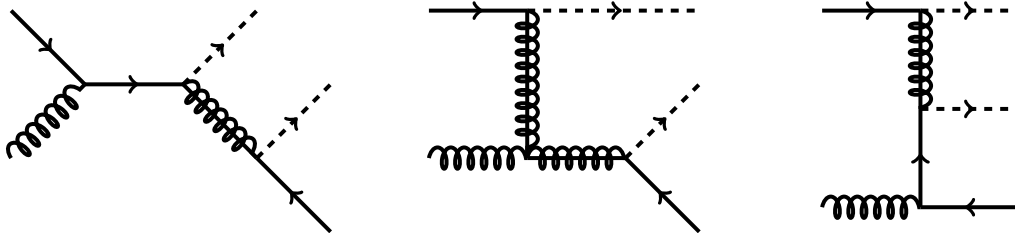


Figure 6.4: A selection of real quark emission diagrams contributing to squark production. The first two diagrams have a gluino propagator which may go on-shell. In this regime of phase space these diagrams should not be included in the correction to squark-production but to a tree-level contribution to squark-gluino-production.

7 Renormalization of the MRSSM

In order to improve the prediction of the cross section of the previous chapter one has to take quantum corrections into account. These are associated with loops in the corresponding Feynman diagrams. Computing these loop diagrams one might encounter infinities which arise from certain momentum configurations of the unspecified loop momentum. These infinities can be classified due to their origin. Infinities which are associated with loop momenta which tend to infinity are referred to as ultraviolet(UV) divergences. Infinities arising from loop momenta approaching zero can occur in loops with massless particles and are called infrared(IR) singularities. Furthermore there are collinear singularities which occur when a massless particle splits into two massless collinear particles.

These infinities are not physical and must therefore be removed to get sensible predictions. To this end one regularizes them to extract them from the quantity in question. UV-divergences can be removed by means of renormalization, i.e. counterterms are inserted into the Lagrangian to cancel UV-divergences. Infrared and collinear divergences are removed by adding up all possible contributions which give rise to the considered observable.

7.1 Regularization Schemes

Dimensional Regularization(DREG)

Dimensional regularization(DREG) is a very common procedure for regularizing infinities which was devised by t'Hooft and Veltman [23]. In this scheme loop momenta, gamma- and epsilon-tensors, phase space and fields are defined in D dimensions. As in every regularization scheme a parameter with mass dimension needs to be introduced. In DREG that is the μ parameter which ensures that the loop integrals still have mass dimension 4:

$$\int \frac{d^4 p}{(2\pi)^4} \rightarrow \mu^{4-D} \int \frac{d^D p}{(2\pi)^D}. \quad (7.1)$$

One often writes $D = 4 - 2\epsilon$. Then the divergences of the loop integral manifest in $\frac{1}{\epsilon}$ poles. However DREG suffers a flaw in supersymmetry. As the degrees of freedom for a massless gauge boson are $D - 2$ but the degrees of freedom for its superpartner are 2 there is a mismatch if $D \neq 4$. As a consequence there are 2ϵ degrees of freedom associated with the gluon¹⁶ which do not have a supersymmetric partner. Therefore DREG violates supersymmetry.

¹⁶These degrees of freedom are identified with scalars and are therefore referred to as ϵ scalars

Dimensional Reduction (DRED)

Dimensional reduction (DRED) was introduced to rectify the imperfections of DREG, i.e. it preserves supersymmetry¹⁷. DRED promotes only loop momenta to D dimensions. All other quantities which are D dimensional in DREG stay in 4 dimensions.

maybe refer to Collins: Renormalization

7.2 Regularization Scheme Dependences

It is useful to introduce the effective action Γ to discuss the subject of this and ensuing subsections. A formal introduction of Γ can be found in [2]. In short Γ can be viewed as a modification of the classical action $\Gamma_{\text{cl}} = \int \mathcal{L}_{\text{cl}}$ by quantum effects:

$$\Gamma = \Gamma_{\text{cl}} + \mathcal{O}(\hbar) \quad (7.2)$$

This means that in addition to the vertices in the classical Lagrangian new vertices arise due to loop effects. As already alluded to loop corrections might a priori not be finite and then need to be rendered finite by the addition of counterterms. For $\mathcal{O}(\hbar)$ corrections one writes

$$\Gamma^{(\leq 1)} \rightarrow \Gamma^{(\leq 1)} + \Gamma^{(1), \text{ ct}} \quad (7.3)$$

These counterterms depend on the regularization (and renormalization) scheme. If one chooses to work with DREG supersymmetry will not be preserved at 1-loop order, i.e. $\Gamma_{\text{DREG}}^{(\leq 1)}$ is not supersymmetric. To maintain supersymmetry invariance of the renormalized effective action the counterterms will not only consist of supersymmetric counterterms $\Gamma_{\text{DREG}}^{(1), \text{ ct, sym}}$ but also of counterterms restoring supersymmetry $\Gamma_{\text{DREG}}^{(1), \text{ ct, restore}}$.

$$\Gamma_{\text{DREG}}^{(1), \text{ ct}} = \Gamma_{\text{DREG}}^{(1), \text{ ct, sym}} + \Gamma_{\text{DREG}}^{(1), \text{ ct, restore}} \quad (7.4)$$

Fortunately a supersymmetry conserving regularization scheme (at 1-loop level) is given by DRED [24]. One way to acquire supersymmetry restoring counterterms is therefore given by

$$\Gamma_{\text{DRED}}^{(\leq 1)} + \Gamma_{\text{DRED}}^{(1), \text{ ct}} \stackrel{!}{=} \Gamma_{\text{DRED}}^{(\leq 1)} + \Gamma_{\text{DRED}}^{(1), \text{ ct}}. \quad (7.5)$$

Equating also the finite terms in $\Gamma^{(1), \text{ ct, sym}}$ in DRED and DREG the choice of the supersymmetry restoring counterterms is fixed by:

$$\Gamma_{\text{DRED}}^{(1), \text{ ct, restore}} = \Gamma_{\text{DREG}}^{(\leq 1)} - \Gamma_{\text{DRED}}^{(\leq 1)}. \quad (7.6)$$

¹⁷It is not clear if DRED preserves supersymmetry at all orders in perturbation theory but it does preserve supersymmetry at the 1-loop level.

This way supersymmetry is preserved by the renormalization constants.

In the case of the MRSSM it will turn out that the only supersymmetry violation comes from corrections associated with the gluon as already alluded to in section 7.1. However supersymmetry restoring will always already be included in δZ^{DREG} . This is $\delta Z^{\text{DREG}} = \delta Z^{\text{DREG, sym}} + \delta Z^{\text{trans}}$ where $\delta Z^{\text{trans}} = \delta Z^{\text{DREG}} - \delta Z^{\text{DRED}}$ is the supersymmetry restoring renormalization constant. The only point where particularly care is required is the coupling: The gauge coupling g_s and the Yukawa coupling \hat{g}_s receive different supersymmetry restoring counterterms due to different loop diagrams. Therefore one has to make a difference between these couplings at 1-loop level. In order to match g_s to the experimentally measured coupling it is renormalized in the $\overline{\text{MS}}$ -scheme (with an additional manipulation for heavy particles, which will be explained in section 7.4). The Yukawa coupling \hat{g}_s therefore needs to be added with the difference of the supersymmetry restoring counterterms from the $q\tilde{q}^\dagger\tilde{g}$ vertex and the $q\bar{q}G$ vertex at 1-loop in order to be renormalized the same way.

7.3 On-Shell Renormalization

A part of the computation of NLO processes is the calculation of renormalization constants. The field and mass renormalization constants have been calculated in DREG in the on-shell scheme. This has the advantage that when turning to the cross section no manipulation of the Green function to the S-matrix element has to be done.

The Quark Self-Energy

The quark self-energy splits into contribution from the SM as well as a supersymmetric analogue which is already present in the MSSM.

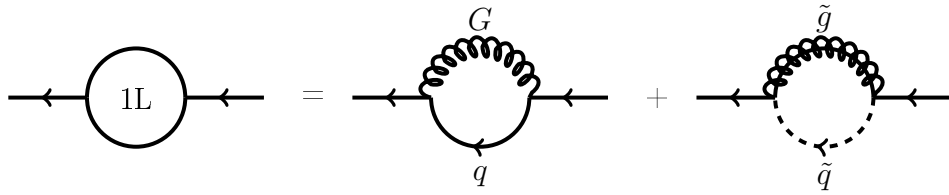


Figure 7.1: Feynman diagrams contributing to the self-energy of the quark at 1-loop level

The 1-PI diagrams evaluate to

$$i\Gamma_{q_i\bar{q}_j}^{1L} = i\frac{g_s^2}{16\pi^2}\delta_{ij}C(F)\left[2\left(B_0(p^2, 0, 0) + B_1(p^2, 0, 0) - \frac{1}{2}\right)\not{p} - 2B_1(p^2, m_{\tilde{g}}^2, m_{\tilde{q}}^2)\not{p}\right]. \quad (7.7)$$

With the counterterm Feynman rule

$$i\Gamma_{q_i\bar{q}_j}^{1L,ct} \hat{=} i \text{---}\leftarrow \text{---}\text{X}\text{---}\leftarrow j \hat{=} i\delta_{ij}\delta Z_q \not{p}$$

and the on-shell renormalization condition

$$\frac{\partial}{\partial \not{p}} \left[\Re(\Gamma_{q_i\bar{q}_j}^{1L}) + \Gamma_{q_i\bar{q}_j}^{1L,ct} \right]_{p^2=0} = 0 \quad (7.8)$$

where $\Re(\dots)$ denotes the real part of \dots one finds

$$\delta Z_q = 2C(F) \frac{g_s^2}{16\pi^2} \Re [B_1(0, m_{\tilde{g}}^2, m_{\tilde{q}}^2)] . \quad (7.9)$$

Note that the term $\frac{1}{2}$ from eq. 7.7 has vanished because the self energy is taken on-shell which means that this factor is absorbed into the on-shell B_0 function which is in DREG defined to be zero if it has no mass scale.

Doing the same calculation in DRED one finds that this very term $\frac{1}{2}$ is absent. Therefore the transition counterterm between DREG and DRED is given by

$$\delta Z_q^{\text{trans}} = \delta Z_q^{\text{DREG}} - \delta Z_q^{\text{DRED}} = C(F) \frac{g_s^2}{16\pi^2} . \quad (7.10)$$

The Squark Self-Energy

The contributions to the self-energy of the left- and right-handed squark are the same. Therefore to avoid unnecessary labeling $\Gamma_{\tilde{q}\tilde{q}^\dagger}$ stands in the following for $\Gamma_{\tilde{q}_L\tilde{q}_L^\dagger} = \Gamma_{\tilde{q}_R\tilde{q}_R^\dagger}$.

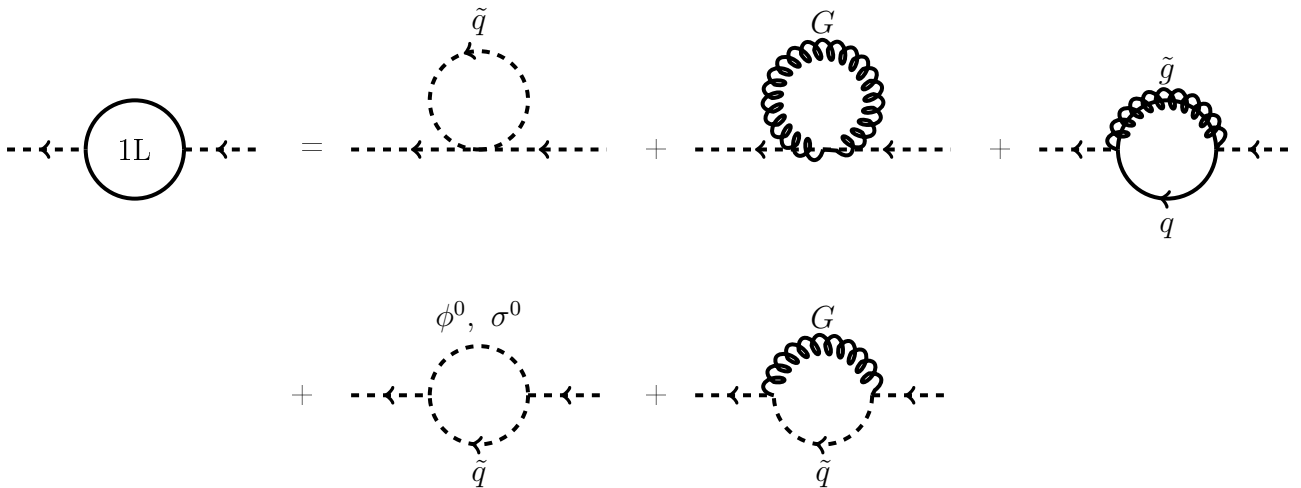


Figure 7.2: Diagrammatic contributions to the self-energy of the squark at 1-loop level

the gluino and may be referred to as the octino.

From the Lagrangian 4.13 one can see that the couplings of the two particles are quite distinct. This is reflected by different field renormalization constants of the left- and right-handed part of the gluino. As for the quarks the fermion (and momentum) flow is from the right to the

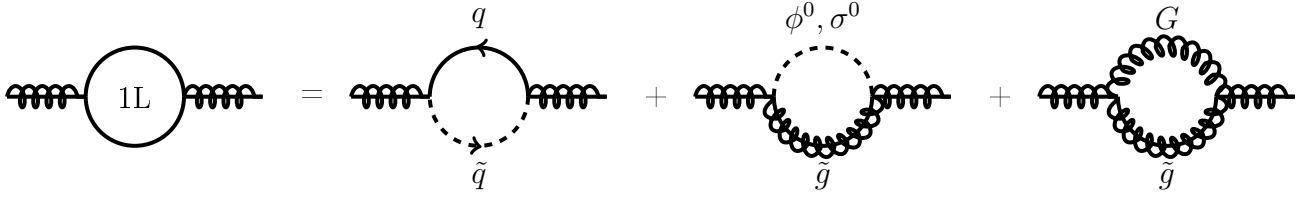


Figure 7.3: diagrammatic contributions to the self-energy of the squark at 1-loop level

left.

$$\begin{aligned}
 i\Gamma_{\tilde{g}^a \tilde{g}^b}^{1L} &= i \frac{g_s^2}{16\pi^2} \delta_{ab} \left[-4T(F) \left((n_f - 1)B_1(p^2, 0, m_{\tilde{q}}^2) + B_1(p^2, m_t^2, m_{\tilde{q}}^2) \right) P_L \not{p} \right. \\
 &\quad + C(A) \left((B_0(p^2, m_{\tilde{g}}^2, m_{\phi^0}^2) - B_0(p^2, m_{\tilde{g}}^2, m_{\sigma^0}^2))m_{\tilde{g}} - (B_1(p^2, m_{\tilde{g}}^2, m_{\phi^0}^2) + B_1(p^2, m_{\tilde{g}}^2, m_{\sigma^0}^2))\not{p} \right) \\
 &\quad \left. + C(A) \left((2 - 4B_0(p^2, 0, m_{\tilde{g}}^2))m_{\tilde{g}} - (1 - 2(B_0(p^2, 0, m_{\tilde{g}}^2) + B_1(p^2, 0, m_{\tilde{g}}^2)))\not{p} \right) \right] \quad (7.17)
 \end{aligned}$$

Where $n_f = 6$ is the number of quark flavors.

The counterterm Feynman rule reads

$$i\Gamma_{\tilde{g}^a \tilde{g}^b}^{1L,ct} \hat{=} a \text{ (crossed wavy lines) } b \hat{=} i\delta_{ab} \left[(\delta Z_{\tilde{g}}^L P_L + \delta Z_{\tilde{g}}^R P_R) \not{p} - \left(\frac{\delta Z_{\tilde{g}}^L + \delta Z_{\tilde{g}}^R}{2} m_{\tilde{g}} + \delta m_{\tilde{g}} \right) \right].$$

The on-shell renormalization conditions for the fields are

$$\frac{\partial}{\partial(P_L \not{p})} \left[\Re(\Gamma_{\tilde{g}^a \tilde{g}^b}^{1L}) + \Gamma_{\tilde{g}^a \tilde{g}^b}^{1L,ct} \right]_{\not{p}=m_{\tilde{g}}} = 0, \quad \frac{\partial}{\partial(P_R \not{p})} \left[\Re(\Gamma_{\tilde{g}^a \tilde{g}^b}^{1L}) + \Gamma_{\tilde{g}^a \tilde{g}^b}^{1L,ct} \right]_{\not{p}=m_{\tilde{g}}} = 0 \quad (7.18)$$

where the derivative of $\Sigma = \Sigma^{VL} P_L \not{p} + \Sigma^{VR} P_R \not{p} + \Sigma^{SL} P_L + \Sigma^{SR} P_R$ with respect to $P_A \not{p}$ ($A \in \{L, R\}$) is defined by

$$\left. \frac{\partial}{\partial(P_A \not{p})} \Sigma \right|_{\not{p}=m} = \Sigma^{VA} + \frac{\partial}{\partial p^2} (m^2 \Sigma^{VL} + m^2 \Sigma^{VR} + m \Sigma^{SL} + m \Sigma^{SR}). \quad (7.19)$$

This leads to the following renormalization constants

$$\begin{aligned}
\delta Z_{\tilde{g}}^L = & \frac{g_s^2}{16\pi^2} \Re \left[4T(F) \left((n_f - 1) B_1(m_{\tilde{g}}^2, 0, m_{\tilde{q}}^2) + B_1(m_{\tilde{g}}^2, m_t^2, m_{\tilde{q}}^2) \right) \right. \\
& + C(A) (B_1(m_{\tilde{g}}^2, m_{\tilde{g}}^2, m_{\phi^0}^2) + B_1(m_{\tilde{g}}^2, m_{\tilde{g}}^2, m_{\sigma^0}^2)) \\
& + C(A) (1 - 2(B_0(m_{\tilde{g}}^2, 0, m_{\tilde{g}}^2) + B_1(m_{\tilde{g}}^2, 0, m_{\tilde{g}}^2))) \\
& + 4T(F) m_{\tilde{g}}^2 \frac{\partial}{\partial p^2} \left(((n_f - 1)) B_1(p^2, 0, m_{\tilde{q}}^2) + B_1(p^2, m_t^2, m_{\tilde{q}}^2) \right) \\
& - 2C(A) m_{\tilde{g}} \frac{\partial}{\partial p^2} \left(B_0(p^2, m_{\tilde{g}}^2, m_{\phi^0}^2) - B_0(p^2, m_{\tilde{g}}^2, m_{\sigma^0}^2) - B_1(p^2, m_{\tilde{g}}^2, m_{\phi^0}^2) - B_1(p^2, m_{\tilde{g}}^2, m_{\sigma^0}^2) \right) \\
& \left. - 4C(A) m_{\tilde{g}}^2 \frac{\partial}{\partial p^2} \left(-B_0(p^2, 0, m_{\tilde{g}}^2) + B_0(p^2, 0, m_{\tilde{g}}^2) \right) \right]_{p^2=m_{\tilde{g}}^2} \quad (7.20)
\end{aligned}$$

and

$$\begin{aligned}
\delta Z_{\tilde{g}}^R = & \frac{g_s^2}{16\pi^2} \Re \left[C(A) (B_1(m_{\tilde{g}}^2, m_{\tilde{g}}^2, m_{\phi^0}^2) + B_1(m_{\tilde{g}}^2, m_{\tilde{g}}^2, m_{\sigma^0}^2)) \right. \\
& + C(A) (1 - 2(B_0(m_{\tilde{g}}^2, 0, m_{\tilde{g}}^2) + B_1(m_{\tilde{g}}^2, 0, m_{\tilde{g}}^2))) \\
& + 4T(F) m_{\tilde{g}}^2 \frac{\partial}{\partial p^2} \left(((n_f - 1)) B_1(p^2, 0, m_{\tilde{q}}^2) + B_1(p^2, m_t^2, m_{\tilde{q}}^2) \right) \\
& - 2C(A) m_{\tilde{g}} \frac{\partial}{\partial p^2} \left(B_0(p^2, m_{\tilde{g}}^2, m_{\phi^0}^2) - B_0(p^2, m_{\tilde{g}}^2, m_{\sigma^0}^2) - B_1(p^2, m_{\tilde{g}}^2, m_{\phi^0}^2) - B_1(p^2, m_{\tilde{g}}^2, m_{\sigma^0}^2) \right) \\
& \left. - 4C(A) m_{\tilde{g}}^2 \frac{\partial}{\partial p^2} \left(-B_0(p^2, 0, m_{\tilde{g}}^2) + B_0(p^2, 0, m_{\tilde{g}}^2) \right) \right]_{p^2=m_{\tilde{g}}^2} . \quad (7.21)
\end{aligned}$$

As for the quark there are constant terms amid the Passarino-Veltman integrals. These arise only in DREG and not in DRED. The transition counterterms are

$$\delta Z_{\tilde{g}}^{A \text{ trans}} = \delta Z_{\tilde{g}}^{A \text{ DREG}} - \delta Z_{\tilde{g}}^{A \text{ DRED}} = C(A) \frac{g_s^2}{16\pi^2} \quad (7.22)$$

for $A \in \{L, R\}$. The gluino mass counterterm is ascertained by the condition

$$\left[\Re(\Gamma_{\tilde{g}^a \tilde{g}^b}^{1L}) + \Gamma_{\tilde{g}^a \tilde{g}^b}^{1L, \text{ct}} \right]_{p=m_{\tilde{g}}} = 0 \quad (7.23)$$

which is equivalent to

$$\delta m_{\tilde{g}} = \Re \left(m_{\tilde{g}} \frac{\Sigma^{VL} + \Sigma^{VR}}{2} + \frac{\Sigma^{SL} + \Sigma^{SR}}{2} \right) \quad (7.24)$$

and yields

$$\begin{aligned} \delta m_{\tilde{g}} = & \frac{g_s^2}{16\pi^2} m_{\tilde{g}}^2 \Re \left[-2T(F) \left((n_f - 1) B_1(m_{\tilde{g}}^2, 0, m_{\tilde{q}}^2) + B_1(m_{\tilde{g}}^2, m_t^2, m_{\tilde{q}}^2) \right) \right. \\ & + C(A) \left(B_0(m_{\tilde{g}}^2, m_{\tilde{g}}^2, m_{\phi^0}^2) - B_0(m_{\tilde{g}}^2, m_{\tilde{g}}^2, m_{\sigma^0}^2) - B_1(m_{\tilde{g}}^2, m_{\tilde{g}}^2, m_{\phi^0}^2) - B_1(m_{\tilde{g}}^2, m_{\tilde{g}}^2, m_{\sigma^0}^2) \right) \\ & \left. + C(A) \left(1 - 2B_0(m_{\tilde{g}}^2, 0, m_{\tilde{g}}^2) + 2B_1(m_{\tilde{g}}^2, 0, m_{\tilde{g}}^2) \right) \right]. \end{aligned} \quad (7.25)$$

Again there is a transition counterterm

$$\delta m_{\tilde{g}}^{\text{trans}} = \delta m_{\tilde{g}}^{\text{DREG}} - \delta m_{\tilde{g}}^{\text{DRED}} = C(A) \frac{g_s^2}{16\pi^2} m_{\tilde{g}}. \quad (7.26)$$

7.4 Renormalization of the Gauge Coupling

The gauge coupling g_s is renormalized in the $\overline{\text{MS}}$ -scheme with the modification that additional logarithms are subtracted, i.e. light particles are treated in the $\overline{\text{MS}}$ -scheme and heavy particles in the zero-momentum subtraction scheme. This is to decouple heavy particles from the running of $\alpha_s = \frac{g_s^2}{4\pi}$. This renormalization procedure allows to adopt the experimental values of α_s from the parton density functions. The running due to effects of heavy particles is then encoded in the logarithms of δg_s .

Extracting δg_s from the quark-quark-gluon vertex requires not only the computation of $i\Gamma_{q_i\bar{q}_j G_a^\mu}^{\text{1L}}$ but also the (re)evaluation of auxiliary field renormalization constants δZ_q^{aux} and δZ_G^{aux} in the above mentioned scheme. These will not be the same as the on-shell scheme.

The Quark Self-Energy Revisited

The quark self-energy has two contribution which are shown in figure 7.1. The first one corresponds to light particles the second one to heavy particles: $i\Gamma_{q_i\bar{q}_j}^{\text{1L}} = i\Gamma_{q_i\bar{q}_j}^{\text{1L,light}} + i\Gamma_{q_i\bar{q}_j}^{\text{1L,heavy}}$. For light particles only the UV-divergent¹⁸ part is kept. The self energy corresponding to the heavy particles is taken at zero momentum $p^2 = 0$.

$$i\Gamma_{q_i\bar{q}_j}^{\text{1L,light}} \Big|_{\text{UV-div}} = iC(F) \frac{g_s^2}{16\pi^2} \Delta_\epsilon \not{p} \delta_{ij} \quad (7.27)$$

$$i\Gamma_{q_i\bar{q}_j}^{\text{1L,heavy}}(p^2 = 0) = -iC(F) \frac{g_s^2}{16\pi^2} 2B_1(0, m_{\tilde{g}}^2, m_{\tilde{q}}^2) \not{p} \delta_{ij} \quad (7.28)$$

The renormalization constant for the evaluation of δg_s is determined by the condition

$$\frac{\partial}{\partial \not{p}} \left[\Gamma_{q_i\bar{q}_j}^{\text{1L,light}} \Big|_{\text{UV-div}} + \Gamma_{q_i\bar{q}_j}^{\text{1L,heavy}}(p^2 = 0) + \Gamma_{q_i\bar{q}_j}^{\text{1L,ct}} \right] = 0 \quad (7.29)$$

¹⁸In contrast to the $\overline{\text{MS}}$ -scheme in the $\overline{\text{MS}}$ -scheme not only the pure ultraviolet divergence but also two additional transcendent numbers are subtracted. It is therefore common to define $\Delta_\epsilon = \frac{1}{\epsilon} - \gamma_E + \ln 4\pi$.

and computes to

$$\delta Z_q^{\text{aux}} = -\frac{g_s^2}{16\pi^2} C(F) [\Delta_\epsilon + B_1(0, m_{\tilde{g}}^2, m_{\tilde{q}}^2)]. \quad (7.30)$$

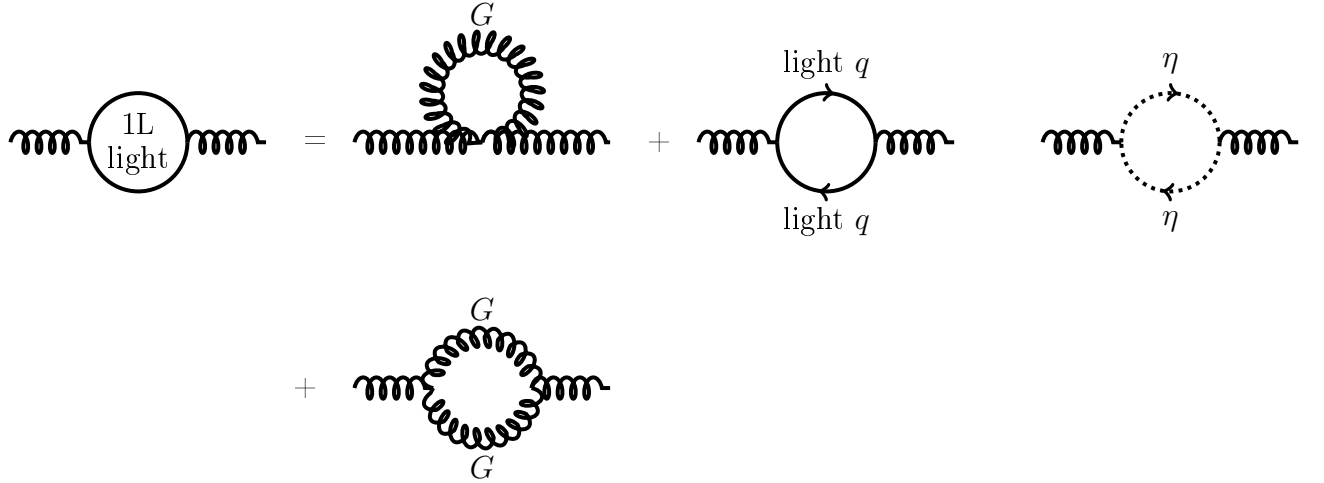


Figure 7.4: Contribution to the self-energy of the gluon originating from light particles

The Gluon Self-Energy

As for the quark self-energy there are again contributions to the self-energy originating from light and heavy particles. Again these are differently dealt with.

$$\begin{aligned} i\Gamma_{G_\mu^a G_\nu^b}^{\text{1L,light}} \Big|_{\text{UV-div}} &= i\frac{g_s^2}{16\pi^2} \Delta_\epsilon \left[0 - \frac{4(n_f - 1)}{3} T(F) (p^2 g^{\mu\nu} - p^\mu p^\nu) + \frac{C(A)}{12} (p^2 g^{\mu\nu} + 2p^\mu p^\nu) \right. \\ &\quad \left. + \frac{C(A)}{12} (19p^2 g^{\mu\nu} - 22p^\mu p^\nu) \right] \delta_{ab} \\ &= i\frac{g_s^2}{16\pi^2} \Delta_\epsilon \left[-\frac{4(n_f - 1)}{3} T(F) + \frac{5}{3} C(A) \right] (p^2 g^{\mu\nu} - p^\mu p^\nu) \delta_{ab} \end{aligned} \quad (7.31)$$

Both the contribution from the gluon loop and the one from the ghost loop are not proportional to $(p^2 g^{\mu\nu} - p^\mu p^\nu)$ but their sum is. The heavy particle contributions are calculated in the zero-

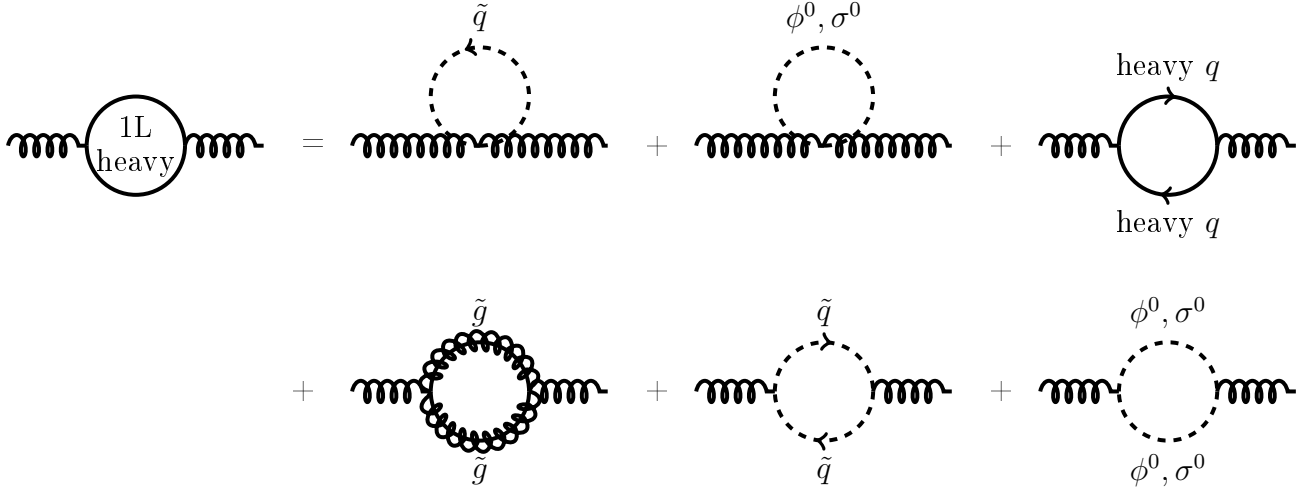


Figure 7.5: Contribution to the self-energy of the gluon originating from heavy particles, in the last diagram either ϕ^0 or σ^0 are running in the loop

momentum subtraction

$$\begin{aligned}
i\Gamma_{G_\mu^a G_\nu^b}^{1L, \text{heavy}}(p^2 = 0) &= i\frac{g_s^2}{16\pi^2}\delta_{ab} \left[-4T(F)n_f \left(\Delta_\epsilon - \ln \frac{m_{\tilde{q}}^2}{\mu^2} \right) m_{\tilde{q}}^2 g^{\mu\nu} - C(A) \left(\Delta_\epsilon - \ln \frac{m_{\phi^0}^2}{\mu^2} \right) m_{\phi^0}^2 g^{\mu\nu} \right. \\
&\quad - C(A) \left(\Delta_\epsilon - \ln \frac{m_{\sigma^0}^2}{\mu^2} \right) m_{\sigma^0}^2 g^{\mu\nu} - \frac{4}{3}T(F) \left(\Delta_\epsilon - \ln \frac{m_t^2}{\mu^2} \right) (p^2 g^{\mu\nu} - p^\mu p^\nu) \\
&\quad - \frac{4}{3}C(A) \left(\Delta_\epsilon - \ln \frac{m_{\tilde{g}}^2}{\mu^2} \right) (p^2 g^{\mu\nu} - p^\mu p^\nu) \\
&\quad - \frac{2}{3}T(F)n_f \left(\Delta_\epsilon - \ln \frac{m_{\tilde{q}}^2}{\mu^2} \right) (p^2 g^{\mu\nu} - p^\mu p^\nu) + 4T(F)n_f \left(\Delta_\epsilon - \ln \frac{m_{\tilde{q}}^2}{\mu^2} \right) m_{\tilde{q}}^2 g^{\mu\nu} \\
&\quad - \frac{1}{6}C(A) \left(\Delta_\epsilon - \ln \frac{m_{\phi^0}^2}{\mu^2} \right) (p^2 g^{\mu\nu} - p^\mu p^\nu) + C(A) \left(\Delta_\epsilon - \ln \frac{m_{\phi^0}^2}{\mu^2} \right) m_{\phi^0}^2 g^{\mu\nu} \\
&\quad \left. - \frac{1}{6}C(A) \left(\Delta_\epsilon - \ln \frac{m_{\sigma^0}^2}{\mu^2} \right) (p^2 g^{\mu\nu} - p^\mu p^\nu) + C(A) \left(\Delta_\epsilon - \ln \frac{m_{\sigma^0}^2}{\mu^2} \right) m_{\sigma^0}^2 g^{\mu\nu} \right] \\
&= i\frac{g_s^2}{16\pi^2}\delta_{ab} \left[-\frac{4}{3}T(F) \left(\Delta_\epsilon - \ln \frac{m_t^2}{\mu^2} \right) (p^2 g^{\mu\nu} - p^\mu p^\nu) \right. \\
&\quad - \frac{4}{3}C(A) \left(\Delta_\epsilon - \ln \frac{m_{\tilde{g}}^2}{\mu^2} \right) (p^2 g^{\mu\nu} - p^\mu p^\nu) \\
&\quad - \frac{2}{3}T(F)n_f \left(\Delta_\epsilon - \ln \frac{m_{\tilde{q}}^2}{\mu^2} \right) (p^2 g^{\mu\nu} - p^\mu p^\nu) \\
&\quad - \frac{1}{6}C(A) \left(\Delta_\epsilon - \ln \frac{m_{\phi^0}^2}{\mu^2} \right) (p^2 g^{\mu\nu} - p^\mu p^\nu) \\
&\quad \left. - \frac{1}{6}C(A) \left(\Delta_\epsilon - \ln \frac{m_{\sigma^0}^2}{\mu^2} \right) (p^2 g^{\mu\nu} - p^\mu p^\nu) \right] \tag{7.32}
\end{aligned}$$

The counterterm Feynman rule for the gluon propagator is

$$i\Gamma_{G_\mu^a G_\nu^b}^{1L,ct} \hat{=} a, \mu \text{---} b, \nu \hat{=} -i\delta Z_G (p^2 g^{\mu\nu} - p^\mu p^\nu) \delta_{ab}.$$

The renormalization condition for δZ_G^{aux} reads

$$\Gamma_{G_\mu^a G_\nu^b}^{1L,light} \Big|_{\text{UV-div}} + \Gamma_{G_\mu^a G_\nu^b}^{1L,heavy}(p^2 = 0) - \delta Z_G^{\text{aux}} (p^2 g^{\mu\nu} - p^\mu p^\nu) \delta_{ab} = 0 \quad (7.33)$$

and yields

$$\begin{aligned} \delta Z_G^{\text{aux}} = \frac{g_s^2}{16\pi^2} \Big\{ & \left[-\frac{4}{3}T(F)(n_f - 1) + \frac{5}{3}C(A) \right] \Delta_\epsilon + \left[-\frac{4}{3}T(F) \left(\Delta_\epsilon - \ln \frac{m_t^2}{\mu^2} \right) \right. \\ & - \frac{4}{3}C(A) \left(\Delta_\epsilon - \ln \frac{m_g^2}{\mu^2} \right) - \frac{2}{3}T(F)n_f \left(\Delta_\epsilon - \ln \frac{m_q^2}{\mu^2} \right) \\ & \left. - \frac{1}{6}C(A) \left(\Delta_\epsilon - \ln \frac{m_{\phi^0}^2}{\mu^2} \right) - \frac{1}{6}C(A) \left(\Delta_\epsilon - \ln \frac{m_{\sigma^0}^2}{\mu^2} \right) \right\}. \end{aligned} \quad (7.34)$$

The $q\bar{q}G$ Vertex Correction

As for the self energies the vertex correction constitutes of loops from light particles which correspond to the Standard Model and additional heavy particle loops. The contributions

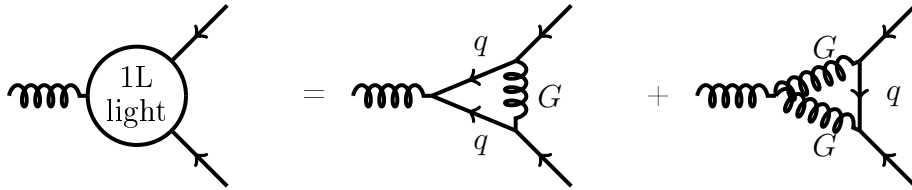


Figure 7.6: Contribution from light (Standard Model) particles to the $q\bar{q}G$ vertex correction

from Standard Model particles to the $q\bar{q}G$ yield

$$\begin{aligned} i\Gamma_{q_i \bar{q}_j G_\mu^a}^{1L,light} \Big|_{\text{UV-div}} &= -ig_s T_{ij}^a \gamma^\mu \frac{g_s^2}{16\pi^2} \left[\left(C(F) - \frac{C(A)}{2} \right) 2(B_0(0,0,0) - 2C_{00}(0,0,0,0,0)) \right. \\ &\quad \left. + C(A)(B_0(0,0,0) + 2C_{00}(0,0,0,0,0)) \right] \\ &= -ig_s T_{ij}^a \gamma^\mu \frac{g_s^2}{16\pi^2} \Delta_\epsilon \left[\left(C(F) - \frac{C(A)}{2} \right) + \frac{3}{2}C(A) \right]. \end{aligned} \quad (7.35)$$

The term in the curved brackets of eq. 7.35 corresponds to the first diagram in fig. 7.6 whereas the term with the prefactor $C(A)$ corresponds to the second diagram. The 3-point-function

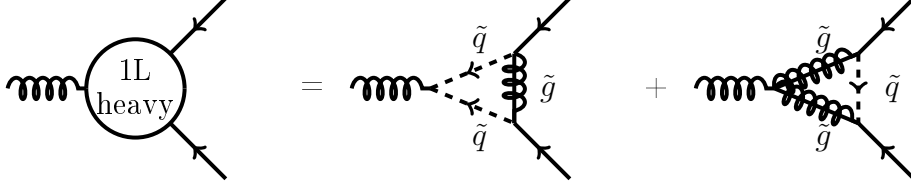


Figure 7.7: Contribution from heavy particles to the $q\bar{q}G$ vertex correction.

with only heavy particles running in the loop evaluates to

$$\begin{aligned}
 i\Gamma_{q_i\bar{q}_j G_\mu^a}^{1L, \text{heavy}}(p_i^2 = 0) &= -ig_s T_{ij}^a \gamma^\mu \frac{g_s^2}{16\pi^2} \left[\left(C(F) - \frac{C(A)}{2} \right) 4C_{00}(0, 0, m_{\tilde{g}}^2, m_{\tilde{q}}^2, m_{\tilde{q}}^2) \right. \\
 &\quad \left. + C(A) (B_0(0, m_{\tilde{g}}^2, m_{\tilde{q}}^2) - 2C_{00}(0, 0, m_{\tilde{g}}^2, m_{\tilde{g}}^2, m_{\tilde{q}}^2)) \right] \\
 &= -ig_s T_{ij}^a \gamma^\mu \frac{g_s^2}{16\pi^2} \left[\left(C(F) - \frac{C(A)}{2} \right) \left(\Delta_\epsilon - \ln \frac{m_{\tilde{g}}^2}{\mu^2} \right) \right. \\
 &\quad \left. + \frac{C(A)}{2} \left(\Delta_\epsilon - \ln \frac{m_{\tilde{g}}^2}{\mu^2} \right) \right] \quad (7.36)
 \end{aligned}$$

The argument $p_i^2 = 0$ of the vertex function denotes, that all external particles are taken on shell, i.e. at zero momentum.

insert B_1 function in order to cancel contribution from quark ren.const

In the second line identities from 10.6 have been used. The renormalization condition for the counterterm of the gauge coupling δg_s reads

$$i\Gamma_{q_i\bar{q}_j G_\mu^a}^{1L, \text{light}} \Big|_{\text{UV-div}} + i\Gamma_{q_i\bar{q}_j G_\mu^a}^{1L, \text{heavy}}(p_i^2 = 0) + \left[-ig_s T_{ij}^a \gamma^\mu \left(\frac{\delta g_s}{g_s} + \delta Z_q^{\text{aux}} + \frac{\delta Z_G^{\text{aux}}}{2} \right) \right] = 0. \quad (7.37)$$

Finally one can read off $\frac{\delta g_s}{g_s}$

$$\begin{aligned}
 \frac{\delta g_s}{g_s} &= \frac{g_s^2}{16\pi^2} \left[\left(\frac{2}{3} T(F)(n_f - 1) - \frac{11}{6} C(A) \right) \Delta_\epsilon + \left(\frac{5}{6} C(A) + \frac{2}{3} T(F) + \frac{1}{3} T(F)n_f \right) \Delta_\epsilon \right. \\
 &\quad \left. - \frac{2}{3} C(A) \ln \frac{m_{\tilde{g}}^2}{\mu^2} - \frac{1}{3} T(F)n_f \ln \frac{m_{\tilde{q}}^2}{\mu^2} - \frac{2}{3} T(F) \ln \frac{m_t^2}{\mu^2} - \frac{1}{12} C(A) \left(\ln \frac{m_{\phi^0}^2}{\mu^2} + \ln \frac{m_{\sigma^0}^2}{\mu^2} \right) \right]. \quad (7.38)
 \end{aligned}$$

Note the only difference to the MSSM is the appearance of the sgluon masses as well as a factor of two in front of the logarithm of the gluino mass which is due to twice as much degrees of freedom of the gluino in the MRSSM.

7.5 The Beta Function

The beta function describes the dependence of the gauge coupling g_s upon the energy scale μ . Writing down the action of a theory in D dimensions one needs to introduce an energy scale μ in order to keep the action dimensionless. But μ is no physical parameter and can be absorbed into the fields and parameters. To this end one defines

$$g_{sB}(g_s, \mu) = \mu^\epsilon g_s \left(1 + \frac{\delta g_s}{g_s} \right) \quad (7.39)$$

which must not depend upon the unphysical scale μ , ergo

$$0 = \frac{dg_{sB}}{d \ln \mu} = \frac{\partial g_{sB}}{\partial \ln \mu} + \beta \frac{\partial g_{sB}}{\partial g_s} \quad (7.40)$$

where the definition of the beta function $\frac{\partial g_s}{\partial \ln \mu}$ has been inserted. Equation 7.40 serves to calculate $\beta(g_s, \epsilon)$. By equating coefficients and using the shortcuts

$$\begin{aligned} \frac{\beta_0^L}{2} &= \frac{2}{3}T(F)(n_f - 1) - \frac{11}{6}C(A) \\ \frac{\beta_0^H}{2} &= \frac{5}{6}C(A) + \frac{2}{3}T(F) + \frac{1}{3}T(F)n_f \\ L &= -\frac{2}{3}C(A) \ln \frac{m_g^2}{\mu^2} - \frac{1}{3}T(F)n_f \ln \frac{m_q^2}{\mu^2} - \frac{2}{3}T(F) \ln \frac{m_t^2}{\mu^2} - \frac{1}{12}C(A) \left(\ln \frac{m_{\phi^0}^2}{\mu^2} + \ln \frac{m_{\sigma^0}^2}{\mu^2} \right) \end{aligned}$$

so that

$$\frac{\delta g_s}{g_s} = \frac{g_s^2}{16\pi^2} \left(\frac{\beta_0^L}{2\epsilon_{UV}} + \frac{\beta_0^H}{2\epsilon_{UV}} + L \right) \quad (7.41)$$

one finds

$$\beta(g_s, \epsilon) = -\epsilon g_s \left(1 + \frac{g_s^2}{16\pi^2} L \right) + \beta(g_s) + \mathcal{O}(2 - \text{loop}) \quad (7.42)$$

$$\beta(g_s) = \frac{g_s^3}{16\pi^2} \beta_0^L + \mathcal{O}(2 - \text{loop}). \quad (7.43)$$

This is the beta function of QCD first found by [Gross, Politzer, Wil]

7.6 Supersymmetry Restoring Counterterm

As already discussed in section 7.2 care is required in terms of supersymmetry restoring when renormalizing the gauge coupling g_s and the Yukawa coupling \hat{g}_s . In doing so one needs the already calculated transition counterterms of the quark, squark and gluino from 7.10, 7.15 and 7.22 as well as the transition counterterm of the gluon.

The Gluon Self-Energy Revisited

The only regularization dependence of the gluon self-energy arises from the gluon loop, i.e. the last diagram in figure 7.4. With the definition of $\Gamma_{\text{DREG}}^{(1),\text{ct},\text{restore}}$ in 7.6 one obtains

$$i\Gamma_{\text{DREG},G_\mu^a G_\nu^b}^{(1),\text{ct},\text{restore}} = -i\frac{1}{3}C(A)\frac{g_s^2}{16\pi^2}(p^2 g^{\mu\nu} - p^\mu p^\nu)\delta_{ab} \quad (7.44)$$

which translates to the transition counterterm

$$\delta Z_G^{\text{trans}} = \frac{C(A)}{3} \frac{g_s^2}{16\pi^2}. \quad (7.45)$$

The $q\bar{q}G$ Vertex Correction Revisited

The diagrams from which the supersymmetry restoring contributions to the gauge coupling correction come from are shown in figure 7.6 and evaluate to

$$i\Gamma_{\text{DREG},q_i\bar{q}_j G_\mu^a}^{(1),\text{ct},\text{restore}} = -ig_s T_{ij}^a \gamma^\mu \frac{g_s^2}{16\pi^2} \left[\left(C(F) - \frac{C(A)}{2} \right) + \frac{C(A)}{2} \right] \quad (7.46)$$

$$= -ig_s T_{ij}^a \gamma^\mu \left[\frac{\delta g_s^{\text{trans}}}{g_s} + \delta Z_q^{\text{trans}} + \frac{\delta Z_G^{\text{trans}}}{2} \right] \quad (7.47)$$

where the second line shows the supersymmetry restoring counterterms. This yields

$$\frac{\delta g_s^{\text{trans}}}{g_s} = -\frac{C(A)}{6} \frac{g_s^2}{16\pi^2}. \quad (7.48)$$

The $q\bar{q}^\dagger\tilde{g}$ Vertex Correction

The supersymmetry restoring corrections to the Yukawa coupling origin from the diagram below. The supersymmetry restoring part is given by

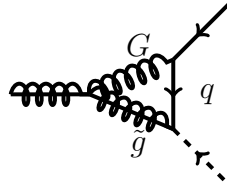


Figure 7.8: diagram of the supersymmetry restoring correction of the $q\bar{q}\tilde{g}$ vertex

$$i\Gamma_{\text{DREG},q_i\bar{q}_j\tilde{g}^a}^{(1),\text{ct},\text{restore}} = -ig_s\sqrt{2}P_L T_{ij}^a \frac{g_s^2}{16\pi^2} C(A) \quad (7.49)$$

$$= -ig_s\sqrt{2}P_L T_{ij}^a \left[\frac{\delta \hat{g}_s^{\text{trans}}}{g_s} + \frac{\delta Z_q^{\text{trans}} + \delta Z_{\tilde{q}}^{\text{trans}} + \delta Z_{\tilde{g}}^{\text{trans}}}{2} \right]. \quad (7.50)$$

The supersymmetry restoring part of the Yukawa renormalization constants is therefore

$$\frac{\delta \hat{g}_s^{\text{trans}}}{g_s} = -\frac{C(F) - C(A)}{2} \frac{g_s^2}{16\pi^2}. \quad (7.51)$$

As a consequence of the two different supersymmetry restoring parts of the coupling renormalization constants an additional renormalization constant $\delta g_s^{\text{restore}}$ needs to be introduced. As described in section 7.2 it is given by

$$\frac{\delta g_s^{\text{restore}}}{g_s} = \frac{\delta \hat{g}_s^{\text{trans}}}{g_s} - \frac{\delta g_s^{\text{trans}}}{g_s} = \frac{g_s^2}{16\pi^2} \left(\frac{2C(A)}{3} - \frac{C(F)}{2} \right). \quad (7.52)$$

In short this means that the gauge coupling g_s is renormalized with δg_s given in 7.38 and the Yukawa coupling \hat{g}_s is renormalized with $\delta \hat{g}_s = \delta g_s + \delta g_s^{\text{restore}}$.

The finite correction $\delta g_s^{\text{restore}}$ is the same as in supersymmetric QCD which should not surprise too much as all its contributions originate from loops with gluons.

7.7 $\overline{\text{MS}}$ - Renormalization

To quickly check for UV-finiteness of a Greenfunction or a physical observable it is useful to have the extracted UV-divergences of the renormalization constants at hand. How these are obtained is described in 10.6.

(In order to obtain these the Passarino-Veltman integrals need to be substituted by their $\frac{1}{\epsilon}$ coefficient. These had been taken from [25] and checked with `FeynArts` and `FormCalc` [26], [?], [26].)

$$\begin{aligned} \delta Z_{\tilde{g}}^L &= -\frac{g_s^2}{16\pi^2\epsilon_{\text{UV}}} 2 [T(F)n_f + C(A)] & \delta Z_{\tilde{g}}^R &= -\frac{g_s^2}{16\pi^2\epsilon_{\text{UV}}} 2C(A) \\ \delta m_{\tilde{g}} &= \frac{g_s^2}{16\pi^2\epsilon_{\text{UV}}} [T(F)n_f - 2C(A)] m_{\tilde{g}} & & \\ \delta Z_{\tilde{q}} &= 0 & \delta m_{\tilde{q}}^2 &= 0 \\ \frac{\delta g_s}{g_s} &= \frac{g_s^2}{16\pi^2\epsilon_{\text{UV}}} [T(F)n_f - C(A)] & & \\ \delta Z_{\phi^0} &= 0 & \delta m_{\phi^0}^2 &= -\frac{g_s^2}{16\pi^2\epsilon_{\text{UV}}} [8T(F)n_f - 16C(A)] m_{\tilde{g}}^2 \\ \delta Z_{\sigma^0} &= 0 & \delta m_{\sigma^0}^2 &= 0 \\ \delta Z_G &= -\frac{g_s^2}{16\pi^2\epsilon_{\text{UV}}} 2T(F)n_f & & \end{aligned} \quad (7.53)$$

8 Squark Production at One-Loop

8.1 The LSZ Theorem

The LSZ theorem [27] or LSZ reduction formula prescribes how to obtain the S-matrix element, i.e. a physical observable, from the time ordered correlation function of the respective field operators. The time ordered correlation function of fields in an interacting theory can be calculated perturbatively with the aid of the Gell-Mann and Low theorem and the Wick theorem.

Considering a physical process with kinematics $\vec{k}_1 \dots \vec{k}_n \rightarrow \vec{p}_1 \dots \vec{p}_m$ and taking for the sake of simplicity only one scalar field ϕ the Fourier transform of the time ordered product of a correlation function is related to the corresponding S-matrix element like¹⁹

$$\begin{aligned} & \prod_{i=1}^n \int dx_i e^{ip_i x_i} \prod_{j=1}^m \int dy_j e^{ik_j y_j} \langle \Omega | \mathcal{T} [\phi(x_1) \dots \phi(x_n) \phi(y_1) \dots \phi(y_m)] | \Omega \rangle \\ & \sim \prod_{i=1}^n \frac{i\sqrt{Z}}{p_i^2 - m^2 + i\epsilon} \prod_{j=1}^m \frac{i\sqrt{Z}}{k_j^2 - m^2 + i\epsilon} \left\langle \vec{p}_1 \dots \vec{p}_n | S | \vec{k}_1 \dots \vec{k}_m \right\rangle. \end{aligned} \quad (8.1)$$

Here \mathcal{T} denotes the time ordering operator, $|\Omega\rangle$ is the ground state of the interacting theory and \sqrt{Z} is the residue of the single particle pole in the two-point function

$$\begin{aligned} \int dx e^{ipx} \langle \Omega | \mathcal{T} [\phi(x) \phi(0)] | \Omega \rangle &= \frac{i}{p^2 - m_0^2} + \frac{i}{p^2 - m_0^2} \left(\frac{i\Sigma(p^2)}{p^2 - m_0^2} \right) + \frac{i}{p^2 - m_0^2} \left(\frac{\Sigma(p^2)}{p^2 - m_0^2} \right)^2 + \dots \\ &= \frac{i}{p^2 - m_0^2 - \Sigma(p^2)}. \end{aligned} \quad (8.2)$$

The parameter m_0 is the tree-level mass and the quantity $-i\Sigma(p^2)$ denotes the sum of all

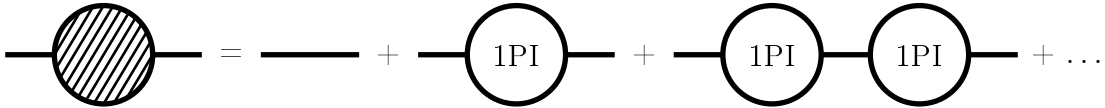


Figure 8.1: Diagrammatic figure of the two-point function of a scalar field: The propagator in an interaction theory can be calculated in a perturbation series in the coupling constant.

one-particle-irreducible contributions to the particle's self-energy. From eq. 8.2 one can read off the physical mass m^2 of the particle which is associated with the field ϕ . It is determined as the value of p^2 where the propagator has a pole, i.e.

$$[p^2 - m_0^2 - \Sigma(p^2)]_{p^2=m^2} = 0 \quad (8.3)$$

¹⁹In this subsection the \sim indicates that the poles on either side are the same provided that all momenta are close to their mass shell, i.e. $p_i^0 \rightarrow E_{\vec{p}_i}$ and $k_j^0 \rightarrow E_{\vec{k}_j}$.

Close to the pole the denominator of eq. 8.2 can be expanded like

$$p^2 - m_0^2 - \Sigma(p^2) = (p^2 - m^2) \left(1 - \frac{\partial \Sigma(p^2)}{\partial p^2} \right)_{p^2=m^2} + \mathcal{O}((p^2 - m^2)^2). \quad (8.4)$$

The residue of the propagator can therefore be written as

$$Z = \left(1 - \frac{\partial \Sigma(p^2)}{\partial p^2} \right)_{p^2=m^2}^{-1}. \quad (8.5)$$

Now considers the full $(n + m)$ -point function in scalar theory. One can decompose it into an amputated $(n + m)$ -point function and "full" propagators like written in eq. 8.2 and depicted in fig. 8.1.

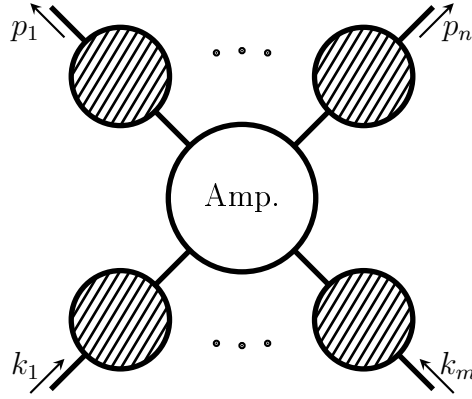


Figure 8.2: Diagrammatic figure of a "full" $(n + m)$ -point function. Apart from the "full" propagators there is the "full" amputated $(n + m)$ -point function

Inserting the expression

$$\frac{i}{p^2 - m_0^2 - \Sigma(p^2)} \sim \frac{iZ}{p^2 - m^2} \quad (8.6)$$

for the full propagators one notices the same singularity as in eq. 8.1. If one now compares the coefficients of these poles in eq. 8.1 one finds

$$\left\langle \vec{p}_1 \dots \vec{p}_n | S | \vec{k}_1 \dots \vec{k}_m \right\rangle = \sqrt{Z}^{n+m}.$$

Now it becomes visible why the renormalization in the on-shell scheme

$$\left. \frac{\partial \Sigma(p^2)}{\partial p^2} \right|_{p^2=m^2} \stackrel{!}{=} 0 \quad (8.7)$$

introduces no further manipulation when turning from the correlation function to the S-matrix-element because $Z = 1$ in on-shell renormalization. Furthermore the on-shell condition for the mass renormalization

$$\Sigma(p^2)|_{p^2=m^2} = 0 \quad (8.8)$$

means that the physical mass equals the tree level mass.

8.2 The Cross Section in the Limit of Large Sgluon Masses

The cross section for squark production does not exist in the limit of an infinitely large sgluon mass, instead it was found that it diverges logarithmically.

$$\lim_{m_{\sigma^0} \rightarrow \infty} \sigma(qq \rightarrow \tilde{q}\tilde{q}) \sim \ln \frac{m_{\sigma^0}^2}{\mu^2} \quad (8.9)$$

This is actually expected as an effective field theory of the MRSSM where the sgluon is integrated out is no longer supersymmetric. This is because the sgluon is together with the octino part of a supermultiplet. Integrating out only the sgluon means that the octino misses its superpartner in the effective field theory. In this case the decoupling theorem [28] does no longer hold.

Refer to super oblique correction and quantify difference of g and \hat{g} from eq 4 in [29]
append plot

9 Summary and Outlook

10 Appendix

10.1 System of Units and Metric

In this thesis the natural units are used, i.e. $c = \hbar (= k_B) = 1$. Furthermore the Minkowski metric is chosen to be

$$g^{\mu\nu} = \text{diag}(1, -1, -1, -1). \quad (10.1)$$

10.2 Constants of the Colour Algebra $SU(N)$

[Marina von Steinkirch]

The Casimir operator $C(R)\mathbb{1}$ of a semi-simple Lie algebra in the irreducible representation R is given by

$$g^{ab}T^a(R)T^b(R) = C(R)\mathbb{1} \quad (10.2)$$

where $T^a(R)$ is the a -th generator of the matrix valued representation R , g^{ab} is the metric of group, $C(R)$ is the Quadratic Casimir invariant of the representation R and $\mathbb{1}$ is the identity in the representation space.

Apart from $C(R)$ it is common to define the Dynkin-Index $T(R)$:

$$\text{Tr} [T^a(R)T^b(R)] = T(R)\delta^{ab}. \quad (10.3)$$

The two constants are connected by

$$C(R) \cdot \dim(R) = T(R) \cdot \dim(G) \quad (10.4)$$

where $\dim(G)$ is the dimension of the group and $\dim(R)$ is the dimension of the irreducible representation R .

In the case of $SU(N)$ one has a diagonal metric $g^{ab} = \delta^{ab}$ and therefore 10.2 turns to

$$\sum_a (T^a(R))^2 = C(R)\mathbb{1}_{\dim(R) \times \dim(R)} \quad (10.5)$$

and one can write down the following useful formulae for the fundamental representation $R = F$: $T_{ij}^a = \frac{\lambda_{ij}^a}{2}$ and the adjoint representation $R = A$: $(T_{ij}^a)^{adj} = -if_{aij}$

$$\begin{aligned} T_{ik}^a T_{kj}^a &= C(F) \mathbb{1}_{ij} & \text{with } C(F) &= \frac{N^2 - 1}{2N} = \frac{4}{3} \\ f^{abc} f^{dbc} &= C(A) \delta^{ad} & \text{with } C(A) &= N = 3 \\ \text{Tr} [T^a T^b] &= T(F) \delta^{ab} & \text{with } T(F) &= \frac{1}{2} \end{aligned} \quad (10.6)$$

where λ_{ij}^a are for $N_c = 3$ the Gell-Mann matrices and f_{abc} are the structure constants of $SU(N_c)$.

10.3 Weyl basis and 2-spinor notation

As representation of the γ -matrices the Weyl or chiral representation is chosen:

$$\gamma^\mu = \begin{pmatrix} 0 & \sigma^\mu \\ \bar{\sigma}^\mu & 0 \end{pmatrix} \quad \gamma_5 = \begin{pmatrix} -\mathbb{1}_2 & 0 \\ 0 & \mathbb{1}_2 \end{pmatrix} \quad (10.7)$$

with

$$\sigma^\mu = \begin{pmatrix} \mathbb{1}_2 & \sigma^i \end{pmatrix}, \quad \bar{\sigma}^\mu = \begin{pmatrix} \mathbb{1}_2 & -\sigma^i \end{pmatrix}, \quad (10.8)$$

where σ^i are the Pauli matrices and $\mathbb{1}_n$ is the $n \times n$ unit matrix. The left and right handed projectors are then given by

$$P_L = \frac{1}{2}(\mathbb{1}_4 - \gamma_5) \begin{pmatrix} \mathbb{1}_2 & 0 \\ 0 & 0 \end{pmatrix} \quad P_R = \frac{1}{2}(\mathbb{1}_4 + \gamma_5) \begin{pmatrix} 0 & 0 \\ 0 & \mathbb{1}_2 \end{pmatrix} \quad (10.9)$$

The representation of generators of the Lorentz group on 4-spinor space are composed of the above matrices. Because of the block form of those it is not surprising that the representation on 4-spinor space is reducible to two representations on 2-spinor (Weyl spinor) spaces. It is therefore sensible to decompose a 4 spinor into a left and a right handed Weyl spinor²⁰

$$\Psi = \begin{pmatrix} \psi_\alpha \\ \bar{\chi}^{\dot{\alpha}} \end{pmatrix} \quad (10.10)$$

where $\alpha, \dot{\alpha} \in \{1, 2\}$. Left handed Weyl spinors are labeled with undotted and right handed Weyl spinors with dotted indices. One distinguishes 4 different Weyl spinors:

$$\psi^\alpha, \quad \bar{\psi}^{\dot{\alpha}} = (\psi^\alpha)^*, \quad \psi_\alpha = \epsilon_{\alpha\beta} \psi^\beta, \quad \text{and} \quad \psi_{\dot{\alpha}} = \epsilon_{\dot{\alpha}\dot{\beta}} \psi^{\dot{\beta}} = (\psi_\alpha)^*, \quad (10.11)$$

²⁰The projectors in the chiral basis (eq. 10.9) explain the names left and right handed Weyl spinors.

where $*$ denotes complex conjugation and indices are lowered with the antisymmetric $\epsilon_{\alpha\beta}$ ($\epsilon_{\dot{\alpha}\dot{\beta}}$), which obeys

$$\epsilon^{\alpha\beta} = \epsilon_{\beta\alpha}, \quad \epsilon^{\dot{\alpha}\dot{\beta}} = \epsilon_{\dot{\beta}\dot{\alpha}} \quad \text{and} \quad \epsilon_{12} = \epsilon_{\dot{1}\dot{2}} = 1. \quad (10.12)$$

By virtue of the antisymmetry of ϵ one finds the Lorentz invariant products:

$$\begin{aligned} \psi\chi &:= \psi^\alpha\chi_\alpha = -\chi_\alpha\psi^\alpha = \chi^\alpha\psi_\alpha = \chi\psi, \\ \bar{\psi}\bar{\chi} &:= \bar{\psi}_{\dot{\alpha}}\bar{\chi}^{\dot{\alpha}} = -\bar{\chi}^{\dot{\alpha}}\bar{\psi}_{\dot{\alpha}} = \bar{\chi}_{\dot{\alpha}}\bar{\psi}^{\dot{\alpha}} = \bar{\chi}\bar{\psi} \end{aligned} \quad (10.13)$$

To make the index structure of the Pauli matrices explicit one writes $\sigma_{\alpha\dot{\alpha}}^\mu$ and $\sigma^{\mu\dot{\alpha}\alpha}$ for the formulae in 10.8. For the definition of the super algebra in section 3.1 the representation of the generators of the Lorentz group on the left and right handed Weyl spinor space are introduced:

$$\begin{aligned} \frac{1}{2}(\sigma^{\mu\nu})_\alpha{}^\beta &:= \frac{i}{4}(\sigma^\mu\bar{\sigma}^\nu - \sigma^\nu\bar{\sigma}^\mu)_\alpha{}^\beta \\ \frac{1}{2}(\bar{\sigma}^{\mu\nu})^{\dot{\alpha}}{}_{\dot{\beta}} &:= \frac{i}{4}(\bar{\sigma}^\mu\sigma^\nu - \bar{\sigma}^\nu\sigma^\mu)^{\dot{\alpha}}{}_{\dot{\beta}} \end{aligned} \quad (10.14)$$

With the definition of bared and charge conjugated 4-spinors²¹

$$\bar{\Psi} := \Psi^\dagger\gamma^0, \quad \Psi^C := i\gamma^2\gamma^0\bar{\Psi}^T \quad (10.15)$$

one obtains:

$$\begin{aligned} \Psi &= \begin{pmatrix} \psi_\alpha \\ \bar{\chi}^{\dot{\alpha}} \end{pmatrix}, & \bar{\Psi} &= \begin{pmatrix} \chi^\alpha & \bar{\psi}_{\dot{\alpha}} \end{pmatrix}, \\ \Psi^C &= \begin{pmatrix} \chi_\alpha \\ \bar{\psi}^{\dot{\alpha}} \end{pmatrix}, & \bar{\Psi}^C &= \begin{pmatrix} \psi^\alpha & \bar{\chi}_{\dot{\alpha}} \end{pmatrix}. \end{aligned} \quad (10.16)$$

The 4-spinor of an arbitrary quark q is given in terms of Weyl spinors q_L and \bar{q}_R by

$$q = \begin{pmatrix} q_L \\ \bar{q}_R \end{pmatrix} \quad (10.17)$$

whereas the 4-spinor of the Dirac gauginos is given in terms of the Weyl spinors λ and $\bar{\chi}$ ²²

$$\tilde{g}^a = \begin{pmatrix} -i\lambda^a \\ i\bar{\chi}^a \end{pmatrix} \quad (10.18)$$

²¹ Ψ^T denotes the transpose of the spinor Ψ and Ψ^\dagger is the Hermitian adjoint of Ψ .

²² λ is the superpartner of the gluon, called the gluino and $\bar{\chi}$ is the Weyl spinor of the chiral superfield which is associated with the gluon, called the octino.

10.4 Anticommuting numbers

Anticommuting numbers θ^α are also referred to as Grassmann numbers and are defined by $\theta^\alpha \theta^\beta = -\theta^\beta \theta^\alpha$ and commute with ordinary numbers.

They occur in superspace formalism in the form of 2 tuples, i.e. θ^α with $\alpha = 1, 2$. The complex conjugate of this tuple is denoted with $\bar{\theta}^{\dot{\alpha}}$. Derivatives are defined by

$$\begin{aligned} \partial^\alpha \theta_\beta &:= \frac{\partial}{\partial \theta_\alpha} \theta_\beta := \delta_\beta^\alpha & \partial_\alpha \theta^\beta &:= \frac{\partial}{\partial \theta_\alpha} \theta^\beta := \delta_\alpha^\beta \\ \bar{\partial}^{\dot{\alpha}} \bar{\theta}_{\dot{\beta}} &:= \frac{\partial}{\partial \bar{\theta}_{\dot{\alpha}}} \bar{\theta}_{\dot{\beta}} := \delta_{\dot{\beta}}^{\dot{\alpha}} & \bar{\partial}_{\dot{\alpha}} \bar{\theta}^{\dot{\beta}} &:= \frac{\partial}{\partial \bar{\theta}_{\dot{\alpha}}} \bar{\theta}^{\dot{\beta}} := \delta_{\dot{\alpha}}^{\dot{\beta}} \end{aligned} \quad (10.19)$$

whereby one needs to be cautious as these definitions imply

$$\partial_\alpha = -\epsilon_{\alpha\beta} \partial^\beta \quad \bar{\partial}_{\dot{\alpha}} = -\epsilon_{\dot{\alpha}\dot{\beta}} \bar{\partial}^{\dot{\beta}}. \quad (10.20)$$

Integrals are defined by:

$$\int d\theta_\alpha (a + b\theta^\beta + c\theta^\beta \theta^\gamma) := b\delta_\alpha^\beta + c(\delta_\alpha^\beta \theta^\gamma - \delta_\alpha^\gamma \theta^\beta) \quad \text{and} \quad \int d\theta_\alpha (a\bar{\theta}^{\dot{\beta}}) := (a\bar{\theta}^{\dot{\beta}}) \int d\theta_\alpha \quad (10.21)$$

where the first line mirrors the claim of translation invariance. One furthermore introduces the shortcuts

$$\int d\theta^2 = \int \frac{1}{4} \epsilon_{\alpha\beta} d\theta^\alpha d\theta^\beta, \quad \int d\bar{\theta}^2 = \int \frac{1}{4} \epsilon_{\dot{\alpha}\dot{\beta}} d\bar{\theta}^{\dot{\alpha}} d\bar{\theta}^{\dot{\beta}}, \quad \text{and} \quad \int d^4\theta := \int d\theta^2 d\bar{\theta}^2 \quad (10.22)$$

10.5 Feynman rules for the RSQCD

The following Feynman rules are derived from 4.13. When compared with the Feynman rules of the supersymmetric QCD the diagrams involving scalar gluons are new. In addition the gluon-quark-squark vertex is different in RSQCD for the gauginos are Dirac fermions.

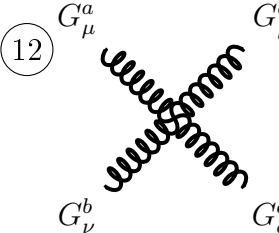
refer to paper cited in Beenakker(Appendix: Feynmanrules)

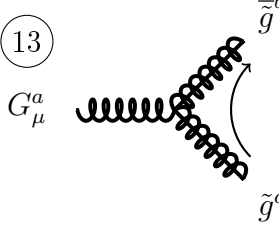
$$\begin{array}{ll}
\textcircled{1} & (\sigma^0)^a \cdots (\sigma^0)^b \hat{=} \frac{i}{p^2 - m_{\sigma^0}^2 + i\varepsilon} \delta_{ab} \\
\textcircled{2} & (\phi^0)^a \cdots (\phi^0)^b \hat{=} \frac{i}{p^2 - m_{\phi^0}^2 + i\varepsilon} \delta_{ab} \\
\textcircled{3} & \tilde{q}_{Ai} \cdots \tilde{q}_{Bj}^\dagger \hat{=} \frac{i\delta_{AB}}{p^2 - m_q^2 + i\varepsilon} \delta_{ij} \\
\textcircled{4} & q_i \cdots \bar{q}_j \hat{=} i \frac{\not{p} + m_q}{p^2 - m_q^2 + i\varepsilon} \delta_{ij} \\
\textcircled{5} & G_\mu^a \cdots G_\nu^b \hat{=} -i \frac{g^{\mu\nu}}{p^2 + i\varepsilon} \delta_{ab} \\
\textcircled{6} & \tilde{g}^a \cdots \bar{\tilde{g}}^b \hat{=} i \frac{\not{p} + m_{\tilde{g}}}{p^2 - m_{\tilde{g}}^2 + i\varepsilon} \delta_{ab} \\
\textcircled{7} & c^a \cdots \bar{c}^b \hat{=} \frac{i}{p^2 + i\varepsilon} \delta_{ab} \\
\textcircled{8} & G_\mu^a \cdots \begin{array}{c} \nearrow \bar{q}_i \\ \searrow q_j \end{array} \hat{=} -ig_s T_{ij}^a \gamma^\mu \\
\textcircled{9} & G_\mu^a \cdots \begin{array}{c} \nearrow \tilde{q}_{Ai}^\dagger(-p_1) \\ \searrow \tilde{q}_{Bj}(p_2) \end{array} \hat{=} -ig_s (p_2 + p_1)^\mu T_{ij}^a \delta_{AB} \\
\textcircled{10} & G_\mu^a \cdots \begin{array}{c} \nearrow \tilde{q}_{Ai}^\dagger \\ \searrow \tilde{q}_{Bj} \end{array} \hat{=} ig_s^2 g^{\mu\nu} \{T^a, T^b\}_{ij} \delta_{AB} \\
\textcircled{11} & G_\rho^c(p_c) \cdots \begin{array}{c} \nearrow G_\mu^a(p_a) \\ \searrow G_\nu^b(p_b) \end{array} \hat{=} -g_s f_{abc} [g_{\mu\nu}(p_a - p_b)^\rho + g_{\nu\rho}(p_b - p_c)^\mu + g_{\rho\mu}(p_c - p_a)^\nu]
\end{array}$$

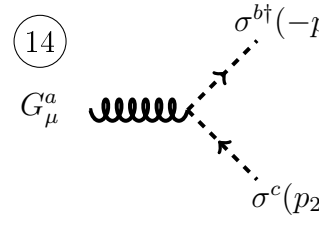
Figure 10.1: In the Feynman diagrams of the propagators the momentum is flowing from the right to the left hand side.

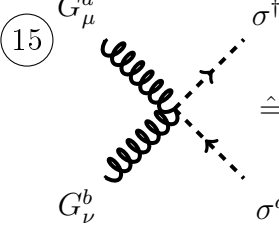
In the Feynman diagrams of the vertices all momenta flow towards the vertex.

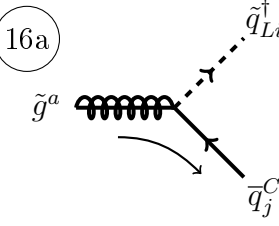
The indices $A, B = L, R$ label the right/left-"handedness" of the squarks. The indices $i, j = 1, 2, 3$ are the color indices in the (anti)fundamental representation where $a, b, c, \dots = 1, \dots, 8$ are the color indices of the adjoint representation.

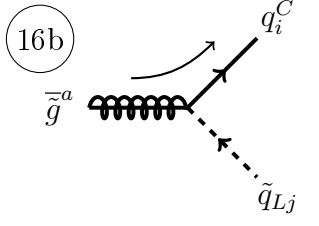
(12)  $\hat{=} -ig_s^2[f^{abe}f^{cde}(g^{\mu\rho}g^{\nu\sigma} - g^{\mu\sigma}g^{\nu\rho}) + f^{ace}f^{bde}(g^{\mu\nu}g^{\rho\sigma} - g^{\mu\sigma}g^{\nu\rho}) + f^{ade}f^{bce}(g^{\mu\nu}g^{\rho\sigma} - g^{\mu\rho}g^{\nu\sigma})]$

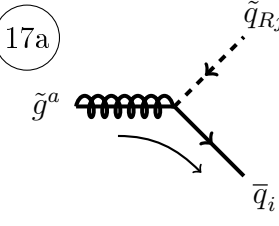
(13)  $\hat{=} -g_s f_{abc} \gamma^\mu$

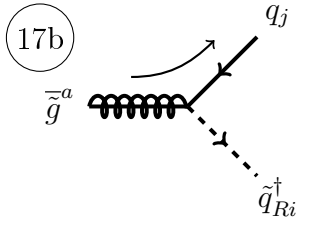
(14)  $\hat{=} -g_s(p_1 + p_2)^\mu f_{abc}$

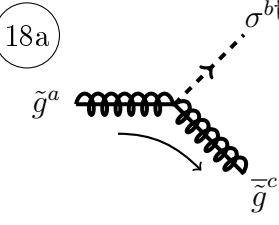
(15)  $\hat{=} +ig_s^2 g^{\mu\nu} [f^{aec}f^{bed} + f^{bec}f^{aed}]$

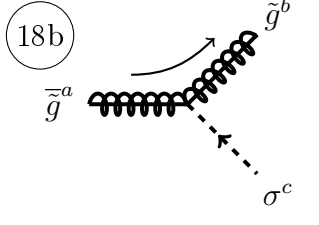
(16a)  $\hat{=} -i\sqrt{2}g_s T_{ij}^a P_L$

(16b)  $\hat{=} -i\sqrt{2}g_s T_{ij}^a P_R$

(17a)  $\hat{=} +i\sqrt{2}g_s T_{ij}^a P_L$

(17b)  $\hat{=} +i\sqrt{2}g_s T_{ij}^a P_R$

(18a)  $\hat{=} -\sqrt{2}g_s f^{abc} P_L$

(18b)  $\hat{=} +\sqrt{2}g_s f^{abc} P_R$

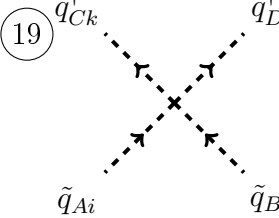
(19)  $\hat{=} -ig_s^2 [T_{ki}^a T_{lj}^a (\delta_{AL}\delta_{CL} - \delta_{AR}\delta_{CR})(\delta_{BL}\delta_{DL} - \delta_{BR}\delta_{DR}) + T_{kj}^a T_{li}^a (\delta_{BL}\delta_{CL} - \delta_{BR}\delta_{CR})(\delta_{AL}\delta_{DL} - \delta_{AR}\delta_{DR})]$

Figure 10.2: The curved arrows indicate the fermion flow. The Feynman rules 16b, 17b and 18b are the complex conjugates of 16a, 17a and 18a respectively. Applying a flipping rule to a vertex one has to reverse the curved arrow, i.e. the fermion flow and replace Ψ with $\bar{\Psi}^C$. In addition one has to add a minus sign for Feynman rule 13.

$$\begin{aligned}
(20) \quad & \begin{array}{c} \tilde{q}_{Aj}^\dagger \quad \sigma^{b\dagger} \\ \diagdown \quad \diagup \\ \times \\ \diagup \quad \diagdown \\ \tilde{q}_{Ai} \quad \sigma^c \end{array} \hat{=} -g_s^2 T_{ij}^a f^{abc} (\delta_{AL} \delta_{CL} - \delta_{AR} \delta_{BR}) \\
(21) \quad & \begin{array}{c} \tilde{q}_{Ai}^\dagger \\ \diagdown \quad \diagup \\ \sigma^a + \sigma^{a\dagger} \quad \tilde{q}_{Bj} \end{array} \hat{=} -i\sqrt{2} g_s m_{\tilde{g}} T_{ij}^a (\delta_{AL} \delta_{BL} - \delta_{AR} \delta_{BR}) \\
(22) \quad & \begin{array}{c} \sigma^{\dagger b} \quad \sigma^{\dagger d} \\ \diagdown \quad \diagup \\ \times \\ \diagup \quad \diagdown \\ \sigma^c \quad \sigma^e \end{array} \hat{=} -g_s^2 (f^{abc} f^{ade} + f^{abc} f^{adc})
\end{aligned}$$

10.6 Passarino-Veltman Integrals

The definition of the Passarino-Veltman integrals in this thesis agrees with the one from `LoopTools` [30] convention. The original paper [31] uses slightly different conventions. A pedagogical introduction to the evaluation of one-loop integrals can be found in [32]

$$\begin{aligned}
\frac{i}{16\pi^2} A_0(m^2) &= \int_l \frac{1}{l^2 - m^2} \\
\frac{i}{16\pi^2} B_{0,\mu,\mu\nu}(p^2, m_1^2, m_2^2) &= \int_l \frac{\{1, l_\mu, l_\mu l_\nu\}}{[l^2 - m_1^2][(l+p)^2 - m_2^2]} \\
\frac{i}{16\pi^2} C_{0,\mu,\mu\nu}(p_1^2, p_2^2, (p_1+p_2)^2, m_1^2, m_2^2, m_3^2) &= \int_l \frac{\{1, l_\mu, l_\mu l_\nu\}}{[l^2 - m_1^2][(l+p_1)^2 - m_2^2][(l+p_1+p_2)^2 - m_3^2]}
\end{aligned} \tag{10.23}$$

with the shortcut $\int_l = \mu^{2\epsilon} \int \frac{d^D l}{(2\pi)^D}$. Furthermore there are suppressed ε 's which prescribe how the poles in the complex plane are avoided. They are hidden in the infinitesimal shift of the masses: $m_i^2 \rightarrow m_i^2 - i\varepsilon$.

The tensor integrals can be decomposed as

$$\begin{aligned}
B_\mu &:= p_\mu B_1 \\
B_{\mu\nu} &:= g_{\mu\nu} B_{00} + p_\mu p_\nu B_{11} \\
C_\mu &= p_{1\mu} C_1 + p_{2\mu} C_2 \\
C_{\mu\nu} &:= g_{\mu\nu} C_{00} + p_{1\mu} p_{1\nu} C_{11} + p_{2\mu} p_{2\nu} C_{22} + (p_{1\mu} p_{2\nu} + p_{2\mu} p_{1\nu}) C_{12}
\end{aligned} \tag{10.24}$$

In the special case of vanishing momenta the integrals take a succinct form.

$$A_0(m^2) = m^2 \left(\Delta_\epsilon - \ln \frac{m^2}{\mu^2} + 1 \right) + \mathcal{O}(\epsilon) \quad (10.25)$$

where the typical UV-divergent constant $\Delta_\epsilon = \frac{1}{\epsilon} - \gamma_E + \ln 4\pi$ is defined. It comprises the Euler-Mascheroni constant γ_E .

$$B_0(0, m_1^2, m_2^2) = \frac{A_0(m_1^2) - A_0(m_2^2)}{m_1^2 - m_2^2} = \Delta_\epsilon + 1 - \frac{m_1^2 \ln \frac{m_1^2}{\mu^2} - m_2^2 \ln \frac{m_2^2}{\mu^2}}{m_1^2 - m_2^2} + \mathcal{O}(\epsilon) \quad (10.26)$$

$$B_0(0, m^2, m^2) = \frac{\partial}{\partial m^2} A_0(m^2) = \Delta_\epsilon - \ln \frac{m^2}{\mu^2} + \mathcal{O}(\epsilon) \quad (10.27)$$

$$B_0(0, 0, 0) = 0 \quad (10.28)$$

$$B_1(0, m_1^2, m_2^2) = -\frac{\Delta_\epsilon}{2} + \frac{1}{2} \ln \frac{m_1^2}{\mu^2} + \frac{-3 + 4t - t^2 - 4t \ln t + 2t^2 \ln t}{4(t-1)^2} + \mathcal{O}(\epsilon) \quad (10.29)$$

$$B_1(0, 0, 0) = 0 \quad (10.30)$$

The scaleless integrals are defined to be zero. The parameter t is given by $\frac{m_2^2}{m_1^2}$. As can be seen from 10.29 B_1 is in contrast to B_0 not symmetric in its masses but it can be shown [Romao] that

$$B_1(p^2, m_1^2, m_2^2) = -(B_0(p^2, m_2^2, m_1^2) + B_1(p^2, m_2^2, m_1^2)) \quad (10.31)$$

It can further be shown that

$$C_{00}(0, 0, 0, m_1^2, m_1^2, m_2^2) = -\frac{1}{2} B_1(0, m_1^2, m_2^2) \quad (10.32)$$

and that $C_{00}(0, 0, 0, m_1^2, m_1^2, m_2^2)$ is a symmetric function of its masses.

From the generic ϵ -expansion of the B_0 integral [25]

$$B_0(p^2, m_1^2, m_2^2) = \Delta_\epsilon - \int_0^1 dx \ln \frac{-x(1-x)p^2 + xm_2^2 + (1-x)m_1^2}{\mu^2} \quad (10.33)$$

and Passarino-Veltman decomposition [31] one can determine the UV-divergent part of all B and C integrals. In chapter 7.7 this was necessary in order to obtain the renormalization constants in the $\overline{\text{MS}}$ -scheme. Infrared and collinear singularities arise from the special case where one or multiple masses tend to zero. These poles are either regularized in terms of a small mass cutoff Λ or also dimensionally as ϵ -poles. In the later case the integral first needs to undergo the limit to zero masses and than being evaluated.

The following list shows all necessary integrals needed to determine the renormalization con-

stants in 7.7.

$$A_0(m^2)|_{\text{UV-div}} = m^2 \Delta_\epsilon \quad (10.34)$$

$$B_0(p^2, m_1^2, m_2^2)|_{\text{UV-div}} = \Delta_\epsilon \quad (10.35)$$

$$B_1(p^2, m_1^2, m_2^2)|_{\text{UV-div}} = -\frac{1}{2} \Delta_\epsilon \quad (10.36)$$

$$C_{00}(p_1^2, p_2^2, (p_1 + p_2)^2, m_1^2, m_2^2, m_3^2)|_{\text{UV-div}} = \frac{1}{4} \Delta_\epsilon \quad (10.37)$$

The UV-divergent part of C_{11} , C_{22} , C_{12} equals zero. As can be seen already from the superficial degree of divergence also $C_i|_{\text{UV-div}} = 0$ for $i \in \{0, 1, 2\}$.

10.7 Cross section and Phase Space Integration

Once the Feynman amplitude \mathcal{M} for a $2 \rightarrow N$ body scattering²³ is computed one can calculate physical observables with it. The differential cross section for $2 \rightarrow N$ scattering is given by

$$d\sigma = \frac{1}{F} d\Phi_N |\mathcal{M}|^2. \quad (10.38)$$

The flux factor is defined by $F = 4\sqrt{(k_a \cdot k_b)^2 - (m_a m_b)^2}$ which equals $F = 2s$ for massless initial state particles. The differential for the N body phase space in D dimensions is given by

$$d\Phi_N = (\mu^{2\epsilon})^{N-1} \left(\prod_{f=1}^N \frac{d^{D-1} p_f}{(2\pi)^{D-1}} \frac{1}{2E_f} \right) (2\pi)^D \delta^{(D)}(k_a + k_b - \sum_{f=1}^N p_f). \quad (10.39)$$

The factor $\mu^{2\epsilon}$ is included to maintain the mass dimension of the cross section. As in this thesis the sum of $|\mathcal{M}|^2$ over helicities and colors $\sum |\mathcal{M}|^2$ has been calculated one can write

$$d\sigma = \frac{1}{2s} d\Phi_2 K_{ab} \sum |\mathcal{M}|^2 \quad (10.40)$$

where K_{ab} encodes the averaging over initial state helicities and colors. Specifying to the center-of-mass frame and assuming that $\sum |\mathcal{M}|^2$ is only a function of the modulus of one of the final state particle's 3-momentum $|\vec{p}_i|$ and the angle θ between \vec{k}_a and \vec{p}_1 one can write

$$\begin{aligned} \int d\Phi_2 &= \mu^{2\epsilon} \int \frac{d|\vec{p}_1| d\Omega_1^{D-1}}{(2\pi)^{D-2} 4E_1 E_2} |\vec{p}_1|^{D-2} \delta \left(k_a^0 + k_b^0 - \sqrt{m_1^2 + |\vec{p}_1|^2} - \sqrt{m_2^2 + |\vec{p}_1|^2} \right) \\ &= \frac{1}{(2\pi)^{D-2}} \frac{2\pi^{\frac{D}{2}-1}}{\Gamma(\frac{D}{2}-1)} \mu^{2\epsilon} \int_0^\infty d|\vec{p}_1| \int_0^\pi d\cos\theta \frac{1}{4E_1 E_2} p_1^{D-2} \sin^{D-4}\theta \\ &\quad \delta \left(k_a^0 + k_b^0 - \sqrt{m_1^2 + |\vec{p}_1|^2} - \sqrt{m_2^2 + |\vec{p}_1|^2} \right). \end{aligned} \quad (10.41)$$

²³with kinematics $k_a + k_b \rightarrow p_1 + \dots p_N$

In the second line the integral over the D-dimensional hypersphere

$$\int d\Omega^D = \int_0^{2\pi} d\phi \prod_{i=1}^{D-2} \int_0^\pi \sin^i \theta_i d\theta_i = \frac{2\pi^{\frac{D}{2}}}{\Gamma(\frac{D}{2})} \quad (10.42)$$

has been used. Because $\sum |\mathcal{M}|^2$ is calculated in terms of Mandelstam variables

$$\begin{aligned} t &= (k_a - p_1)^2 \\ t &= -2 \left(|\vec{k}_a| \sqrt{m_1^2 + |\vec{p}_1|^2} - |\vec{k}_a| |\vec{p}_1| \cos \theta \right) + m_1^2 \end{aligned} \quad (10.43)$$

$$\begin{aligned} u &= (k_a - p_2)^2 \\ u &= -2 \left(|\vec{k}_a| \sqrt{m_2^2 + |\vec{p}_1|^2} + |\vec{k}_a| |\vec{p}_1| \cos \theta \right) + m_2^2 \end{aligned} \quad (10.44)$$

it is useful to perform a change of coordinates yielding

$$d|\vec{p}_1| d\cos \theta = -\frac{E_1 E_2}{4|\vec{k}_a|^2 |\vec{p}_1|^2 (E_1 + E_2)} du dt. \quad (10.45)$$

Inserting 10.45 into 10.41 and using $2|\vec{k}_a| = \sqrt{s} = E_1 + E_2$ gives

$$\begin{aligned} \int d\Phi_2 &= \frac{1}{s} \frac{\pi^{-\frac{D}{2}+1}}{2^{D-3} \Gamma(\frac{D}{2}-1)} \int du dt \left(\frac{tu - m_1^2 m_2^2}{\mu^{2\epsilon} s} \right)^{\frac{D-4}{2}} \\ &\quad \frac{1}{4} \Theta(tu - 4m_1^2 m_2^2) \delta(s + t + u - m_1^2 - m_2^2) \end{aligned} \quad (10.46)$$

where the Θ -function comes from the bounds of $|\vec{p}_1|$ and θ visible in 10.41 and the combination of 10.43 and 10.44. Working in $D = 4 - 2\epsilon$ dimensions and inserting $\Theta(s - 4m^2)$ with $m = \frac{m_1 + m_2}{2}$ to account for the production threshold one finds

$$\begin{aligned} \frac{d^2\sigma}{dt du} &= \frac{K_{ab}}{s^2} \frac{\pi S_\epsilon}{\Gamma(1-\epsilon)} \left[\frac{tu - m_1^2 m_2^2}{\mu^2 s} \right]^{-\epsilon} \Theta(tu - m_1^2 m_2^2) \\ &\quad \Theta(s - 4m^2) \delta(s + t + u - m_1^2 - m_2^2) \sum |\mathcal{M}|^2 \end{aligned} \quad (10.47)$$

where $S_\epsilon = (4\pi)^{-2+\epsilon}$ as defined in [16]. The averaging factors K_{ab} are given by

$$K_{qq} = \frac{1}{4N_c^2} \quad K_{GG} = \frac{1}{4(1-\epsilon)^2(N_c^2-1)^2} \quad K_{qG} = \frac{1}{4(1-\epsilon)N_c(N_c^2-1)}. \quad (10.48)$$

11 References

- [1] M. Maggiore, *A modern introduction to quantum field theory*. Oxford master series in physics 12, Oxford University Press, 2005.
- [2] M. E. Peskin and D. V. Schroeder, *An introduction to quantum field theory*. Advanced book program, Boulder (Colo.): Westview Press Reading (Mass.), 1995. Autre tirage : 1997.
- [3] C. N. Yang and R. L. Mills, “Conservation of isotopic spin and isotopic gauge invariance,” *Phys. Rev.*, vol. 96, pp. 191–195, Oct 1954.
- [4] P. W. Higgs, “Broken symmetries, massless particles and gauge fields,” *Phys. Lett.*, vol. 12, pp. 132–133, 1964.
- [5] P. W. Higgs, “Broken Symmetries and the Masses of Gauge Bosons,” *Phys. Rev. Lett.*, vol. 13, pp. 508–509, 1964.
- [6] P. W. Higgs, “Spontaneous Symmetry Breakdown without Massless Bosons,” *Phys. Rev.*, vol. 145, pp. 1156–1163, 1966.
- [7] F. Englert and R. Brout, “Broken Symmetry and the Mass of Gauge Vector Mesons,” *Phys. Rev. Lett.*, vol. 13, pp. 321–323, 1964.
- [8] G. S. Guralnik, C. R. Hagen, and T. W. B. Kibble, “Global Conservation Laws and Massless Particles,” *Phys. Rev. Lett.*, vol. 13, pp. 585–587, 1964.
- [9] T. W. B. Kibble, “Symmetry breaking in nonAbelian gauge theories,” *Phys. Rev.*, vol. 155, pp. 1554–1561, 1967.
- [10] A. D. H. J. Manfred Böhm, Manfred Böhm (Dr. rer. nat.), *Gauge Theories of the Strong and Electroweak Interaction*. Vieweg + Teubner, 3rd rev. ed. 2001 ed., 2001.
- [11] N. Cabbibo, “Leptonic Decays in the Unitary Symmetry Scheme,” in *Proceedings, International Conference on Fundamental Aspects of Weak Interactions*, pp. 299–302, 1964.
- [12] M. Kobayashi and T. Maskawa, “CP Violation in the Renormalizable Theory of Weak Interaction,” *Prog. Theor. Phys.*, vol. 49, pp. 652–657, 1973.
- [13] C. Becchi, A. Rouet, and R. Stora, “The Abelian Higgs-Kibble Model. Unitarity of the S Operator,” *Phys. Lett.*, vol. B52, pp. 344–346, 1974.
- [14] C. Becchi, A. Rouet, and R. Stora, “Renormalization of the Abelian Higgs-Kibble Model,” *Commun. Math. Phys.*, vol. 42, pp. 127–162, 1975.

-
- [15] C. Becchi, A. Rouet, and R. Stora, “Renormalization of Gauge Theories,” *Annals Phys.*, vol. 98, pp. 287–321, 1976.
 - [16] W. Beenakker, R. Hopker, M. Spira, and P. M. Zerwas, “Squark and gluino production at hadron colliders,” *Nucl. Phys.*, vol. B492, pp. 51–103, 1997.
 - [17] L. A. Harland-Lang, A. D. Martin, P. Motylinski, and R. S. Thorne, “Parton distributions in the LHC era: MMHT 2014 PDFs,” *Eur. Phys. J.*, vol. C75, no. 5, p. 204, 2015.
 - [18] G. Dissertori, I. Knowles, and M. Schmelling, *Quantum Chromodynamics: High Energy Experiments and Theory*. International series of monographs on physics, Clarendon Press, 2003.
 - [19] J. C. Collins, D. E. Soper, and G. F. Sterman, “Factorization of Hard Processes in QCD,” *Adv. Ser. Direct. High Energy Phys.*, vol. 5, pp. 1–91, 1989.
 - [20] R. Brock *et al.*, “Handbook of perturbative QCD: Version 1.0,” *Rev. Mod. Phys.*, vol. 67, pp. 157–248, 1995.
 - [21] T. Kinoshita, “Mass Singularities of Feynman Amplitudes,” *Journal of Mathematical Physics*, vol. 3, pp. 650–677, July 1962.
 - [22] T. D. Lee and M. Nauenberg, “Degenerate systems and mass singularities,” *Phys. Rev.*, vol. 133, pp. B1549–B1562, Mar 1964.
 - [23] G. ’t Hooft and M. J. G. Veltman, “Regularization and Renormalization of Gauge Fields,” *Nucl. Phys.*, vol. B44, pp. 189–213, 1972.
 - [24] W. Hollik and D. Stockinger, “Regularization and supersymmetry restoring counterterms in supersymmetric QCD,” *Eur. Phys. J.*, vol. C20, pp. 105–119, 2001.
 - [25] A. Denner, “Techniques for the Calculation of Electroweak Radiative Corrections at the One-Loop Level and Results for W-physics at LEP 200,” *Fortschritte der Physik*, vol. 41, pp. 307–420, 1993.
 - [26] T. Hahn, “Generating Feynman diagrams and amplitudes with FeynArts 3,” *Comput. Phys. Commun.*, vol. 140, pp. 418–431, 2001.
 - [27] H. Lehmann, K. Symanzik, and W. Zimmermann, “On the formulation of quantized field theories,” *Nuovo Cim.*, vol. 1, pp. 205–225, 1955.
 - [28] T. Appelquist and J. Carazzone, “Infrared Singularities and Massive Fields,” *Phys. Rev.*, vol. D11, p. 2856, 1975.

-
- [29] H.-C. Cheng, J. L. Feng, and N. Polonsky, “Superoblique corrections and nondecoupling of supersymmetry breaking,” *Phys. Rev.*, vol. D56, pp. 6875–6884, 1997.
 - [30] T. Hahn and M. Perez-Victoria, “Automatized one loop calculations in four-dimensions and D-dimensions,” *Comput. Phys. Commun.*, vol. 118, pp. 153–165, 1999.
 - [31] G. Passarino and M. J. G. Veltman, “One Loop Corrections for $e^+ e^-$ Annihilation Into $\mu^+ \mu^-$ in the Weinberg Model,” *Nucl. Phys.*, vol. B160, pp. 151–207, 1979.
 - [32] R. K. Ellis, Z. Kunszt, K. Melnikov, and G. Zanderighi, “One-loop calculations in quantum field theory: from Feynman diagrams to unitarity cuts,” *Phys. Rept.*, vol. 518, pp. 141–250, 2012.

Erklärung

Hiermit erkläre ich, dass ich diese Arbeit im Rahmen der Betreuung am Institut für ??
Physik ohne unzulässige Hilfe Dritter verfasst und alle Quellen als solche gekennzeichnet habe.
Vorname Nachname

Dresden, Monat 2012